Naval Research Reviews

Office of Naval Research
Four / 1996
Vol XLVIII

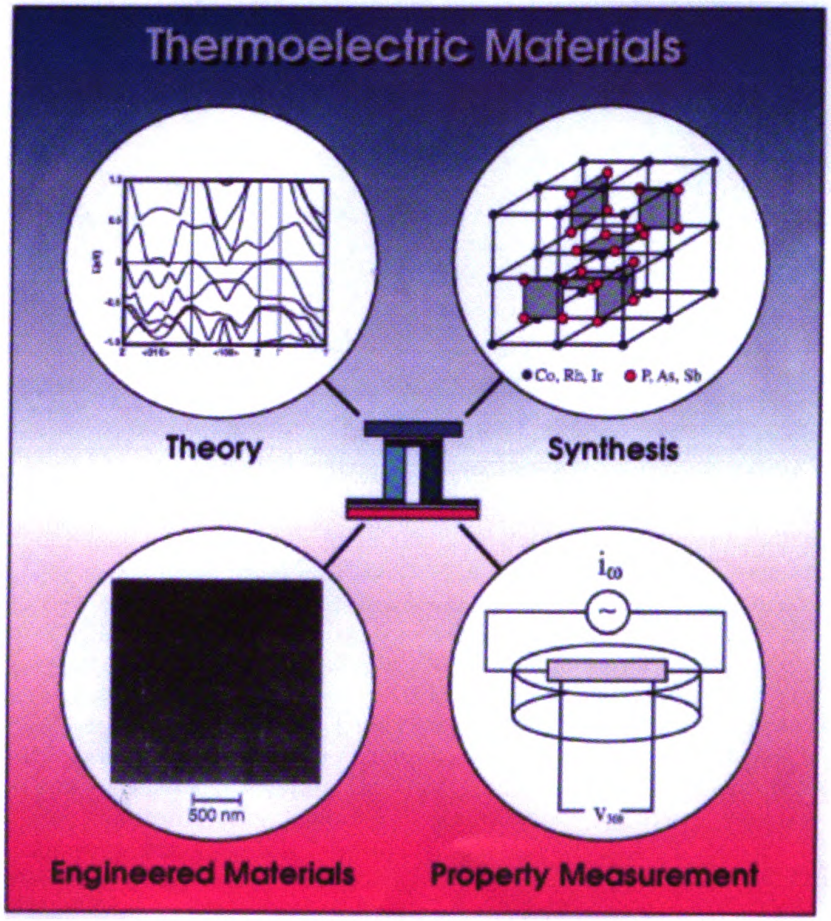

Thermoelectric Materials

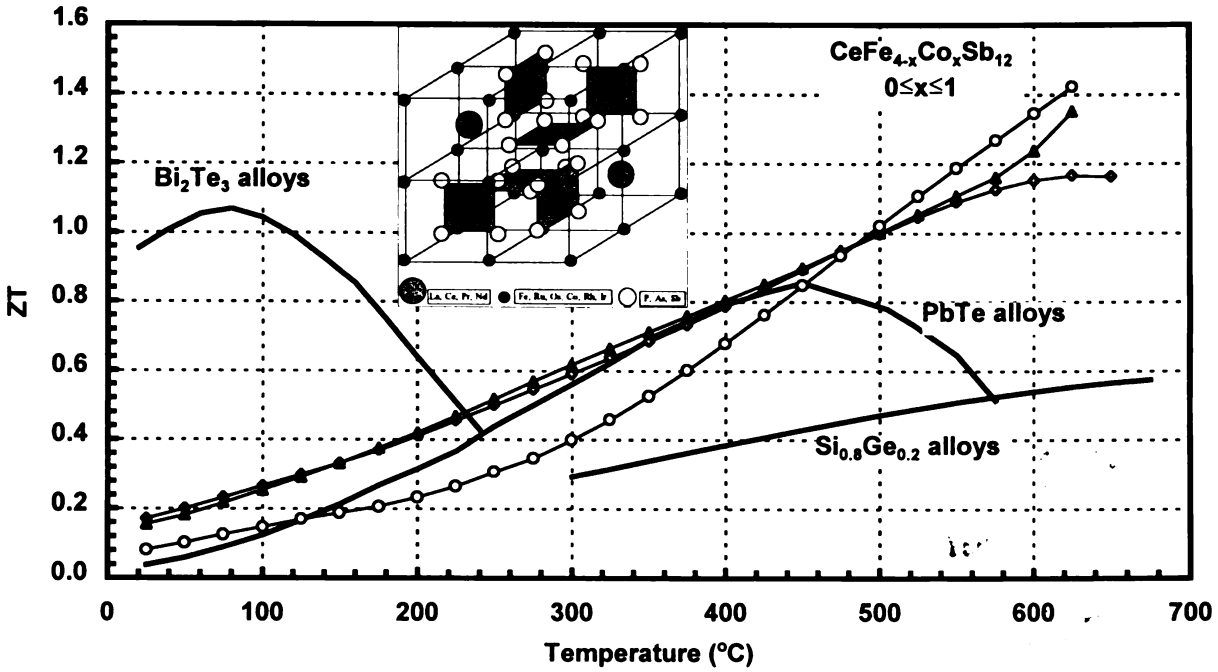

New thermoelectric materials with superior transport properties at high temperatures have been discovered. These materials are part of the large family of skutterudites, a class of compounds which have shown a good potential for thermoelectric applications. The composition of these novel materials, called filled skutterudites, can be represented by the formula LnT_4Pn_{12} (Ln = rare earth, Th; T = Fe, Ru, Os, Co, Rh, Ir; Pn = P, As, Sb). In these compounds, the empty octants of the skutterudite structure which are formed in the TPn_3 (~ T_4Pn_{12}) framework are filled with a rare earth element. Some of these compositions, based on $CeFe_4Sb_{12}$, have been prepared and have shown exceptional thermoelectric properties in the 350-700°C temperature range. At room temperature, $CeFe_4Sb_{12}$ behaves as a p-type semimetal, but with a low thermal conductivity and surprisingly large Seebeck coefficient. These results are consistent with some recent band structure calculations on these compounds. Replacing Fe with Co in $CeFe_4Sb_{12}$ and increasing the Co:Fe atomic ratio resulted in an increase in the Seebeck coefficient values. Measurements on bulk samples with a $CeFe_{3.5}Co_{0.5}Sb_{12}$ atomic composition and p-type conductivity resulted in dimensionless figure of merit ZT values of 1.4 at 600°C.

Naval Research Reviews

Office of Naval Research
Four/1996
Vol XLVIII

Articles

Departments

About the cover

The ability to produce a simple pn-junction-based thermoelectric device with enhanced performance (pictured in the center of the cover) is reliant upon fundamental chemistry and materials research of topics ranging from theory to property measurement. Each circle represent one of the key research elements necessary to achieve the goal of improved thermoelectric devices. The electronic band structure plot for $Cs_2BaCu_8Te_{10}$ is depicted in the theory circle and the synthesis circle contains the unit cell of promising new class of solid state thermoelectric materials known as skutterudites. The engineered materials circle depicts an SEM of a Si/Ge superlattice and the property measurement circle depicts a schematic of the 3 omega technique used to measure thermal conductivity in thin films.

Naval Research Reviews publishes articles about research conducted by the laboratories and contractors of the Office of Naval Research and describes important naval experimental activities. Manuscripts submitted for publication, correspondence concerning prospective articles, and changes of address, should be directed to Code 00PA, Office Naval Research, Arlington, VA 22217-5660. Requests for subscriptions should be directed to the Superintendent of Documents, U.S. Government Printing Office, Washington, DC 20403. *Naval Research Reviews* is published from appropriated funds by authority of the Office of Naval Research in accordance with Navy Publications and Printing Regulations. NAVSOP-35.

Thermoelectric Science and Technology - An Overview

John C. Pazik, Guest Editor
Office of Naval Research

Thermoelectric (TE) materials, and devices prepared from them, are of interest to the Navy for two basic reasons: 1) the devices can be used in reliable, quiet, solid state coolers and 2) the devices can be used for exhaust heat recovery and/or power conversion. Based on these two fundamental capabilities (cooling and power generation), thermoelectric materials can have broad impact on Navy warfighting capabilities including Forward Presence, Readiness, Support and Infrastructure, and Joint Strike. Exhaust heat recovery and power generation aspects of thermoelectric materials may ultimately lead to reduced fuel usage which "can minimize the logistic footprint without loss of capability" and "increase naval facilities' energy independence." Since TE devices used for cooling applications are solid state (no moving parts, lubricants, seals, etc) they also impact the area of "design-in reliability, maintainability, and availability." From an environmental perspective, the non-CFC based cooling offered by TE technology can positively impact the Navy's "capability to operate unimpeded by environmental issues" and provides a "substitute for hazardous materials and processes." Ultimately one can envision TE cooling devices which "allow strike assets to manage their signatures to delay detection and targeting from threat sensors." Specific cooling applications where TE technology is currently used in Navy systems (or envisioned for use) include ship-board air-conditioning, IR detection systems, cryogenic electronics (microprocessors, high temperature superconductors), and environmental suits. Thermoelectric power generation applications include exhaust heat recovery (gas-turbine engines, exhaust stacks, diesel engines) and silent auxiliary power sources (submarines, UUV). Commercial applications of TE technology are equally enormous and include cooling units for cellular base stations, high technology home refrigeration, increased fuel efficiency for trucks and automobiles, and recreational coolers.

Clearly there are other technologies available which can meet many of the cooling and power conversion needs of the Navy and private sector. So what exactly is it about thermoelectric technology that makes it so attractive for the various applications? The simple answer is that TE cooling and power generation devices are solid state. There are no moving parts, no refrigerants, no lubricants, and no seals. Quiet, non-emissive, vibrationless, and reliable operation are the key aspects of TE technology which set it apart from all the competing technologies. If TE technology is so great why isn't it everywhere? Quite simply, the efficiency of current systems is too low to be used in anything but the most demanding applications where the higher cost (i.e. low efficiency) is outweighed by the mission requirements. For example, TE has been the technology of choice for power generation on NASA deep space missions because of its inherent long term reliability and vibrationless operation.

The most critical issue for researchers in TE science and technology today is the development of new materials and devices with intrinsic properties much better than those currently in use today. It's helpful at this point to recall the basic thermoelectric effects. When any material is placed in a temperature gradient a potential will be produced which will depend on the magnitude of the temperature gradient and the physical properties of the material. Similarly, if a current is passed through the junction of two dissimilar materials, heat will either be liberated or absorbed at the junction depending on the direction of current flow and material properties. The magnitude of these "thermoelectric effects" determine the quality (figure of merit) of a given set of thermoelectric materials. A typical thermoelectric device on the market today is based on semiconductor materials which are n and p doped and connected in series (as depicted on the front cover of this issue). For a cooling application, one can conceptually imagine that electrons will gain or loose energy (depending on direction of current flow) to the surroundings as they move over the potential barrier at the p-n junction. The ultimate performance of a thermoelectric based system (cooling or power generation) is determined by the intrinsic materials figure of merit (FOM) defined in equation 1 where S is the Seebeck coefficient, σ is the electrical conductivity, and κ is the thermal conductivity, and T is the absolute temperature.

$$ZT = \frac{S^2 \sigma T}{\kappa} \qquad (1)$$

Equation 1 provides general guidance for the type of materials needed to maximize ZT and ultimately improve device performance. The Seebeck coefficient is a measure of the ability of a material to generate an EMF in a temperature gradient. The larger the EMF the material can generate for a given temperature gradient the better the material will be for TE technology. It is also desirable to maximize the electrical conductivity, σ, because a large σ will result in small internal heat loss (I^2R heating). Finally, one wishes to choose a material which has low thermal conductivity, κ, since this will minimize the equalization of the temperature gradient. One quickly sees that the relationship between the various material parameters is complex and must be considered when designing new materials. For example, κ has two components, an electrical and phonon contribution (equation 2) and the electrical component, κ_{el}, is related to σ via the Wiedemann-Franz Law.

$$\kappa = \kappa_{el} + \kappa_{ph} \qquad (2)$$

Essentially any increase in σ will result in an increase in κ (via κ_{el}) and thus the effective ZT will not be improved. Thus for a material whose electrical component is the major contribution to the thermal conductivity (i.e. a metal), strategies to improve ZT via improvements in electrical conductivity or reduction in thermal conductivity will not be fruitful.

Metals typically have low Seebeck coefficients (1-10 μV/K) and high electrical ($\geq 10^6$ ohm-cm^{-1}) and thermal conductivity (10-1000 W/m-K) giving a relatively low FOM, ~10^{-3}. Conversely, insulators have high Seebeck coefficients (1000 μV/K) and low thermal conductivities (.01 -1 W/m-K), however the electrical conductivity is extremely low ($\leq 10^{-8}$ ohm-cm^{-1}) resulting in ZT's around 10^{-10}. Semiconductors are currently the materials of choice. Seebeck coefficients range from 100-500 μV/K, electrical conductivity ranges from 10^3-10^4 ohm-cm^{-1}, and thermal conductivities between 1-100 W/m-K. The best, well understood, thermoelectric materials[1] are based on the Bi-Te-Se-Sb alloys and have FOM's of approximately 1.0. It is also important to recognize that the fundamental materials properties are temperature dependent. So a material may make an outstanding thermoelectric device over one range of temperatures but could and is likely to be useless over other temperature ranges. Si-Ge materials function optimally between 1100-1300K while Bi_2Te_3 based materials operate best between 200-500K.

A final word about measuring the performance of thermoelectric materials and devices. In addition to the intrinsic FOM, the TE device performance properties may be defined by a coefficient of performance (COP), equation 3 and 4

Cooling Equation:

$$COP = \frac{T_c}{T_h - T_c} \frac{(\sqrt{1+ZT}) - \frac{T_h}{T_c}}{(\sqrt{1+ZT}) + 1} \qquad (3)$$

Power Generation Equation:

$$COP = \frac{T_h - T_c}{T_h} \frac{(\sqrt{1+ZT}) - 1}{(\sqrt{1+ZT}) + \frac{T_c}{T_h}} \qquad (4)$$

where T_c is the temperature of the cold side and T_h is the temperature of the hot side. It is important to realize that ultimately one must consider the ΔT available for power generation or for the cooling requirement and that the actual device efficiency is dependent on this temperature differential. When ΔT is small, TE based cooling technologies become more competitive than traditional Rankine cycle systems for a given cooling application. It should also be pointed out that for ZT values ranging from 3-8, TE based cooling could compete head on with Rankine cycle cooling in almost every cooling application.

This issue of Naval Research Reviews provides an overview of the direction current thermoelectric research is taking. The five general articles represent the core of the ONR program in thermoelectric materials science and technology: theory, experiment and property measurement. The article by Singh and Reinecke (et. al.) describes the current theoretical approaches to designing better thermoelectric materials. It includes discussions of band structure calculations for complex inorganic materials and describes methods of improving ZT through quantum confinement. Venkatasubramanian has provided a report on experimental efforts currently underway to synthesize thin film TE structures and how the design of these structures could impact the FOM. Kanatzidis and DiSalvo provide an overview of current approaches in solid state chemistry for synthesizing bulk materials which may exhibit enhanced ZT. The focus of their discussion involves molten flux synthesis of multinary chalcogenides and an exploration of valence fluctuation compounds, metals with unusually large Seebeck coefficients. Slack and Fleurial describe an interesting class of compounds referred to as skutterudites[1]. These materials have large, complex unit cells and have properties which show promise as TE materials. Uher provides an overview of techniques currently being used to measure the properties of new thermoelectric materials. This is a critical area of research since accurate, reproducible measurements are critical to the identification of promising materials.

[1]Recent reports indicate that a new material of nominal composition, $CeFe_{4-x}Co_xSb_{12}$ ($0 \leq x \leq 1$), has a FOM of 1.4 (see inside front cover).

Theoretical Approaches for Understanding and Optimization of Thermoelectric Materials

D.J. Singh, T.L. Reinecke, W.E. Pickett and P.J. Lin-Chung, Naval Research Laboratory, Washington, D.C.

Introduction

Materials research has unearthed a plethora of interesting, useful and often unanticipated phenomena. Some more notable recent examples include the fullerenes, high temperature superconductivity, colossal magnetoresistance in manganites, the quantum hall effects, superhard magnetic materials, ductile ordered structural intermetallics and oscillatory couplings in magnetic multilayers. Discoveries have often come through serendipity or at least through a great deal of searching based on physical intuition and qualitative theoretical ideas. No doubt there are many materials with unanticipated but useful properties remaining to be found. However, the task of finding a material meeting a given set of specifications is often akin to finding the proverbial needle in a haystack. This article describes advances in theory and modeling that permit more systematic approaches and illustrates these as they are being applied to ONR supported research seeking better thermoelectrics (TE). Two aspects are highlighted: (1) The use of first principles calculations to understand materials properties and thereby point to possible improvements; and (2) The use of theory to understand nanostructural effects and to suggest novel quantum well structures for enhancing TE properties. These comprise the two main sections of this article.

Recent years have seen tremendous advances in our ability to fabricate and characterize a wide variety of tailor-made structures on nanometer (nm) length scales, using such techniques as molecular beam epitaxy, organo-metallic vapor phase epitaxy, lithography and etching as well as novel chemical processes. The properties of systems structured on these small length scales are often radically different from the bulk materials of which they are composed and depend on a wide range of changeable variables such as specific materials compositions and well widths.

Fabricating a sufficient variety of materials and structures using the Edisonian approach for testing can be time consuming and costly. It has been found in this field that

model calculations of the properties of these systems carried out in conjunction with experiment and fabrication are a powerful tool in predicting novel phenomena, in understanding observations and in guiding the fabrication of new materials and structures. The electronic states involved in these systems are often shallow states near band edges, and the length scales of interest typically are of the order of 10's of nanometers or more. Under these conditions the electronic properties can be described very well within generalized effective mass methods and transport within Boltzmann equation approaches.

Searching for improved materials by synthesizing and characterizing great numbers of different compositions and structures, guided by physical intuition and simple models, has lead to remarkable discoveries. However, recent advances in theory, both of the computational variety driven by new algorithms and data processing technology, as well in model calculations for structures of experimental interest, have provided alternate and more efficient strategies. These are iterative in nature and in the best developed cases consist of strongly interacting theoretical, computational and experimental efforts. Theory, both formal and computational, play several roles in these efforts. Besides suggesting promising candidate materials and structures, theory plays a key role in unraveling the properties of new materials, and the understanding thus gained provides important guidance in the subsequent optimization of the properties.

The work described here is aimed at developing improved thermoelectrics. TE materials are characterized by the TE figure of merit $Z = \sigma S^2/\kappa$, where σ is the electrical conductivity, S is the Seebeck coefficient (also called thermopower) and κ is the thermal conductivity. ZT (T is temperature) is a dimensionless quantity which slightly exceeds one at present in the best materials. Higher values of Z yield better TE performance. There is no known fundamental limit on Z; Carnot efficiency corresponds to infinite Z.

Understanding Materials from First Principles

Materials are fundamentally collections of electrons and atomic nuclei; the interactions are those of charged particles (Coulombic) and the dynamics are those of quantum mechanics. From this reductionist perspective, the underlying principles have been well understood since the early part of the 20th century. Nonetheless, most important discoveries in materials science were unanticipated and several have proven remarkably resistant to explanation from basic principles. Clearly, this perspective misses the tremendous complexity and richness of phenomena that is materials science. Substantial progress in understanding materials from first principles has only occurred in the last decade or so. The origin of the difficulties in bridging the microscopic physics and the real world lies in the quantum mechanical equations and the large number of particles. Although simple in form, these are 3N dimensional differential equations, where N is the (practically infinite in materials) number of particles; as a result the quantum mechanics is intractable in its most basic form.

The major breakthrough that allowed progress from first principles came in the mid 1960's from ONR sponsored basic research in quantum mechanics, and consisted of the development of density functional theory (DFT) by Hohenberg, Kohn and Sham [1] and especially practical computational schemes based on it. The DFT and particularly the local density approximation (LDA) to it, along with algorithmic developments and advances in computing technologies, have now made possible realistic studies of a wide variety of materials and properties. The DFT framework reduces the intractable problem of solving of a 3N dimensional differential equation to that of solving a set of N three dimensional equations, albeit coupled by a non-linear, density dependent potential. With modern computers and algorithms, representative samplings of these systems of equations can be solved on a routine basis, provided that the complexity of the material, as characterized by the unit cell size, is not too great.

Computational Approaches for Thermoelectrics

The performance of a thermoelectric material is characterized by the figure of merit, Z. The numerator of Z consists of electronic transport quantities; these depend on the band structure (the energies of allowed states as functions of their net crystal momentum) near the Fermi energy and the scattering mechanisms for the charge carriers. These terms depend strongly on the doping level with the result that obtaining high Z requires careful optimization of the doping level, and in fact even discerning whether or not a given semiconductor has TE potential requires exploration of the variation with doping. Knowledge of the band structure, which can be obtained reliably using modern electronic structure methods, permits the doping dependence to be calculated, thereby bypassing time consuming experimental searches.

The denominator, κ, is the sum of an electronic thermal conductivity (related to σ) and a lattice contribution, the latter normally dominating in semiconductors. Understanding κ requires an understanding of the lattice vibrations and the scattering processes affecting them.

The work discussed here is based on the Linearized Augmented Planewave Method [2], which is very general with regard to the materials that it can be applied to and is state-of-the-art as regards accuracy in solving the DFT equations. No adjustment of the DFT band gaps is made. DFT gaps, although smaller than experiment in certain semiconductor classes, agree well with experiment in well hybrid-

ized transition metal compounds, like skutterudites. Because these methods are essentially microscopic and derived from the underlying quantum mechanics and interactions, they do not depend on experimentally determined parameters. Rather, one may calculate properties of a material, starting from just the atomic numbers and usually the crystal structure. This first principles aspect is often crucial in understanding novel materials, as experiments are often unavailable, incomplete or subject to interpretation. The importance of such an approach is well illustrated by the electronic structures of the binary skutterudites, which have been under investigation as potential TE materials. Theory has led to a complete revision in the description of their TE properties.

Binary Skutterudites: New Excitement from Old Materials

The binary skutterudites, MX_3 (M = Co, Rh, Ir; X = P, As, Sb), although cubic in symmetry, have a rather complex crystal structure (Fig. 1) containing sixteen atoms per cell and large open voids. They have been known and generally characterized as rather conventional semiconductors with moderate band gaps [3], although Ackerman and Wold did observe a weak optical signal extending to low energy and questioned this characterization. Recently, these materials have come under investigation as a potential basis for improved thermoelectrics [4,5].

Slack and co-workers measured high carrier mobilities (i.e. high σ for a given doping level) and reasonably large values of the Seebeck coefficient in hole doped $IrSb_3$. However, the measured κ was more than an order of magnitude higher than the estimated minimum thermal conductivity (see the article by Slack in this issue), resulting in relatively low values of Z at room temperature. Furthermore, since TE is a bulk application, the use of Ir (an expensive precious metal) raises serious cost issues. Several questions were raised by these seminal studies: (1) What is the band structure and what does it imply for the variation of Z with doping level and temperature; specifically, is there a doping regime where this material has a high ZT? (2) What modifications can be made to reduce κ while maintaining electrical properties favorable for high ZT? (3) Can Ir be replaced by any less expensive elements without degrading TE performance?

The starting point for addressing these questions is the electronic band structure, which we calculated from first principles [6]. Accurate calculations for complex materials such as these were made possible by use of the supercomputers supported by the DoD high performance computing modernization program and algorithmic improvements in the LAPW method made with ONR support at NRL and elsewhere.

Figure 1.

Crystal structure of the binary skutterudites, MX_3. This body centered cubic structure may be viewed as consisting of interpenetrating simple cubic lattices, the first consisting of M atoms on each lattice site and the second consisting nearly square X_4 rings oriented with alternating x, y, z and empty sites. The filled skutterudite structure derives from filling these empty sites with a third element. First principles methods described in this article allow computation of electronic, vibrational and other properties from knowledge of the crystal structure.

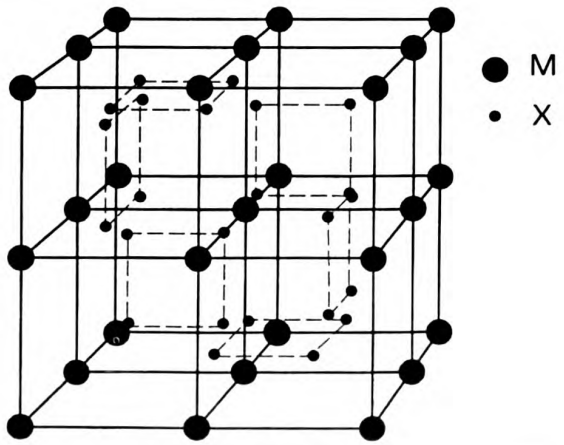

Figure 2.

Electronic band structure of $IrSb_3$ along representative direction in the Brillouin zone. The dashed horizontal line denotes the Fermi energy (E_F). Note the valence band dispersing upwards to the conduction band minimum at the Γ point. This is at odds with previous views of the material as a moderate band gap semiconductor.

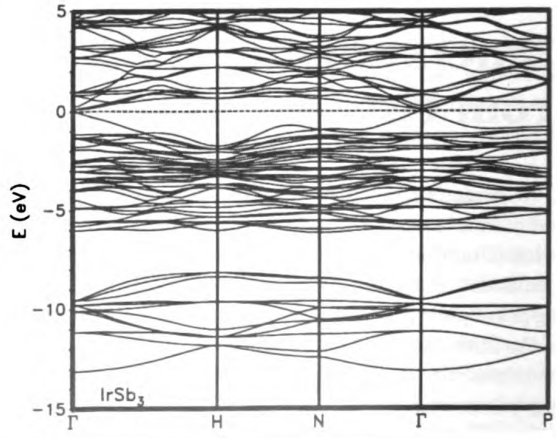

The band structure of $IrSb_3$ is shown in Fig. 2, and the corresponding electronic density of states (DOS) in Fig. 3. The apparent complexity of these plots results from the fact

Figure 3.

Electronic DOS of $IrSb_3$ and projections. E_F is denoted by the dashed vertical line. Note the low DOS in the gap-like region just below E_F.

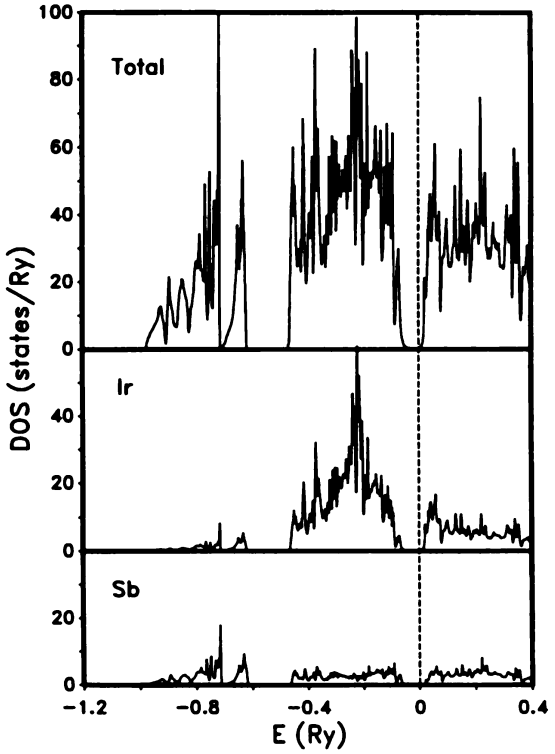

that the number of bands is roughly proportional to the number of atoms in the unit cell (2 for Silicon or GaAs; 16 for $IrSb_3$). There is a rather well defined pseudo-gap between manifolds of valence (occupied states below the Fermi energy, E_F) and conduction (unoccupied states above E_F) bands, and this is reflected in the DOS by very low values in the first 1.2 eV below E_F. This corresponds to the gap seen in optical experiments and assigned as the band gap.

However, the DOS in this region, although small, is not exactly zero, and this non zero DOS is critical to understanding the electrical transport (σ and S). Instead, there is a single band that crosses this pseudogap reaching the conduction band minimum at the Γ point. The reason why this was not previously established in experiments is that it is one dispersive band out of many, and therefore gives a very weak optical signal that is difficult to distinguish from artifacts e.g. due to defect states in imperfect samples. All reported measurements on $IrSb_3$ were on lightly hole doped material, which apparently forms most readily. In this case, E_F lies slightly below the nominal (undoped) position, and the electrical transport properties are determined almost entirely by the properties of this unanticipated band.

In ordinary semiconductors, the valence and conduction bands are parabolic in shape at least near E_F, so that the band is a smooth curve reaching (for valence bands) its maximum with zero slope. The transport properties are then understood in terms of the effective mass m^*, which gives the curvature, and a handful of other parameters, such as scattering times. Remarkably, the valence band in $IrSb_3$ does not fit this picture. Rather than being parabolic as in conventional band structures, it is linear almost exactly up to the band edge. For hole doping above about $n = 3x10^{16}$ cm^{-3} (TE materials typically have $n \sim 10^{19}$ cm^{-3}), E_F will occur in this linear regime with the implication that the electrical transport will scale differently than in conventional semiconductors. For example, S is predicted to vary as $n^{-1/3}$ instead of $n^{-2/3}$ and σ will vary approximately as $n^{2/3}$ instead of n. Our calculations show a very similar linearly dispersing band crossing the gap in $CoSb_3$; $CoAs_3$ also has a gap crossing state but its dispersion has the conventional parabolic shape. ($CoAs_3$ becomes interesting because it is predicted to be a member of the very small class of true gap-less semiconductors.) These predictions, which require a revision of the previous understanding of the materials, are in quantitative agreement with the Seebeck coefficients measured by Slack and have now been confirmed by additional experiments testing these scalings and carefully searching the gap region [7,8].

Besides the new semiconductor physics that this discovery opens up, there are important implications for TE: (1) Z in p-type $IrSb_3$ will depend only weakly on doping, so high Z will not arise in p-type $IrSb_3$ through optimization of n alone; (2) the linear dispersion yields large shifts in E_F for given n, so non-degenerate behavior and roughly linearly increasing S will persist to high T (favorable for high temperature TE applications); (3) the parabolic conduction bands have reasonably high effective masses (~ 0.5 m_e), so that if n-type mobilities are comparable to p-type values, the n-type material will have significantly higher ZT after optimization of n; and (4) highly covalent electronic band structures are found including notably strong bonding in the Sb_4 rings. The implication of this last point is that κ in $CoSb_3$ should not be much degraded relative to $IrSb_3$. Since the electronic properties are similar, the cheaper Co based materials may be good substitutes for Ir containing skutterudites.

Evaluation before Synthesis

These studies of the binary skutterudites indicated that modifications that would lower κ and/or improve the electrical properties are needed to make them into competitive room temperature TE materials. This suggests studies of n-type binary skutterudites, which may have improved electrical properties (numerator of Z), and the exploration of strategies for lowering the thermal conductivity (denominator of Z).

Slack and co-workers noted that κ of $IrSb_3$ is more than an order of magnitude higher than theoretical estimates of the minimum κ for skutterudite and that the structure contains large voids that should accept atoms. Based on this, he speculated that κ could be lowered considerably if weakly bound atoms could be inserted into these voids, where they might "rattle" about and scatter low energy phonons. He suggested the possibility of inserting heavy rare gas atoms, particularly Xe, by high pressure synthesis. This choice was motivated by the expectation that these inert atoms would not strongly scatter electrons, presumably leaving the electronic properties unchanged, and that being weakly bound they might be particularly good scatterers of low energy phonons. However, testing these conjectures experimentally is difficult because of the need to construct a high pressure apparatus, the high cost of Xe gas, and the potential need to explore a wide range of processing conditions. Accordingly, we used first principles calculations for the postulated compound, $XeIr_4Sb_{12}$ to explore some of these issues.

The calculated band structure of $XeIr_4Sb_{12}$ was found to be practically identical to that of the corresponding unfilled skutterudite, $IrSb_3$, with no discernable change near E_F. This lends strong support to one of Slack's conjectures, i.e. Xe will not scatter electrons so that the electronic properties will not be degraded relative to $IrSb_3$. Unfortunately, this is not the whole story.

The DFT computational framework directly gives the total binding energies of solids. These can be compared to obtain the relative stability of various structures, as well as to compute such properties as defect energies, diffusion barriers and phonon spectra. Calculations for $XeIr_4Sb_{12}$ indicate that the compound is energetically unfavorable relative to separated Xe and $IrSb_3$ by 5-10 Kcal/mole. This substantial energy, and the inertness of Xe, which makes chemical synthesis routes unlikely, suggests that $XeIr_4Sb_{12}$ will be exceedingly difficult to stabilize, if it can be done at all. Insertion of lighter (and smaller) rare gas atoms is more likely to be feasible.

Alternate Filled Skutterudites

Although it may be difficult to synthesize rare-gas filled skutterudites, the basic idea of filling the voids in the structure to obtain lower thermal conductivity may be sound, and in fact a number of filled skutterudite structure compounds are known to exist. These are derived from the binary skutterudites (e.g. $CoSb_3$) by replacing the transition metal by the element to the left in the periodic table, and inserting a di- or tri-valent cation forming e.g. $BaFe_4Sb_{12}$ or $LaFe_4Sb_{12}$. These compounds have lower valence electron counts than the binary skutterudites since replacement of the transition metal results in four fewer electrons (one for each of four atoms), and the cation insertion leads to the addition of two or three valence electrons. Compounds without the transition metal substitution would have higher electron counts, but these have not been successfully synthesized, a fact probably related to the tendency of binary skutterudites to form with p-type (lower electron count) dopings and the antibonding nature of the conduction band states.

Metallic conduction is generally unfavorable for TE applications because normal metals have Fermi energies lying in broad bands leading to very low Seebeck coefficients. (Note the exception of f-band valence fluctuation materials discussed in this volume by DiSalvo.) Unfortunately, almost all of these filled skutterudites are known to be metallic. $LaFe_4P_{12}$ is even a superconductor.

This metallic character has been rationalized by supposing that the band structures are substantially the same as in the binary skutterudites, but that the Fermi level is lowered corresponding to the reduced electron count. Within this so-called rigid band picture, dispersive bands will cross the Fermi level and the material will be metallic. However, there is no good reason for supposing that these materials follow rigid band behavior, and in fact there are some semiconducting filled skutterudites, notably UFe_4P_{12}, $CeFe_4As_{12}$ and $CeFe_4P_{12}$. $CeFe_4Sb_{12}$ has been reported as a possibly low carrier density metal, although it is unclear whether this is due to experimental difficulties in finding a very small gap in doped samples.

Semiconductivity in $CeFe_4X_{12}$ (X=P,As) has been rationalized in terms of the rigid band picture (above) by supposing that Ce is tetra-valent in these compounds, yielding the same electron count as CoX_3. However, the fact that the much larger trivalent La ion enters the same structure, with the implication that tri-valent Ce would fit as well, is at odds with this view.

We have used first principles calculations of the electronic structure to resolve this issue and to assess the TE potential of the Ce filled skutterudites. One immediate difficulty was that the crystal structures (normally an input to the calculations) of $CeFe_4As_{12}$ and $CeFe_4Sb_{12}$ were only partially known, and in particular the two parameters giving the pnictogen (P, As, Sb) positions in the unit cells had not been determined experimentally. At the same time, Morelli and Meisner [9] reported transport measurements on $CeFe_4Sb_{12}$, raising questions about its electronic structure and showing that it does indeed have a much lower thermal conductivity than $CoSb_3$ - a result that increases interest for potential TE application. As mentioned, one of the main quantities that density functional calculations provide is the total energy for any given structure. Accordingly, it is possible to determine structural parameters by performing calculations of the energy as a function of these coordinates, thereby determining the minimum energy configuration, which then corresponds to the actual crystal structure. A by-product of this mapping of the energy surface is its curvature about the minimum, which yields vibrational frequencies or phonons. This prescription was used to determine the pnictogen positions and the associated A_g Raman active phonon frequencies in

$CeFe_4As_{12}$ and $CeFe_4Sb_{12}$. A full set of phonon dispersions was calculated using this procedure combined with force constant models for the unfilled skutterudite $CoSb_3$ [10].

Our first principles calculations for $CeFe_4P_{12}$, $CeFe_4As_{12}$ and $CeFe_4Sb_{12}$ show that these materials have qualitatively similar electronic structures with smooth variation from the lighter to the heavier pnictogen compounds [11]. All three compounds are found to be semiconducting, albeit with small gaps of 0.34, 0.16 and 0.10 eV in the P, As and Sb compounds, respectively. The band structure for $CeFe_4As_{12}$ is shown in Fig. 4.

The topmost valence (occupied) bands consist of hybridized Fe 3d and pnictogen p states, while the lower valence bands are mainly dominated by pnictogen p character. On the other hand, the lowest conduction bands are comprised of nearly flat spin orbit split manifolds of Ce 4f states, and are apparently situated in a gap formed by the other bands. However, analysis of the wavefunctions reveals that this picture is only qualitative.

In fact, there is considerable Ce 4f character in bands below E_F. When integrated, this occupied 4f character amounts to one electron per Ce atom, i.e. tri-valent Ce at odds with the previous explanation of the semiconducting character as being due to tetra-valency of Ce. Rather, the band gaps in these compounds arise because of hybridization or mixing of Ce 4f states with the skutterudite Fe 3d - pnictogen p states. This hybridization, which is strongest in the phosphide and weakest in the antimonide, leads to an interesting combination of small band gaps (possibly overestimated for f-bands within the LDA), and large effective masses. This is in contrast to the low effective masses more commonly found in small band gap materials.

Figure 4.

Band structure of $CeFe_4As_{12}$. The dashed horizontal line denotes E_F.

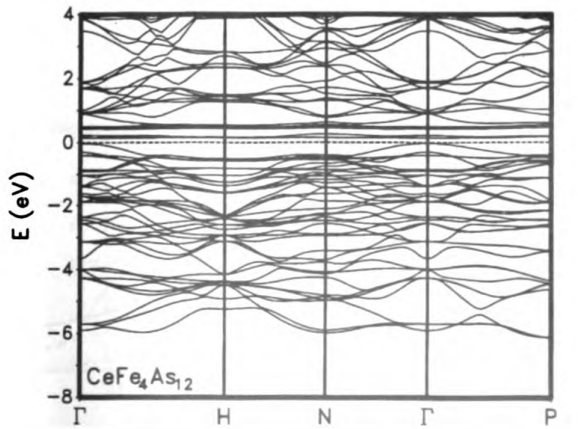

High band masses lead to high Seebeck coefficients for a given doping level, and as such are favorable for TE applications, provided other conditions are met as well. In particular, a low lattice thermal conductivity, κ_L is needed, along with reasonably high carrier mobilities (for high σ). High mobilities arise in materials with highly itinerant band states. In these materials, the hybridization, and itinerancy is strongest in $CeFe_4P_{12}$, and weakest in $CeFe_4Sb_{12}$. The arsenide is intermediate.

Morelli and Meisner have, as mentioned, shown that $CeFe_4Sb_{12}$ does indeed have very low values of κ. Calculated Raman phonon modes in $CeFe_4As_{12}$ are similar to those of $CeFe_4Sb_{12}$, but are shifted to about 50% higher frequency. Based on this and the highly covalent picture of the bonding that emerges from analysis of the calculated electronic structures, it seems likely that $CeFe_4As_{12}$ also has low κ, though probably not as low as the antimonide. The presence of light atoms in the phosphide and its considerably contracted lattice parameter, which would not favor soft Ce modes, imply that its thermal conductivity may be substantially higher. These considerations, and the calculated band structures, suggest that the arsenide and antimonide may be favorable TE materials. Experimental measurements of the transport properties of n- and p-type crystals will be needed to establish this.

Nanoscale Structures: High Performance Superlattices

Remarkable advances have been achieved in recent years in our ability to fabricate a wide variety of novel materials in the form of superlattices and other low dimensional and composite structures. Among the best known of these structures are quantum well superlattices, prepared in the form of multilayers. The existence of conduction and valence band offsets between adjacent material layers creates potential wells separated by potential barrier layers. The charge carriers in the quantum wells are confined to move perpendicular to the superlattice direction and thus give rise to two-dimensional conduction. Recent advances in growth and microfabrication techniques, as well as etching and lithography techniques, have also made it possible to obtain quasi-one-dimensional wire like superlattice structures of one material within another. Such wires have cross-sectional areas ranging from a few atoms to square micrometers or more.

The properties of these systems can be modified in controlled ways by a variety of changes in structure and materials. For example, the potential off-sets between different materials can give rise to the confinement of carriers in effectively two dimensional or in one dimensional subbands. In two dimensions the density of states is proportional

to the inverse of the well width, and in one dimension to the inverse square of the effective wire width. This can lead to greatly enhanced densities of states and transport properties. In addition, the thermal properties of these systems can be changed through changes in the phonon scattering at interfaces and due to disorder (Recall that decreases in the thermal conductivity lead to more desirable TE materials). For reasons such as these, superlattices and related composite systems are of considerable interest in the search for materials with improved thermoelectric properties.

An interesting proposal involving superlattice systems for TE applications was made recently by Hicks and Dresselhaus [12] who argued that the TE figure of merit of a material, for transport parallel to the quantum well planes, could be enhanced greatly in a quantum well superlattice geometry as a result of an effectively two-dimensional density of states for the electrons. They calculated ZT for model Bi_2Te_3 superlattices with varying well widths in which the potential barriers of the wells were taken to be infinite and the widths of the barriers were neglected, and they found that ZT increased monotonically with decreasing well width attaining values much greater than that for bulk Bi_2Te_3. They also argued that quantum wire superlattices would give further enhancements in the figure of merit [13].

The proposals of Hicks and Dresselhaus attracted considerable attention because of the possibility of obtaining greatly improved materials for thermoelectric applications from superlattices. However, because these authors did not consider the effects of the barrier layers, their calculations neglected two physical effects, which are essential to describe the figure of merit of realistic superlattice systems even at a qualitative level. The first of these effects is that thermal current flows through the barrier layers in addition to the well layers, thus producing a decreased ZT. Secondly, electron tunneling occurs through the barriers, and the resulting superlattice dispersion leads to a decreased density of states and correspondingly reduced ZT.

In order to evaluate realistic composite systems for thermoelectric applications, it is necessary to have a description of their thermoelectric transport properties. This should include realistic results for the dependencies of the transport properties on the parameters of the systems. Calculations of the thermopower [14] and of other properties have been reported over the years. Recently, several workers have provided a realistic description of the figure of merit for model superlattice systems [15-19].

Quantitative Calculations for Superlattice Thermoelectrics

Lin-Chung and Reinecke [15] included the effects of thermal currents in the barrier materials for quantum well superlattice systems, which have quasi-two dimensional electronic properties in the quantum well regions. They considered Bi_2Te_3/PbSnTe superlattices and derived the effective transport properties as functions of barrier and well widths. They found that the thermal currents in the barriers reduced the values of ZT at a given well width but that the composite superlattice systems nevertheless could have values of ZT considerably greater than for the bulk. In this work they did not allow carrier tunneling into the barrier regions. Mahan and Lyon [20] have also discussed the role of heat transfer in the barriers of superlattices.

Broido and Reinecke [16] included both the effect of carrier tunneling for finite potential barriers as well as the effect of thermal current flows in the barriers having finite widths in order to address these two issues in a unified way. A Bi_2Te_3 superlattice was considered in which a fixed potential offset V_0 was present at the boundaries between the wells and barriers. The electronic band structure was given by a Kronig-Penney description within the effective mass approximation, and the transport properties were treated within a constant relaxation time approximation to the Boltzmann equation using bulk relaxation times.

They took the superlattice axis to be in the direction of the c-axis of the hexagonal unit cell and the x-direction to be in the quantum well plane along the a-axis. For current transport along the quantum well perpendicular to the superlattice direction, Fig. 5 illustrates the calculated figure of merit of the superlattice, Z_ST, as a function of the superlattice period d for several different potential barrier heights. Fig. 6 shows Z_ST as a function of the quantum well width for several ratios of the barrier width to the well width. In these figures, ZT is shown scaled to the corresponding bulk value, which is calculated to be $Z_{3D}T=0.53$.

From these figures, it is seen that ZT has a maximum

Figure 5.

The figure of merit Z_ST of Bi_2Te_3 superlattice (scaled by $Z_{3D}T$) as a function of the superlattice period d for several potential barrier heights (b=a).

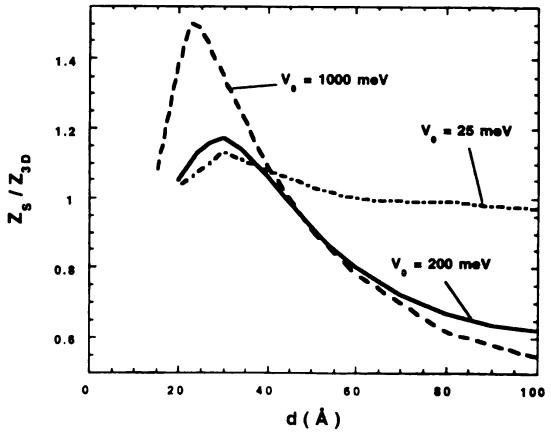

for decreasing well widths. This arises from the effects of carrier tunneling, which become greater at smaller well widths. For sufficiently small well widths the structure goes over into an effectively three dimensional system. From Fig. 5 one sees that the enhancement in ZT occurs as a result of the quantum confinement of carriers, which is greater for larger values of V_0. For larger V_0, the carrier dispersion along the superlattice direction is flatter and the effective density of states is enhanced by the confinement. It is seen that $Z_S T$ can be enhanced by some 50% over $Z_{3D} T$ for modest barrier heights of 1 eV. Barrier heights on this order can be obtained in semiconductor systems such as InAs/AlSb, as well as other composite systems involving wider band gap materials such as in systems having insulators for the barriers. From Fig. 6 it is seen that for a fixed V_0 the well width at which the maximum of ZT occurs depends on the barrier width. This well width dependence results from the combined effects of thermal currents through the barriers and carrier tunneling through the barriers. Recently, Sofo and Mahan [19] have made a similar treatment of thermoelectric transport in superlattice systems.

The effects of superlattice geometry on semi-metals having two carrier components (electrons and holes) such as Bi have also been considered [17,21]. A homogeneous system having one type of carrier component has a higher ZT than a corresponding two component system because the contributions of carriers with different charges tend to cancel in the thermoelectric power. The effects of the superlattice potential and of quantum confinement split the electron and hole energies into sub-bands; this can transform the material into an effective one-carrier system. For example, in superlattices such as the Bi/PbTe, the Bi may have a higher ZT than in its bulk, semi-metallic form. Such superlattice systems involving Bi have been studied [17] using the techniques developed earlier [16]. A substantial enhancement of ZT in the one component superlattice geometry over that of bulk Bi was found. It is particularly noteworthy that in this case the maximum of ZT occurs for relatively wide wells of the order of 60 - 80 Å.

Figure 6.

The figure of merit $Z_S T$ of Bi_2Te_3 superlattice (scaled by $Z_{3D} T$) as a function of the quantum well width a for several barrier widths b for a potential off-set of 200 meV.

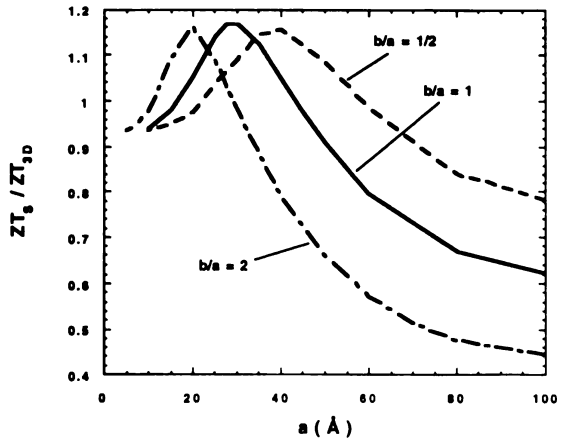

Exploration of Further Geometries

The thermoelectric properties of quantum wire superlattices have also been studied [18]. Quantum wire structures are now being fabricated in a number of ways, such as lithographic techniques, in situ growth of materials in glass arrays, and injection of materials into chemical templates. Quantum wire superlattices have been studied [18] using techniques similar to those used to study quantum well superlattices [16]. Results for ZT for a rectangular array of quantum wires of Bi_2Te_3 for transport along the wire direction as functions of potential off-set and quantum wire width are similar to those shown for quantum well superlattices shown in Figs. 5 and 6. It has been found that the degree of enhancement of ZT over that for the bulk is greater in the quantum wire superlattices than in the quantum well superlattices for a given potential offset above 1 eV. This is attributed to the effects of greater confinement in the quantum wire case [18].

Thermoelectric transport in superlattices along the superlattice direction has also been considered [22,23]. Recent preliminary measurements for GaAs/AlAs superlattices suggest that the thermal conductivity for transport in this direction can be reduced by as much as a factor of ten [24]. The physical origin of this reduction is not yet known in detail, but it most likely involves scattering due to disorder or interfaces. Calculations of ZT of superlattices involving Bi_2Te_3 for transport in this direction have been made for a Bi_2Te_3 superlattice with several values of the thermal conductivity, and it has been found that ZT is increased by more than a factor of two for decreases in the thermal conductivity of a factor of ten.

Tuning Properties for Performance in Composite Systems

Superlattice and other composite systems are attractive for thermoelectric applications because a wide variety of parameters can be varied to achieve desired properties. From the theoretical work to date on quantum well and quantum wire superlattices we are developing a basic knowledge of the thermoelectric transport properties of realistic systems.

In particular, it has been found that it is essential to include carrier tunneling through the barriers and thermal transport in the barriers to describe realistic systems. It has been found that a considerable enhancement of the figure of merit, ZT, over the corresponding bulk values can be achieved through carrier confinement in these systems. This theoretical work should stimulate advances in fabricating systems of interest as thermoelectric materials as well as further experimental work on them.

There are several important physical effects that need to be addressed in describing the thermoelectric transport properties of confined systems. It is known that the carrier relaxation rates in confined structures depend on the structure involved and have complex energy dependencies [25]. It is important to include these in describing thermoelectric transport in realistic systems. Another important aspect of the physics both of confined systems, and also of bulk systems, which is not yet fully understood is their thermal transport. The effects of disorder and interface scattering in these systems are expected to decrease thermal transport by phonons, and that should produce an improved thermoelectric figure of merit. Measurements of the thermal conductivity in AlAs/GaAs superlattices [26] indicate that it is less than either of the bulk values. A theoretical framework for understanding these effects on thermoelectric transport is needed. In particular, it will be necessary to know how the thermal transport in these systems depends on their materials and structure in order to predict how best to exploit them in producing better thermoelectric materials. In summary, the basis of a realistic theoretical treatment of thermoelectric transport in superlattice systems has been developed, but key physical issues still need to be investigated.

Outlook

Exploration of the huge parameter spaces required to find specific materials and structures that provide sought after properties remains one of the most daunting challenges in materials research. Nonetheless, there has been a great deal of progress, both on the experimental front, where new or greatly improved tools for controlled synthesis and characterization have been developed (e.g. molecular beam epitaxy for growing superlattices), and, as discussed in this article, on the theoretical and computational side. These advances are beginning to allow a new paradigm in which advances in materials research come from a strong synergism between theory, computation, characterization and synthesis efforts. As discussed in this article, theory has been used to advantage in understanding properties of skutterudite based materials and in understanding the TE properties of superlattice and composite systems. Ongoing efforts include the application of first principles methods to other novel materials with TE potential, such as the newly synthesized Cu-Te compounds discussed by Kanatzidis in this volume and detailed predictions of TE properties in novel nanostructured geometries in conjunction with experiment.

Acknowledgments

This work was supported by the Office of Naval Research. The authors are grateful for helpful interactions with D.A. Broido, J.L. Feldman, L. Nordstrom, H. Krakauer, G.A. Slack and D.T. Morelli. Computations were performed at the DoD computer centers at CEWES and NAVO as well as the Arctic Region Supercomputing Center.

The editor wishes to acknowledge Professor Gerald Mahon of the University of Tennessee for assistance in the review of the scientific and technical details reported in this article.

Biographies

Dr. David J. Singh received his B.Sc and Ph.D. degrees in Physics from the University of Ottawa in 1980 and 1985, respectively. He was a postdoctoral fellow at the College of William and Mary from 1985 to 1988, when he moved to the Complex Systems Theory Branch at NRL. He is an expert on applications of first principles methods in solid state physics and materials science. He is the author of a book on methodology for electronic structure calculations, in addition to approximately 125 refereed papers and chapters. Dr. Singh's current interests include new first principles algorithms and the use of density functional methods to understand complex materials.

Dr. Thomas L. Reinecke did his Ph.D. degree at Oxford University in 1972 as a Rhodes Scholar. He was a lecturer and research associate at Brown University from 1972 to 1974. He came to NRL in 1974 and has been head of the Theory Section of the Semiconductors Branch (1980-1990) and head of the Electronic and Optical Properties Section of the Electronic Materials Branch (1990 to present). He received the Sigma Xi Award for outstanding research in pure science in 1982, was elected fellow of the American Physical Society in 1982, received the Humbolt Prize in Physics in 1994 and has authored 150 papers. His interests have involved a wide range of condensed matter physics and currently concentrate on the electronic and optical properties of low dimensional semiconductor systems. He has been a visiting scientist at several institutions and at present is spending a year at the Max-Plank Institute in Stuttgart, Germany on the Humbolt Award.

Dr. Warren E. Pickett received his Ph.D. in theoretical solid state physics from State University of New York at Stony Brook in 1975. Since 1979 he has been a condensed matter

theorist at NRL, studying semiconductors, metals and superconductors, and indulging an avid interest in new materials with novel properties. He has spent sabbatical years at Daresbury Laboratory, England and Cambridge University, England. He received the Scientific Achievement Award from the Washington Academy of Sciences in 1985 and was elected a Fellow of the American Physical Society in 1989. At NRL he has been the recipient of the E.O. Hulburt Award and the Sigma Xi Technical Achievement Award. In 1992 he was named NRL senior scientist for Condensed Matter Theory. Dr. Pickett has authored 225 scientific publications.

Dr. Pay-June Lin-Chung received her bachelors degree in physics at the National Taiwan University in 1958 and masters and doctoral degrees in physics from the University of Pennsylvania, Institute of Metals (1961 and 1965). She did postdoctoral work at the University of Chicago and the Physics Department, University of California Berkeley. She taught at Northridge State University of California before joining NRL in 1967. She has been visiting scientist at Argonne National Laboratory, University of Durham and Cavendish Laboratory, University of Cambridge. Dr. Lin-Chung has authored 90 publications in condensed matter physics. Her research spans electronic band theory, fermi surface studies, defects and impurities, lattice dynamics, electron-phonon interactions, magnetism, optics and transport phenomena.

REFERENCES

1. P. Hohenberg and W. Kohn, *Inhomogeneous Electron Gas*, Phys. Rev. **136**, B864 (1964); W. Kohn and L.J. Sham, *Self-Consistent Equations Including Exchange and Correlation Effects*, Phys. Rev. **140**, A1133 (1965).
2. D.J. Singh, *Planewaves, Pseudopotentials and the LAPW Method* (Kluwer, Boston, 1994).
3. A. Kjekshus and T. Rakke, *Compounds with the Skutterudite Type Crystal Structure*, Acta Chem. Scand. A **28**, 99 (1974); J. Ackermann and A. Wold, *The preparation and characterization of the cobalt skutterudites CoP_3, $CoAs_3$ and $CoSb_3$*, J. Phys. Chem. Sol. **38**, 1013 (1977).
4. T. Caillat, A. Borshchevsky and J.P. Fleurial, *Proc. Eleventh Int. Conf. on Thermoelectrics* (University of Texas Press, Arlington, 1993).
5. G.A. Slack and V.G. Tsoukala, *Some properties of semiconducting $IrSb_3$*, J. Appl. Phys. **76**, 1665 (1994).
6. D.J. Singh and W.E. Pickett, *Skutterudite antimonides: Quasilinear bands and unusual transport*, Phys. Rev. B **50**, 11235 (1994).
7. D.T. Morelli *et al.*, *Low-temperature transport properties of p-type $CoSb_3$*, Phys. Rev. B **51**, 9622 (1995).
8. D. Mandrus *et al.*, *Electronic transport in lightly doped $CoSb_3$*, Phys. Rev. B **52**, 4926 (1995).
9. D.T. Morelli and G.P. Meisner, *Low temperature properties of the filled skutterudite $CeFe_4Sb_{12}$*, J. Appl. Phys. **77**, 3777 (1995).
10. J.L. Feldman and D.J. Singh, *Lattice dynamics of skutterudites: first principles and model calculations for $CoSb_3$*", Phys. Rev. B **53**, (in press, 1996).
11. L. Nordstrom and D.J. Singh, *Electronic Structure of Ce-filled skutterudites*, Phys. Rev. B **53**, 1103 (1996).
12. L.D. Hicks and M.S. Dresselhaus, *Effect of quantum-well structures on the thermoelectric figure of merit*, Phys. Rev. B **47**, 12727 (1993).
13. L.D. Hicks and M.S. Dresselhaus, *Thermoelectric figure of merit of a one-dimensional conductor*, Phys. Rev. B **47**, 16631 (1993).
14. L. Friedman, *Thermopower of superlattices as a probe of the density of states distribution*, J. Phys. C **17**, 3999 (1984).
15. P.J. Lin-Chung and T.L. Reinecke, *Thermoelectric figure of merit of composite superlattice systems*, Phys. Rev. B **51**, 13244 (1995).
16. D.A. Broido and T.L. Reinecke, *Effects of superlattice structure on the thermoelectric figure of merit*, Phys. Rev. B **51**, 13797 (1995).
17. D.A. Broido and T.L. Reinecke, *Comment on Use of quantum well superlattices to obtain high figure of merit from nonconventional materials*, Appl. Phys. Lett. **67**, 1170 (1995).
18. D.A. Broido and T.L. Reinecke, *Thermoelectric figure of merit of quantum wire superlattices*, Appl. Phys. Lett. **67**, 100 (1995).
19. J.O. Sofo and G.D. Mahan, *Thermoelectric figure of merit of superlattices*, Appl. Phys. Lett. **65**, 2690 (1994).
20. G.D. Mahan and H.B. Lyon, *Thermoelectric devices using semiconductor quantum wells*, J. Appl. Phys. **76**, 1899 (1994).
21. L.D. Hicks, T.C. Harman and M.S. Dresselhaus, *Use of quantum-well superlattices to obtain a high figure of merit from nonconventional thermoelectric materials*, Appl. Phys. Lett. **63**, 3230 (1993).
22. D.A. Broido and T.L. Reinecke (unpublished).
23. S.Y. Mensah and G.K. Kangah, *The thermoelectric effect in a semiconductor superlattice in a non-quantizing electric field*, J. Phys. Condens. Mater **4**, 919 (1994).
24. H. Maris (unpublished).
25. See for example, P.A. Knipp and T.L. Reinecke, *Electron-phonon scattering rates in quantum wires*, Phys. Rev. B **48**, 5700 (1993).
26. T. Yao, *Thermal properties of AlAs/GaAs superlattices*, Appl. Phys. Lett. **51**, 1798 (1987).

Thermoelectric Materials: Solid State Synthesis

Mercouri G. Kanatzidis, Department of Chemistry, Michigan State University and
Francis J. DiSalvo, Department of Chemistry, Cornell University

Introduction

It is remarkable that during the last 35 years the efficiency of the best thermoelectric materials has not improved to any significant extent. This is despite spectacular advances in some areas of materials research and technology in that period: semiconductor devices, advanced ceramics, superconductors, superalloys, laser, optical and non-linear optical materials, photovoltaics and composites, to name but a few. The efficiency of thermoelectric coolers operating near room temperature is only about 10% of Carnot efficiency; yet the thermodynamics of thermoelectric cooling suggest that achieving close to 100% of Carnot efficiency may be possible. To put that in context, modern freon-based home refrigerators operate at 30 to 35% of Carnot efficiency and large building air conditioning units at over 80%.

An efficient thermoelectric device is fabricated from two materials, one n-type and the other a p-type conductor. Each material is separately chosen to optimize the figure of merit, z, where $z = S^2\sigma/\kappa$; S is the thermopower, σ the electrical conductivity, and κ the thermal conductivity (1). All three of these materials properties are determined by the details of the electronic structure and scattering of charge carriers (electrons or holes) and thus are not independently controllable parameters. κ also has a contribution from lattice vibrations, κ_{ph}, the phonon thermal conductivity. Thus $\kappa = \kappa_{el} + \kappa_{ph}$, where κ_{el} is the carrier thermal conductivity.

In order to carry a heat flux of reasonable magnitude, moderate to high carrier densities are needed (small band gap semiconductors with carrier densities of 10^{18}/cm^3 to metals at 10^{23}/cm^3). In this range of carrier densities, κ_{el} usually is much larger than κ_{ph}. In that case, the ratio κ/σ is given approximately by the Wiedemann-Franz law, $\kappa/\sigma = L_oT$, where L_o has the value 2.45×10^{-8} watt-Ohm/K^2 (2). Indeed in the best thermoelectric materials currently known, Bi_2Te_3 and PbTe, the Wiedemann-Franz law is almost exactly obeyed in the range of temperatures of optimal device performance. For the Bi_2Te_3 material used in commercial devices (3), the value of zT at room temperature is about 0.9 (T is the absolute temperature; z always appears in combination with T in engineering calculations.). As zT increases, the cooling efficiency increases, a little less than linearly in this range of zT.

Thus improving device performance means improving $zT = S^2/L_o$, or increasing S while keeping moderate to large carrier densities of one carrier type. Since the

thermopower of optimally n or p doped Bi_2Te_3 is on the order of ± 220 μV/K (3), significant improvements in thermoelectric cooling efficiencies - to 20 or 30% - could occur if materials of reasonable carrier density with thermopowers of 300 to 350 μV/K can be found.

In this article we focus on the efforts to synthesize bulk materials with figures of merit two to four times higher than those attainable with Bi_2Te_3. There are two basic approaches: the synthesis of new, structurally and/or compositionally complex, materials and the exploitation of new phenomena in solids that produce high thermopowers. Both approaches rely on advanced synthetic capabilities, on the now routine capability to determine complex crystal structures (very difficult and extremely time consuming 35 years ago - computers have made it all possible), and on automated measurement of electrical and thermal properties.

Along with chemical and structural complexity usually comes the degrees of freedom to produce and control more complex electronic structures. This is certainly evident in the field of high temperature superconductors, where the structures and six or more element compositions of the materials are well adapted to chemical control and modification of the properties. Boltzmann transport theory describes both electrical and thermal transport in the vast majority of solids (4). This theory provides a general understanding of the thermopower that is expressed in the following equation:

$$S = \pi^2 k_B^2 T/3e[d(\ln\sigma(E)/dE] \text{ at } E = E_F$$

$\sigma(E)$ is the electrical conductivity determined as a function of band filling or Fermi energy, E_F. If the electronic scattering is independent of energy, then $\sigma(E)$ is just proportional to the density of states at E. In the general case S is a measure of the difference in $\sigma(E)$ above and below the the Fermi surface - specifically through the logarithmic derivative of σ with E.

Since the thermopower of a material is a measure of the asymmetry in electronic structure and scattering rates near the Fermi level, we desire to produce complexities in either or both in a small energy interval (a few kT) near E_F. While simple materials usually have simple band structures, in a few materials interactions between conduction electrons or interactions of conduction electrons with local magnetic spins lead to sharp features in the electronic excitations near the Fermi level that sometimes produce high thermopowers.

Here, then, we discuss these two approaches to new thermoelectric materials, exploring complex materials and investigating relevant electron interaction phenomena, by choosing examples from our current research.

Synthetic Methodologies

a. Complex Materials from the alkali-metal polychalcogenide flux method

Structural and compositional complexity can result in corresponding complexities in the electronic structure. Such complexities may produce the required asymmetry in $\sigma(E)$ to obtain large thermopowers. The phonon contribution to the thermal conductivity can also be lowered by such structural complexity as well as by choosing heavy elements as components of the material and by choosing combinations of elements that normally make moderate to weak chemical bonds. These latter two factors lower the Debye temperature and thereby decrease the thermal conductivity. This is just what happens in Bi_2Te_3 and PbTe. In general, these latter conditions will be met by compounds of main group elements beyond the third period. Since the known materials that are used in thermoelectric devices are chalcogenide compounds (the chalcogenides are sulfur, selenium and tellurium), we are searching for more complex semiconducting compounds of this type.

Since many chalcogenides - especially those that are complex - decompose at relatively low temperature (perhaps 500 to 1000 °C), a low temperature synthesis method is needed. We have been exploiting polychalcogenide fluxes for exactly these purposes.

The use of molten salts as solvents for reaction and crystal growth of solid state materials has expanded in the last few decades to a highly versatile synthetic method. Such media have been employed for well over 100 years for high temperature single crystal growth but only recently for new materials synthesis (5). Although many salts melt at high temperatures (≥ 700 °C), eutectic combinations of binary salts and salts of polyatomic species often have melting points well below the temperatures of classical solid state syntheses, making possible their use in the exploration of new chemistry at intermediate temperatures. In some cases, such salts act not only as solvents, but also as reactants, providing species which can be incorporated into the final product.

a.1. Flux Choice

One class of low melting salts that are especially intriguing is the alkali-metal polychalcogenides, A_2Q_x (A=alkali metal, Q=chalcogenide). Both the solids of these compositions and the melts contain Q_x^{-2} anions, in which x Q atoms form a covalently bonded one dimensional chain. As solvents for intermediate temperature reactions, A_2Q_x salts are especially well suited because the melting points range

between the extremes of K_2S at about 850 °C to K_2S_4 at 145 °C, with the majority of compositions melting at <300 °C. Although few detailed phase diagram studies of the other congeners have been performed, the melting points of many polychalcogenide salts are lower than 550 ° C. The minimum melting points are higher for the heavier chalcogenides, being about 250 °C for the polyselenides and 350 °C for the polytellurides. Low melting, A_2Q_x fluxes remain nonvolatile over a wide temperature range, and so once above the melting point, reaction temperatures can be varied considerably without concern for solvent loss.

Reactions between metals and molten A_2Q_x are performed *in situ*. The powdered reagents (polychalcogenide and metal or metal chalcogenide) are mixed under inert atmosphere and loaded into reaction vessels of either pyrex or quartz. Once evacuated, the tubes are flame sealed and subjected to the desired heating program in a computer controlled furnace.

The polychalcogenide salts can be made by reacting stoichiometric amounts of elemental chalcogenide with alkali metal in liquid NH_3 at -70 °C. To synthesize new compounds, one or more metals are added directly to the A_2Q_x/Q reaction mixture and heated in a sealed pyrex or quartz container. Crystalline products either precipitate from the melt or form on slow cooling of the melt, depending on the specific stoichiometric and processing conditions.

Polychalcogenide fluxes are highly reactive towards metals because they are very strong oxidants. This phenomenon arises from the fact that, although the terminal atoms of the $(Q_x)^{2-}$ chains have a formal oxidation state of 1-, the internal atoms are all zero valent and thus are good oxidizing agents. Metals are drawn into solution by being oxidized by the internal atoms of the $(Q_x)^{2-}$ chains, which, upon being reduced, split into smaller fragments. The solvated metal cations are then coordinated by the basic terminal atoms of the $(Q_x)^{2-}$ ligands, forming some manner of soluble intermediate, which is followed by nucleation into solid crystals. Presumably, the nucleated species are in equilibrium with the soluble intermediates, especially if the flux is present in excess, and hence a solvation/reprecipitation effect (often referred to as the mineralizer effect) occurs. This aids in the growth of high quality single crystals because the flux can redissolve small or poorly formed crystallites and then reprecipitate the species onto larger, well-formed crystals.

At this stage of development of this method, each ternary metal explored must be treated as a new and unique system, and similarities to the reactivity of other metals can only be drawn afterwards. Of course, the complexity of the resulting compounds may be further increased by adding several metals at once to the melt to produce quaternary, quintenary, etc. phases.

a.2. Novel Bismuth Chalcogenides

Despite the empirical guidelines we have, it is still challenging to choose the particular system for exploration. The fact that Bi_2Te_3 is the best material known to date suggests that it combines many of the necessary features for high figure of merit. If there is something special about bismuth in giving rise to simultaneously high electrical conductivity and thermoelectric power, it should be manifested in other compounds of bismuth as well. This suggests a research direction where we could explore other, more complex, chalcogenides of bismuth in the hope that some (or all) of the key properties would be superior to those of Bi_2Te_3. Further, structurally and compositionally more complex bismuth chalcogenides would, most likely, have a low lattice thermal conductivity. This is because a structure with a large unit cell is expected for complex materials, which would decrease the acoustic phonon mode velocities that are responsible for the transfer of heat in materials. The relatively weak Bi-Te bonding and the large atomic masses contribute as well to the low phonon velocities. Therefore, exploratory synthesis in this region of the periodic table becomes a reasonable activity and, as the preliminary results show, quite promising.

We have obtained many interesting new bismuth containing phases by reacting the metal with alkali metal chalcogenide salts in polychalcogenide melts. One such phase is the orthorhombic $BaBiTe_3$, which was prepared at 600 °C from a K_2Te_5 flux in which a mixture of Bi and BaTe were dissolved (6). The structure of this material is two-dimensional with $[BiTe_3]^{2-}$ layers alternating with Ba cations (Figure 1). Many interesting features exist in the structure, one of which is the presence of Te-Te bonds between Te atoms arranged in ribbons. The flat Te ribbons contain zig-zag Te chains and they are alternating between Bi-Te blocks, which look like they have been excised out of a rock-salt structure.

Figure 1.

The layered structure of $BaBiTe_3$. The two distinct sections of the lattice are shown.

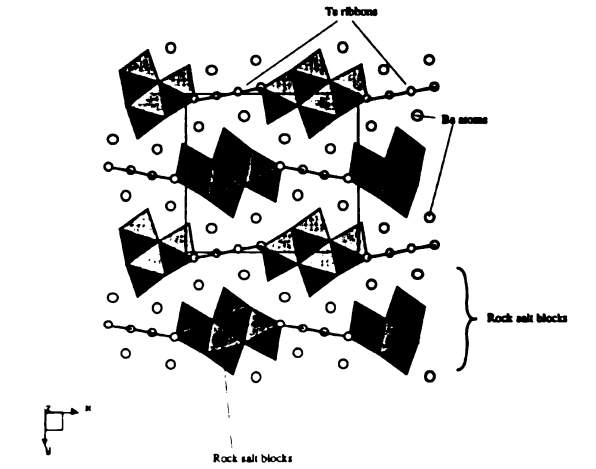

Figure 2.

Structure of $KBi_{6.33}S_{10}$. The parts of the structure related to Bi_2Te_3 and CdI_2 structures are shown.

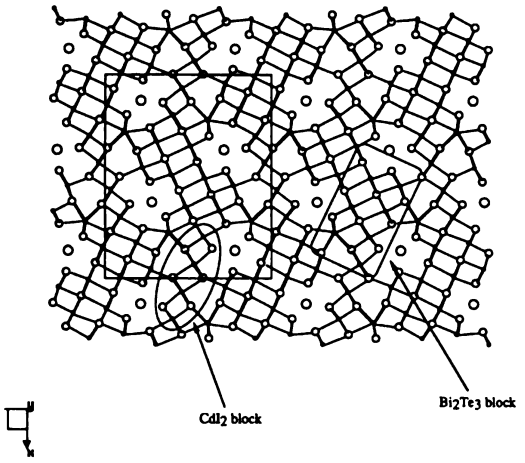

$BaBiTe_3$ is a semiconductor with a narrow band-gap of 0.35 eV and quite promising electrical properties. The electrical conductivity is reasonably high at ~100 S/cm and the thermoelectric power reaches +220 μV/K at room temperature. Therefore, the compound is p-doped. The thermal conductivity, which is crucial in assessing the compound's potential, is only 65-70% that of the rhombohedral Bi_2Te_3. The thermal conductivity is suppressed because of the low symmetry and because unit cell is much larger than that of Bi_2Te_3. The compound also contains additional soft phonon modes from the Ba—Te interactions. The latter are absent in Bi_2Te_3. This result suggests that generally ternary or quaternary compounds may possess lower thermal conductivity than the corresponding binary compounds. In order to fully assess the potential of this material for cooling devices, controlled n and p doping to moderately high levels must be achieved.

Two other interesting phases discovered recently are the sulfides $KBi_{6.33}S_{10}$ and $K_2Bi_8S_{13}$ (7). They belong to the general family of compounds $(A_2Q)_n(Bi_2Q_3)_m$ (A=alkali metal; Q=S, Se) with n=1 and m=6.33, 4, respectively. In an architectural context, both compounds can be thought of as an intimate composite of two different structure types interconnected to form a 3-D network. They have three-dimensional orthorhombic structures made up of Bi_2Te_3-type (NaCl-type) blocks and CdI_2-type fragments that connect to form tunnels filled with eight-coordinate K^+ cations. This may be beneficial to the electronic properties of the compounds which may bear similarities to those of Bi_2Te_3. The lower symmetry they possess may result in low thermal conductivity and could give rise to a superior thermoelectric material. The $[Bi_{6.33}S_{10}]^-$ framework is made of edge-sharing BiS_6 octahedra, as shown in Figure 2. The structure of $K_2Bi_8S_{13}$ is similar but the Bi_2Te_3-type (NaCl-type) blocks and CdI_2-type fragments are arranged differently.

These ternary bismuth sulfides have promising electrical properties with maximum conductivity and thermopower of 200 S/cm and ~90μV/K, respectively. These are unoptimized values, and we believe they can be greatly improved by further processing. Using the measured values of the electrical resistivity in conjunction with the Wiedemann-Franz law, we estimate the maximum possible value of the electronic thermal conductivity contribution to be below 1% of the total thermal conductivity. Thus, essentially all heat in these compounds is carried by lattice phonons. The pleasant surprise in these compounds comes from the rather low thermal conductivity they possess, as found especially in the sulfide $KBi_{6.33}S_{10}$. Taking as a bench mark the room temperature value of the total thermal conductivity of Bi_2Te_3 (κ = 1.7 W/m-K), we note that the total thermal conductivity of $KBi_{6.33}S_{10}$ (8) is actually lower (Figure 3). Hence, at least from the perspective of thermal transport, these compounds satisfy one of the key requirements for a useful thermoelectric material, they possess low lattice thermal conductivity. This is an important finding because $KBi_{6.33}S_{10}$, being a sulfide, is expected to possess higher thermal conductivity compared to the heavier tellurides. If controlled doping can enhance the electrical conductivity and at the same time preserve or even increase the thermopower, in the case of $KBi_{6.33}S_{10}$ we indeed might have a promising thermoelectric material. To achieve this, we need additional information regarding the transport properties including carrier concentrations and mobilities. This work is currently underway (8). Both $KBi_{6.33}S_{10}$ and $K_2Bi_8S_{13}$ melt with no

Figure 3.

The thermal conductivity of polycrystalline cylindrical samples of $KBi_{6.33}S_{10}$ (open squares)and $K_2Bi_8S_{13}$ (open circles) as a function of temperature. The arrow indicates the room temperature value of the lattice thermal conductivity of Bi_2Te_3.

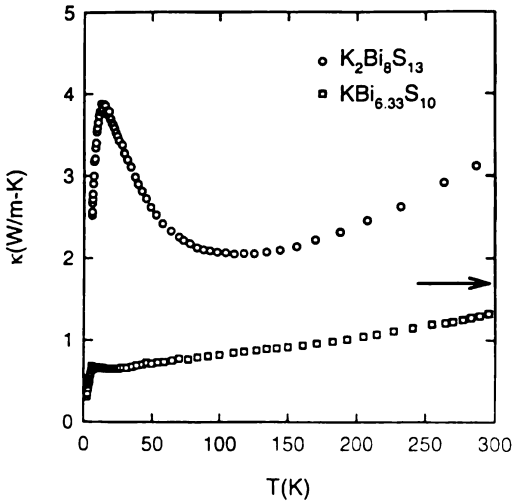

decomposition at 710 °C and 713 °C, suggesting they will be amenable to thermoelectric element fabrication and processing similar to that currently used in Bi_2Te_3 technology.

While we expect to find many new bismuth chalcogenide compounds by this method, it is not necessary to limit the search to bismuth. Other heavy main group metals may also lead to high thermopower materials. The synthetic search is well underway; although much remains to be done.

b. Electron Interactions: Intermediate Valence in Rare Earth Intermetallic Compounds

Many new phenomena have been discovered in solids since the early 60's. Of particular interest is the unusual behavior of rare earth atoms in some intermetallic compounds, since this behavior can include very high thermopowers relative to other metallic systems.

Normally, the f electrons of rare earth atoms are well shielded from bonding interactions by the s and d valence electrons. The f state of rare earth atoms in compounds is only weakly perturbed from that found in free rare earth atoms or ions. In some materials, the f electrons of the rare earth elements Ce, Sm, Eu, Tm and Yb interact with the conduction electrons to produce a variety of electronic states (9): Heavy Fermions, Kondo Insulators, Kondo Lattices, and Intermediate Valence (IV). In the IV state the occupancy of the f state appears to be non-integral. While the details of the unusual states that result from this conduction electron - f state interaction are still being examined by experimentalists and theorists, it is experimentally apparent that these IV compounds have very unusual electronic transport properties, including large thermopowers.

$CePd_3$ is a metallic conductor and is the prototypical IV material with a large thermopower. $YbAl_3$ (10) another IV material has a thermopower of opposite sign to that of $CePd_3$ ($YbAl_3$ is n-type while $CePd_3$ is p-type). Thus IV materials exist with both types of carriers, a necessary condition to obtain devices with the highest cooling efficiencies. The thermopowers of these IV materials are higher than for any other kind of metallic system. Note also that the thermopower of both $CePd_3$ and $YbAl_3$ is rather insensitive to temperature above 100 K, in contrast to that of metals or of Bi_2Te_3 (11) where $S\alpha T$. Since these IV compounds are metallic, we expect that the ratio κ/σ will be near the Wiedemann-Franz limit. In $CePd_3$ this ratio is quite sample dependent, probably due to slight differences in stoichiometry or to the presence of anti-site and other defects. Nevertheless, the ratio we measure is about a factor of two larger than expected.

The IV state produces considerable changes in the electronic and magnetic properties of the material. In most intermetallic compounds the valence electron configuration of Ce is the same as in a free Ce atom: $4f^15d^16s^2$. The one f electron produces a magnetic moment of 2.54 μ_B (Bohr magnetons) per Ce atom, while the remaining s and d states become delocalized as part of the electronic band structure. Consequently, most intermetallic Ce compounds are paramagnetic with a moment that is also typical of Ce^{+3} ions in an ionic solid (a $4f^1$ electron configuration for the single remaining valence electron). Thus, even in intermetallic compounds, when the normal 2.54 μ_B moment is observed, the Ce atom is referred to as trivalent. In a few Ce compounds the f moment disappears, probably because of a change in the Ce valence electron configuration to $5d^26s^2$. While such a change in configuration costs energy, increased overlap of the d orbitals with conduction band states may result, lowering the electronic energy sufficiently to make up for the initial cost of the configuration change. When Ce has no moment in such intermetallic phases, it is called tetravalent, since the moment is also lost in ionic Ce^{+4} compounds, where no valence electrons remain.

This latter view of tetravalent Ce is not the only way that tetravalent-like behavior can be observed. In some Ce intermetallics and below a certain temperature, called the Kondo temperature, the conduction electrons interact with the Ce so as to screen the Ce moment. In compounds where no moment is observed, it may be that the Kondo temperature is well above room temperature. In typical trivalent Ce compounds the Kondo temperature is low or zero.

The IV state is intermediate between typical trivalent and tetravalent states. In the IV state the magnetic moment is reduced below 2.54 μ_B, and is often temperature dependent. The IV compounds have room temperature susceptibilities only half that expected for Ce with the full f^1 moment, and most of the temperature dependence is lost. At low temperatures, current theories would suggest that the Ce magnetic moment is effectively cancelled (screened) by the conduction electrons through a Kondo resonance. The IV state is also signaled by changes in all other properties, such as electrical conductivity, thermopower and Ce to near-neighbor bond lengths. In some cases, before measuring thermopower, it is easier to look at other properties to see if the IV state is present, and if not, different properties may not need to be measured.

That is the good news. Now for the challenges. The IV state is rather rare. It has been identified in a few dozen intermetallic compounds out of perhaps 3 or 4 thousand compounds containing one of the five rare earths named above. The IV state is also rather sensitive to chemical perturbations. For example, non-stoichiometry or chemical substitution for either Ce or Pd in $CePd_3$, cause large changes in the physical properties and supress the IV state (see for example refs. 12 and 13).

Given these facts about the known IV materials, many questions remain, such as: Can we find other IV compounds? What is the highest thermopower we can obtain from such a material? Can we optimize the figure of merit by chemical

doping and other crystal-chemical techniques in IV materials - without destroying the IV state? Since intermetallic compounds tend to be brittle, can we find ways to make the IV materials less so?

In order to explore the potential of IV materials to be used in higher efficiency thermoelectric devices, it is clear from the above questions that the synthesis of new and modified materials must play a major role. Here, we focus on our synthetic techniques and recent results to illustrate how such materials are synthesized, and we show some of their crystallographic or physical properties.

Intermetallic compounds are usually prepared from the metallic elements by melting at high temperatures (from 1000 to 2500 °C). We typically use an arc furnace, in which an electric arc is used to melt the reactants on a water cooled copper hearth and the product is rapidly cooled when the arc is turned off. With sufficient care the inclusion of Cu in the product can be avoided. In other cases, where more control of the reaction temperature is needed, an RF furnace is used. An RF furnace couples an RF field generated in a cylindrical coil to an electrically conducting susceptor (usually made from Ta or Mo) inside the coil. The susceptor is also the sample container, if the susceptor is non-reactive with the sample under the preparation conditions. Otherwise the sample is put in some other non-reactive container inside the susceptor. Particular cases may require a modified approach. For example, Yb has a high vapor pressure at its melting point, so its compounds are best synthesized in a sealed container. Mo crucibles that are welded shut and then heated in the RF furnace are suitable as both container and susceptor in that case.

Depending upon the reactant composition chosen, the molten product will freeze either into a single intermetallic compound (a congruently melting solid) or the melt will freeze into a mixture of solid phases. In most cases annealing at modest temperatures (700 to 1000 °C) is needed to produce a well-ordered crystalline product and/or the equilibrium phases that result from that starting composition. When searching for new phases, the compound stoichiometry is generally not known, but often is in the ratio of small integers. By making samples of different starting compositions and comparing powder X-ray diffraction patterns, we can identify the compositions at which a single homogeneous phase exists. In many cases the structure of the phases produced can be identified by powder diffraction. In other cases single crystals are needed so that the structure (and thus the composition) can be determined by single crystal X-ray diffraction methods. By heating a homogeneous material at temperatures just below the point at which some melting occurs, or just below where decomposition occurs, small crystals often grow within a polycrystalline mass by grain coarsening, and the crystals may be separated by lightly crushing the sample.

Our synthetic program currently has two foci: finding new ternary or quaternary rare earth compounds that are IV and modifying known IV materials. We next discuss examples of each to give a a better sense of the synthetic challenges and the spectrum of materials that we are synthesizing.

b.1. New Ce Intermetallic Compounds

$CePd_3$ and $CeSn_3$ are both IV materials. What happens if all three elements are included in a ternary compound? Will more IV materials be produced? Will mixing the non-rare earth elements, especially in an ordered fashion, produce larger thermopowers? These kinds of questions lead us to the study of the Ce-Pd-Sn phase diagram. The phase diagram, when completely explored, indicates the stoichiometry and structure of the compounds that exist and often indicates other information such as melting points, etc. All the binary compounds of Ce-Pd and Ce-Sn were already known, as well as two ternary phases: CePdSn and $CePd_2Sn_2$. In our studies we discovered several new ternaries, but discuss only one here.

When a small amount of Sn is added to $CePd_3$, an unusual compound results, $Ce_8Pd_{24}Sn$ (14), which crystallizes in a new structure type. The structure is an ordered and partly filled superstructure of $CePd_3$. This compound is surprising in that it is uncommon to find intermetallic phases with stoichiometric coefficients so much larger than 1. The compound is produced by arc melting and annealing at 900 °C for several weeks. Interestingly, we have discovered that Sn may be replaced by a wide variety of main group metals. So far, the resistivity of two compounds, $Ce_8Pd_{24}Ga$ and $Ce_8Pd_{24}In$, indicate strong interactions with the conduction electrons (figure 4). Magnetic studies and thermopower measurements

Figure 4.

The resistivity of $Ce_8Pd_{24}In$ and $Ce_8Pd_{24}Ga$ show considerable increases in resistivity over that of $La_8Pd_{24}In$, a compound with identical structure but no f electrons. It appears that the Ce compounds have Kondo temperatures on the order of 20 K, but since the room temperature thermopowers are low and Ce magnetic moments are normal, they do not qualify as IV materials.

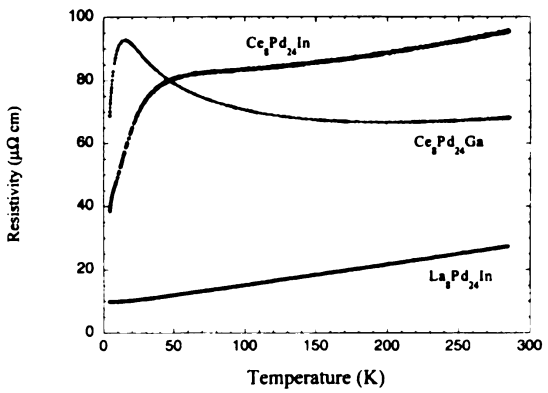

show, however, that the strong IV character of $CePd_3$ is lost with even this small perturbation on the composition and structure.

Even though we have synthesized several dozen new Ce intermetallics, we have so far found hints of only one new IV compound, Ce_2CoSi_3 (15). At present there are no theoretical or even empirical guidelines which help in deciding which particular materials will be IV, and, given the small number of known IV materials in the family of Ce compounds, the expected success rate of discovering new ones is low. The magnetic susceptibility of the series $Ce_2Au_{1-x}Co_xSi_3$ (figure 5) shows the evolution of the behavior from typical Ce^{3+} moments at small x to apparent reduced moments at x = 1.0. Ce_2CoSi_3 is quite brittle in polycrystalline form, and we have not yet been able to determine the thermopower. Since single crystals should be mechanically more robust, we are attempting to prepare them for thermopower and other property measurements. Also since Ce_2CoSi_3 has a hexagonal structure, its properties are expected to be anisotropic, and single crysta! measurements will be necessary to investigate such anisotropy as well.

b.2. Modifying known IV materials

We are also trying to understand the doping behavior of the known IV materials to see how the thermopower is affected by such chemical manipulation. In particular, some theoretical models suggest that the thermopower should be independent of Ce concentration in an IV compound, if all other structural and electronic factors remain unchanged. Our studies of the dilution of Ce in $CePd_3$ show that the situation is complex and not yet completely understood. Figure 6 shows the room temperature thermopower of several different alloy systems: $Ce_{1-x}Y_xPd_3$ (16), $Ce_{1-x}(La_{0.5}Y_{0.5})_xPd_3$ (17), and $Ce_{1-x}Nd_xPd_3$ (17). To prepare homogeneous samples of such complex alloys, great care must be taken. In many cases reported in the literature, such care is clearly not taken and essentially meaningless studies are performed on inhomogeneous materials. When such alloys are melted they always form with composition gradients on solidifying. These gradients can be rather large. The composition gradients can only be removed after melting by prolonged annealing at temperatures approaching the point at which some melting first occurs. At this point the diffusion coefficient is usually large enough that, for gram size samples, the material becomes homogeneous in a few days. Such synthesis strategies will not work for large samples. On a technological scale a powder metallurgical approach could work, if processing temperatures are low enough to prevent the formation of any melt.

Figure 5.

The magnetic susceptibility of $Ce_2Au_{1-x}Co_xSi_3$ shows typical IV like susceptibility at x = 1.0. At the Au rich end of the alloys (small x), typical trivalent behavior is observed.

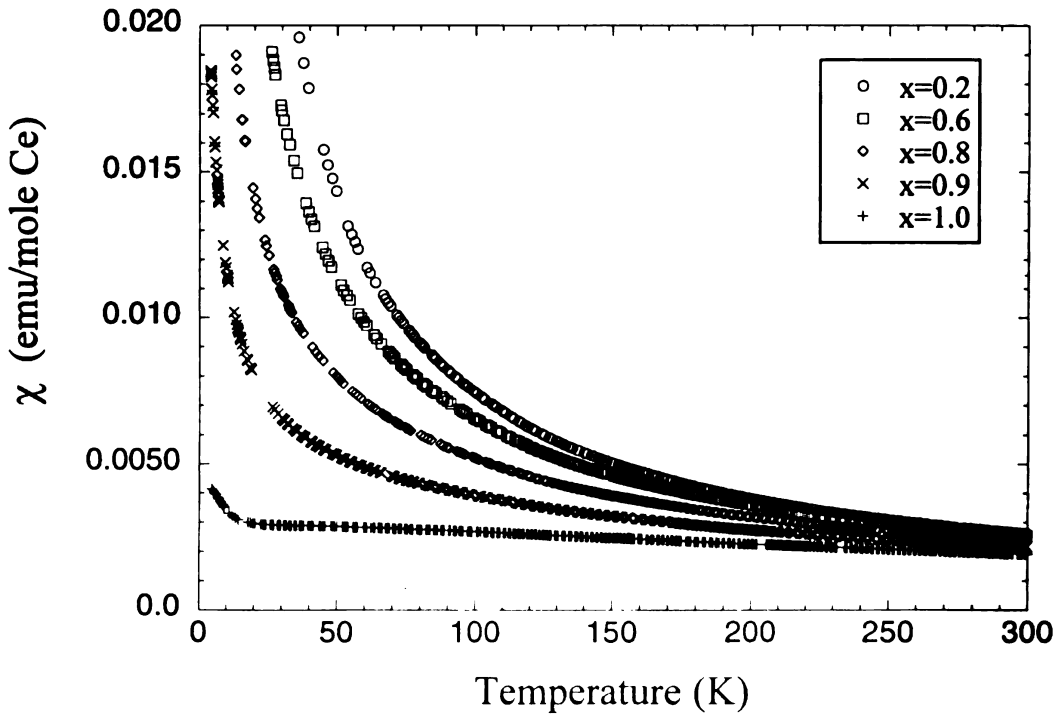

Figure 6.
The thermopower of $Ce_{1-x}Y_xPd_3$ (●), $Ce_{1-x}(La_{0.5}Y_{0.5})_xPd_3$ (+), and $Ce_{1-x}Nd_xPd_3$ (▲) is shown vs. x. The solid line is the theoretcial dependence based on the single Ce model and the Nordheim-Gorter rule.

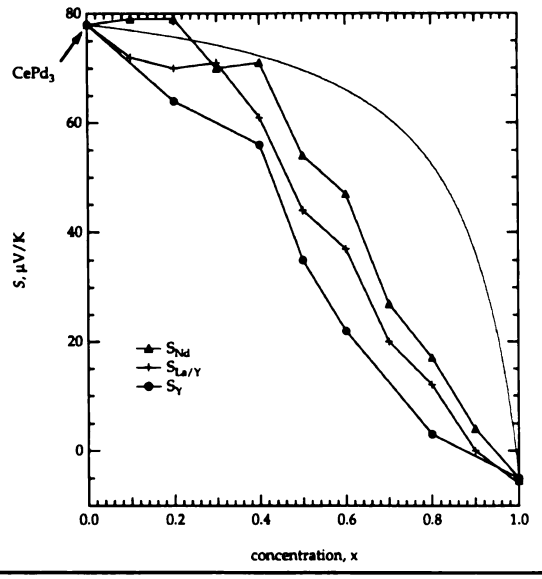

The data for $Ce_{1-x}Y_xPd_3$, taken from the literature, show a decline of the thermopower with doping. Such doping also leads to a decrease in the unit cell volume. The decrease in thermopower has been interpreted as due to the chemical "pressure" caused by the replacement of Ce by the smaller Y. Pressure favors the formation of tetravalent Ce, since it is also smaller than trivalent Ce.

If chemical pressure were the only reason for the reduced thermopower, then replacement of Ce by the correct mixture of La (larger than Ce) and Y (smaller than Ce) would keep the crystallographic unit cell exactly the same size. The data on such an alloy shows that the thermopower decreases nonetheless, but not quite as rapidly as for Y alone. This reduction, however, might be due to atomic scale fluctuations in the lattice strain due to the different size of La and Y. Such fluctuations would not be apparent in the normal x-ray diffraction pattern where the lattice parameters are found to be independent of x.

In order to avoid lattice strain effects, we looked at dilution of Ce with Nd. $NdPd_3$ and $CePd_3$ have lattice parameters that differ by a very small amount (the cubic lattice parameters for both compounds are 4.128(2) Å). However, the thermopower again decreases with increasing Nd concentration, but not quite as rapidly as for the previous two materials. It would appear then that the Ce electronic state is not independent of concentration when we control the lattice and electronic features to be as close to those of $CePd_3$ as is possible. This may indicate that the effects we seek to control are collective, and not single Ce ion effects. However, further studies and comparisons with theoretical models are needed in order to fully understand the implications of these measurements.

Our exploration of IV materials as potential thermoelectric devices is just beginning. Our fundamental understanding of the IV phenomenon is elementary; our ability to predict the composition of new IV materials is virtually nil; and our understanding of how to manipulate the IV state by doping is just starting. We have a considerable way to go to see if IV phenomena will be useful for the purpose of thermoelectric cooling.

Summary

Bulk Bi_2Te_3 is a relatively simple small bandgap semiconductor whose electronic properties have been understood both experimentally and theoretically for more than 30 years. It's thermoelectric performance is near optimal for a bulk material with a single conventional conduction and valence band. Yet it is clear that we still cannot predict which specific materials will have significantly better thermoelectric properties. However, as discussed in the text, we do have general "guidelines" that help focus our attention on broad classes of materials. Generally, materials with electronic structures that are complex in a narrow range of energy near E_F are the focus of the searches underway.

New synthetic methods to prepare complex materials, an ability to easily determine the structure of those phases, and recent discoveries of new phenomena in conducting solids give us hope that we will someday replace the Bi_2Te_3 family as the highest efficiency thermoelectric materials. We as a materials community have yet to find the desired materials. There are promising leads, but the task is challenging and time intensive. The search is so far highly empirical: it is guided by our past knowledge, but it is not a predictable or easily definable path. We hope that a continued and growing interaction with theorists may provide better guidance in this process. The potential payoff is enormous in both economic and environmental terms; yet the "risk" is high: it may take many years of focused research to find such materials. And as is usually the case, it will likely take a considerable development and engineering effort before new devices will be affordable and generally available. However, without the ability to synthesize and characterize high quality materials of considerable complexity, our chances of success are very slim indeed.

Acknowledgments

We would like to acknowledge the support of ONR in the above endeavors. We especially would like to thank the graduate students and postdocs who carried out the research discussed and who critically read the manuscript: B. K. Cho,

R. A. Gordon, Y. Ijiri, C. D. W. Jones, C. M. Spencer in the DiSalvo group and Duck Young Chung, Xiang Shang, Lykougos Iordanidis and Tim McCarthy in the Kanatzidis group.

The editor wishes to acknowledge Professor Galen Stucky of the University of California, Santa Barbara for assistance in the review of the scientific and technical details reported in this article.

Biographies

Dr. Frank DiSalvo received his B.S. in Physics from MIT in 1966 and his Ph.D. in Applied Physics from Stanford University in 1971. He then joined the research staff at AT&T Bell Laboratories, where he later headed several research departments. In 1986 he moved to the Department of Chemistry at Cornell University, where he has taught freshman chemistry for engineers, senior level inorganic chemistry, and a graduate course in solid state chemistry. In 1991 he was awarded the American Physical Society International Prize for New Materials and was elected to the National Academy of Sciences. He is a Fellow of the American Academy of Arts and Sciences. The main goal of Dr. DiSalvo's research has been the discovery and understanding of new chemical and physical phenomena in solids. Particular research emphasis is on the synthesis of novel compounds and the subsequent characterization of their structural, thermal, electrical, and magnetic properties. Compound types extensively examined include chalcogenides, oxides and more recently nitrides, structurally low-dimensional phases, metal cluster phases, and intermetallic compounds. Phenomena of interest have included thermoelectric effects, intercalation reactions, reversible reactions for battery cathodes, structural phase transitions, magnetic properties of crystalline and amorphous materials, charge density waves, and superconductivity.

Dr. Mercouri G. Kanatzidis is a professor in the chemistry department at Michigan State University. He received a B.S. in chemistry in 1979 from Aristotle University of Thessaloniki and a Ph.D. in inorganic chemistry in 1984 from the University of Iowa. He then completed postdoctoral appointments at the University of Michigan (D. Coucouvanis) and Northwestern University (Tobin J. Marks). He joined the Michigan State University faculty in 1987. Dr. Kanatzidis was an NSF Presidential Young Investigator and Alfred P. Sloan Fellow. He is currently a Camille and Henry Dreyfus Teaching Scholar. Dr. Kanatzidis is a member of numerous professional societies, and in addition to his teaching responsibilities, he serves on the editorial boards for Chemistry of Materials and the Journal of Alloys and Compounds. Dr. Kanatzidis' research interests primarily involve inorganic chemistry, with particular emphasis on the solid state chemistry of metal chalcogenides. He also is interested in the fields of conducting polymers, intercalation chemistry, and bioinorganic chemistry. He is an author of over 180 publications.

REFERENCES

1. see for example: "Thermoelectric and Thermomagnetic Effects and Applications," T. C. Harman and J. M. Honig, McGraw Hill (pub) 1967
2. see for example: "Solid State Physics," N. W. Ashcroft and N. D. Mermin, Holt, Rinehart and Winston (pub) 1976
3. We thank Bill Kolander and Hi Lyon from Marlow Industries for data concerning commercial Bi_2Te_3 thermoelectric cooling devices.
4. "Thermoelectricity in Metals and Alloys," R. D. Bernard, Taylor and Francis (pub) 1972
5. D. Elwell and H. J. Scheel, *Crystal Growth from High-Temperature Solutions,* Academic Press, New York, 1975.
6. D.-Y. Chung and M. G. Kanatzidis, manuscript in preparation.
7. M. G. Kanatzidis, T. J. McCarthy, T. A. Tanzer, L.-H. Chen, L. Iordanidis, T. Hogan, C. R. Kannewurf, C. Uher and B. Chen, Chem. Mater. submitted.
8. C. Uher, B. Chen , L. Iordanidis, T. J. McCarthy, T. A. Tanzer, L.-H. Chen and M. G. Kanatzidis, work in progress.
9. R. B. Coles, Contemp. Phys. **28**, 143 (1994); F. Steglich, C. Geibel, K. Gloos, G. Olesch, C. Schank, C. Wassilew, A. Loidl, A. Krimmel, and G. R. Stewart, J. Low Temp. Phys. **95**, 3 (1994); M. B. Maple, Physica B **171**, 389 (1991); G. Aeppli and Z. Fisk, Comments Cond. Mat. Phys. 16, 155 (1992); Z. Fisk and J. R. Schrieffer, MRS Bulletin, 23 August 1993; and references therein
10. H. J. Van Daal, P. B. Van Aken, and K. J. H. Buschow, Phys. Lett. 49A, 246 (1974)
11. M. V. Vedernikov, Chapter 20 in "Thermoelectric and Electrical Applications of Intermetallic Compounds: Principles and Practice" J. H. Westbrook and R. L. Fleischer, J. Wiley (pub) 1995
12. P. Scoboria, J. E. Crow and T. Mihalisin, J. Appl. Phys. 50, 1896 (1979)
13. T. Gambke, B. Elschner and K. Schaafhausen, Physics Letters, 78A, 413 (1980)
14. R. A. Gordon, C. D. W. Jones, M. G. Alexander and F. J. DiSalvo, Physica B, **225**, 23 (1996)
15. R. A. Gordon, C. D. W. Jones and F. J. DiSalvo to be published J. Alloys & Compounds
16. D. Jaccard, M. J. Besnus and J. P. Kappler, J. Magnetism and Mag. Matls. 63/64, 572 (1987)
17. Y. Ijiri and F. J. DiSalvo, to be published Physica B

The Thermoelectric Properties of Skutterudites

Glen A. Slack, Department of Physics, Rensselaer Polytechnic Institute, Troy, New York and Jean-Pierre Fleurial and Thierry Caillat, Jet Propulsion Laboratory, Pasadena, California

Introduction

Skutterudites are a class of compounds based on $CoAs_3$, which is actually the mineral skutterudite. This name comes from the Norwegian town of Skutterud, near the location where the mineral was originally found. There are nine binary semiconducting compounds in this group: CoP_3, $CoAs_3$, $CoSb_3$, RhP_3, $RhAs_3$, $RhSb_3$, IrP_3, $IrAs_3$, and $IrSb_3$. In some ways they resemble the III-V semiconductors AlP, AlAs, AlSb, GaP, GaAs, GaSb, InP, InAs, and InSb. Both sets of compounds are covalent semiconductors with cubic crystal structures. They can be made into both n-type and p-type variants by suitable doping techniques.

One of the requirements for a good thermoelectric compound is a high carrier mobility which correlates with a small electronegativity difference between the elements in the compound [1]. The smaller the value, the more nearly covalent the compound. Skutterudites are significantly more covalent than the III-V compounds. A number of recent papers have appeared describing the thermoelectric properties of the skutterudites [2-7].

Figure of merit

The performance of a material in a thermoelectric refrigerator or generator can be related to the dimensionless figure of merit, ZT, where T is the absolute temperature, and Z at the temperature T is computed from:

$$Z = S^2\sigma/\Lambda \qquad (1)$$

where S= the absolute Seebeck coefficient, σ= the electrical conductivity, and Λ= the thermal conductivity. From Eq.(1) we can see that a good thermoelectric material will have a high electrical conductivity and a low thermal conductivity. The Wiedemann-Franz-Lorenz law states that for a metal:

$$\Lambda_e = L_0\sigma T \qquad (2)$$

where Λ_e is the electronic component of the thermal conductivity, and L_0 is the Lorenz number. In a semiconductor the lattice phonons or quantized lattice vibrations contribute significantly to the total thermal conductivity so that

$$\Lambda(\text{TOTAL}) = \Lambda_e + \Lambda_g \qquad (3)$$

Here Λ_g = the lattice thermal conductivity. In the case of semiconductors we have:

$$ZT = \frac{S^2\sigma T}{\Lambda_e+\Lambda_g} = \frac{S^2\sigma T}{L_0\sigma T+\Lambda_g} = \frac{S^2}{L_0+(\Lambda_g/\sigma T)} \qquad (4)$$

Eq.(4) shows the influence of Λ_g on the figure of merit.

As explained by Slack [1] the ideal semiconducting material for a thermoelectric device is one which is a "phonon glass and electron crystal" or PGEC. A phonon glass has the very smallest possible value of Λ_g because the atomic disorder reduces the phonon propagation distances to their absolute minimum value. Hence Λ_g becomes Λ_{MIN}. The electron crystal should appear to the electrons (or holes) as a very perfectly ordered, covalent solid so that the electrons are not scattered very much as they propagate through the crystal. This dual nature of disorder for phonons and order for electrons is the critical feature for finding new and better thermoelectric materials. We shall show that skutterudites have a very special nature that may make this possible.

Low Lattice Thermal Conductivities

The best currently employed thermoelectric materials are Ge-Si, Bi_2Te_3-Sb_2Te_3, PbTe-PbSe and Bi-Sb mixed crystals. The mixed crystals have higher ZT values than either parent because the atomic mixture produces what is termed "mass fluctuation" scattering of the lattice phonons[8]. This effect was discovered by Eucken and Kuhn[9] in 1928. This randomness of the mass, size and charge of the atoms on a particular lattice position in the crystal can also tend to scatter electrons as well[1]. Thus mixed-crystal thermoelectrics have to be carefully tailored to produce some decrease in Λ_g without too much of a decrease in σ. Mixed crystals can be made between the various III-V compounds, and they can also be made in the skutterudite system.

The special structure of the skutterudites offers a second method of reducing Λ_g that is not found in the III-V compounds or any of the other currently used compounds. Each cubic unit cell of the skutterudite structure contains two ordered voids[10]. These voids can be populated with "extra" atoms whose job it is to scatter phonons but not electrons. The possibility of tailoring these "extra" atoms to yield a PGEC behavior of the skutterudites is creating much current interest in these materials.

Both n-type and p-type conductivity samples have been obtained for skutterudites, using several preparation techniques[4,5]. Associated with a low hole effective mass, very high carrier mobilities, low electrical resistivities and moderate Seebeck coefficients are obtained in p-type skutterudites[5]. For a comparable doping level, the carrier mobilities of n-type samples are about an order of magnitude lower than the values achieved on p-type samples[5]. But the much larger electron effective masses and Seebeck coefficients make n-type skutterudites even more promising candidates. However, the thermal conductivities of the binary skutterudite compounds are too large (100-150 mW/cm K at 300K), particularly at low temperatures, to be useful for thermoelectric applications. Substantial reductions in the lattice thermal conductivity must be obtained to achieve values comparable to those of state of the art thermoelectric materials (10-40 mW/cm K at 300K). Several approaches to a low lattice thermal conductivity in skutterudites are presented in the next section.

Reducing the Lattice Thermal Conductivity

Because of the importance of Λ_g on the value of ZT a great deal of effort is being devoted to understanding the mechanisms that may be employed for reducing the Λ_g of skutterudites. These may be listed as methods for scattering the lattice phonons:

Mass and Strain Fluctuation
Void Fillers
Charge Carriers from Dopants
Mixed-Valence Cations
Inner-Shell Excitations (d-shell & f-shell)
Grain Boundaries, Precipitates, Others

We shall discuss a number of these possibilities.

The phonon heat transport in crystals occurs over the whole range of phonon energies from zero up to an energy of $k\theta_0$ where k = Boltzmann's constant and θ_0 = the Debye temperature. Each one of the phonon scattering mechanisms listed will scatter phonons in some particular energy range while interacting weakly with all of the other phonons. For example the mass fluctuation scattering cross-section increases as ν where ν is the phonon frequency. It is termed Rayleigh scattering. Thus it is very effective on phonons with energies near $k\theta_0$ but allows the low frequency phonons to travel almost unimpeded. We can only reduce Λ_g to Λ_{MIN} if phonons of all energies have a mean-free path equal to one-half their wavelength. Thus simple mass fluctuation scattering, produced by making mixed crystals or alloy crystals, can never yield Λ_{MIN}. The best hope is to combine mass fluctuation scattering with another mechanism that interacts with the lower frequency phonons. This technique was employed by Dismukes et al.[11] in Si-Ge samples where the lowest frequency phonons were scattered by interaction with the

free carriers in these degenerately doped materials. The mass fluctuation scattering was produced by using samples with 70 atom % Si and 30 atom % Ge. The combination of these two mechanisms produces quite low thermal conductivities, but these materials still do not possess $\Lambda_g = \Lambda_{MIN}$ as shown by Slack and Hussain[8].

Intrinsic Thermal Conductivity

Before we discuss in detail the results on reducing the Λ_g of skutterudites we need to know how the pure crystals behave. In Fig. 1 we show the present data on the lattice thermal conductivity of $CoSb_3$, $RhSb_3$, and $IrSb_3$. Data on the other skutterudites is quite limited. Note in Fig. 1 the almost exponential rise in Λ as the temperature decreases below 300K. This feature is characteristic of pure, isotopically clean crystals for $T<\theta_0$. Since θ_0 is close to 300K for all three crystals, this rise starts below room temperature. A similar rise is observed in InSb[12] below its Debye temperature of 207K. The decreasing Λ below 10K in Fig. 1 is caused in $CoSb_3$ by phonons being scattered from the walls of the 1 millimeter diameter single crystal. In $RhSb_3$ the decrease is caused by some unknown internal defects, possibly Sb precipitates. In the polycrystalline $IrSb_3$ it is caused by phonon scattering at the boundaries of the 7 μ diameter grains. In Fig. 1 it is apparent that the Λ of $CoSb_3$ rises above 700K. This rise is caused by the bipolar diffusion of carriers which are thermally excited across the small band gap (Eg ~ 0.63 eV) of $CoSb_3$. The band gap of $IrSb_3$ is too large for this effect to appear. Such bipolar heat transport has been well documented[13] in Si and Ge at high temperatures.

Figure 1

The Lattice Thermal Conductivity of Pure, Undoped $CoSb_3$ and $RhSb_3$ crystals and polycrystalline $IrSb_3$ Versus Temperature. The $RhSb_3$ curve stops at 300K, the $CoSb_3$ at 1000K.

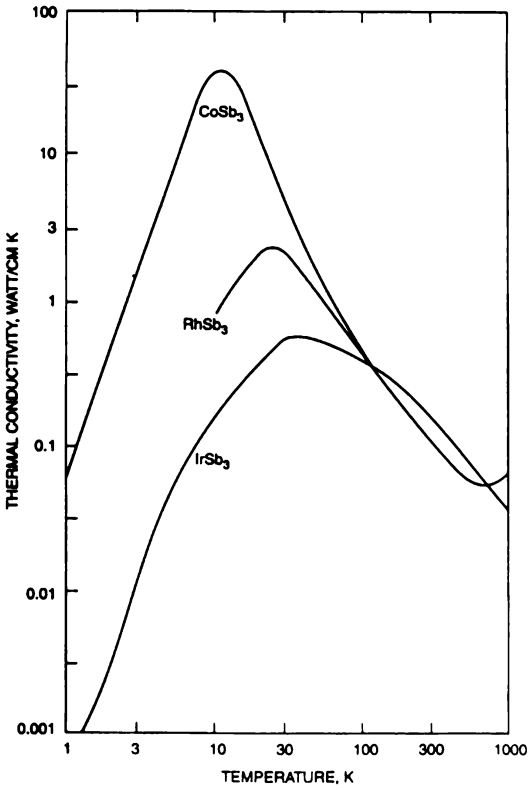

Minimum Thermal Conductivity

Every crystal has a lower limit to its lattice thermal conductivity. This concept and the method of calculating this value of Λ_{MIN} has been explained by Slack[1]. The minimum value will be attained when all of the acoustic phonons have a mean-free-path equal to one-half of their wavelength and all optic phonons have a mean-free-path equal to the average interatomic distance. The sum of these two contributions gives Λ_{MIN}. The calculated values of Λ_{MIN} for $IrSb_3$ versus temperature are given in Fig. 2. The values for $IrSb_3$ and $CoSb_3$ are almost identical.

Figure 2.

The calculated minimum thermal conductivity versus temperature for $IrSb_3$.

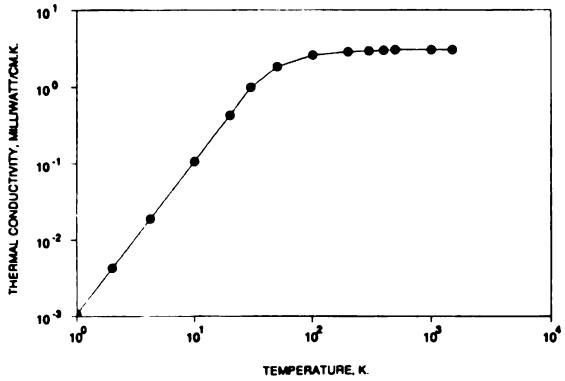

Mass and Strain Fluctuation Scattering

The mass and strain fluctuation scattering of phonons in crystals is usually produced either by isotopic substitution or isoelectronic substitution of one or several elements. In the skutterudite compounds solid solutions have been reported to exist in the $IrSb_3$ - $RhSb_3$ and $CoAs_3$ - CoP_3 systems over the whole range of compositions [4,14,15]. Recent results at the Jet Propulsion Laboratory show that the $IrSb_3$ - $CoSb_3$ system also forms a complete series of solid solutions. In the $CoSb_3$ - $CoAs_3$ system there is a wide miscibility gap[15] over the central 80 mole % of the system. These and other recent results[16,17] are summarized in Table 1.

An example of the possible thermal conductivity reduction from mixed crystals is useful. Mixed crystals of $RhSb_3$ - $IrSb_3$ can be made over the whole composition range. The thermal conductivity of mixed crystals of 50 mole % $RhSb_3$ with 50 mole % $IrSb_3$ has been measured above room temperature. A careful analysis of these results shows that the decrease in Λ is caused only by the mass difference between the Rh and Ir, there is no strain-fluctuation component. Thus Rh behaves much like a very light isotope of Ir. A similar result has been found in AlAs - GaAs mixed crystals by Afromowitz[18], where Al acts like a light isotope of Ga. The $Rh_{0.5}Ir_{0.5}Sb_3$ crystal has a thermal conductivity at 300K of Λ_g(50-50) = 90 mW/cm K. This is 68% of that of the average of the two parents, $RhSb_3$ and $IrSb_3$, and is much larger than Λ_{MIN} of 3.1 mW/cm K. Some recent data on mixed crystals at 300K are shown in Figure 3, where measured values of the lattice thermal conductivity are given. The measured total Λ has had the electronic component subtracted, and also has been corrected for small porosity effects. Thus the numbers correspond to theoretically dense samples.

The effect of the mass and strain fluctuation scattering of phonons by these point defects in skutterudites can be calculated using the theory developed by Callaway[19]. This theory permits us to calculate Λ_g versus chemical composition over the whole composition range. Some of the results are shown in Fig. 3 for various $CoSb_3$ mixed crystals. Curves 2 and 3 are for samples that are miscible over the whole composition range while the other five curves are predictions for samples that have a limited range of actual miscibility. We have found, for example, that $CoSb_3$ will accept up to 12 mole % IrP_3, see curve 7. This means that the expected Λ_g will be about 13 mW/cm K at 300K. This reduction in Λ_g is quite substantial compared to pure $CoSb_3$ at 104 mW/cm K. Further studies of these effects are presently underway.

Table 1.

Some Known Skutterudite Mixed Crystals

Compound	Partial Range of Solid Solutions with	Full Range of Solid Solutions with
CoP_3		$CoAs_3$
$CoAs_3$	$CoSb_3$, $IrAs_3$	
$CoSb_3$	$CoAs_3$	$IrSb_3$
$RhSb_3$	$CoSb_3$	$IrSb_3$
$IrAs_3$	$CoAs_3$, $IrSb_3$	
$IrSb_3$	$IrAs_3$	$CoSb_3$, $RhSb_3$
$Fe_{0.5}Ni_{0.5}Sb_3$	$CoSb_3$, $IrSb_3$	$Ru_{0.5}Pd_{0.5}Sb_3$
$Ru_{0.5}Pd_{0.5}Sb_3$	$CoSb_3$, $IrSb_3$	$Fe_{0.5}Ni_{0.5}Sb_3$
$FeSb_2Te$	$CoSb_3$, $RuSb_2Te$	
$RuSb_2Te$	$FeSb_2Te$	$IrSb_3$

Figure 3.

The Calculated Lattice Thermal Conductivity of $CoSb_3$ Mixed Crystals at 300K as a Function of the Mole Percent of $CoSb_3$. The circular points have been measured for $CoSb_3$-$IrSb_3$, the square point is for the ninth sample ($CoSb_3$ -$Fe_{0.5}Ni_{0.5}Sb_3$) in Table 7 with 79 mole % $CoSb_3$.

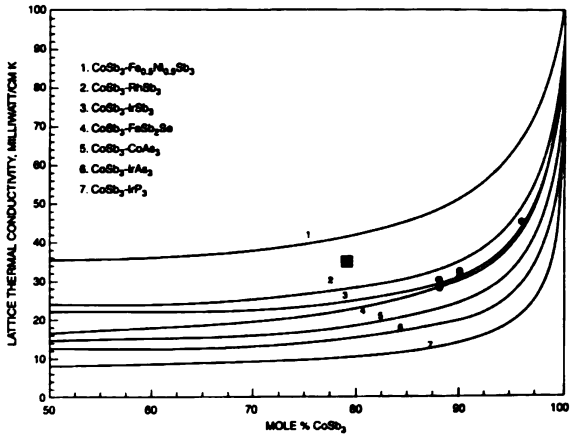

Scattering by Void Fillers

Numerous different atoms have been introduced into the voids in skutterudite crystals[20]. Among these are Ba, Sr, La, Ce, Th, U, Nd and Sm. In $IrSb_3$, for example, Ba^{2+} ions just fill the voids with no space left over. If all of the voids in the crystal, which are always periodically arranged, are filled with Ba atoms so that the chemical formula is Ir_4BaSb_{12}, the phonon propagation will detect no disorder and the thermal conductivity will be high, i.e. about 160 mW/cm K at room temperature. If we fill only one-half of the voids with Ba and leave the others vacant, than we will have mass fluctuation scattering similar to that discussed previously. This ef-

fect scatters predominantly the higher frequency phonons. However if we place smaller size atoms in the voids such as Nd^{3+} or Sm^{3+}, these "rattle about" because the voids are significantly larger in diameter than the Sm or Nd ions. Thus looser bonding of undersize atoms will change (decrease) the frequency of the lattice phonons that are being scattered. Furthermore, the undersize atoms will not vibrate in phase with one another. This means that all of the voids can be filled with undersize atoms and the atomic "disorder" caused by the uncoordinated "rattling of the atoms in their cages" will scatter the lower frequency lattice phonons. The result is a drastic reduction in the thermal conductivity as shown in Fig. 4. Here La, Nd, or Sm atoms in the voids in $IrSb_3$ have

Figure 4.

The Lattice Thermal Conductivity of Pure, Unfilled, Polycrystalline $IrSb_3$ and of Rare-Earth Filled $IrSb_3$ Versus Temperature The curve for Λ_{MIN} is also shown. See reference #20.

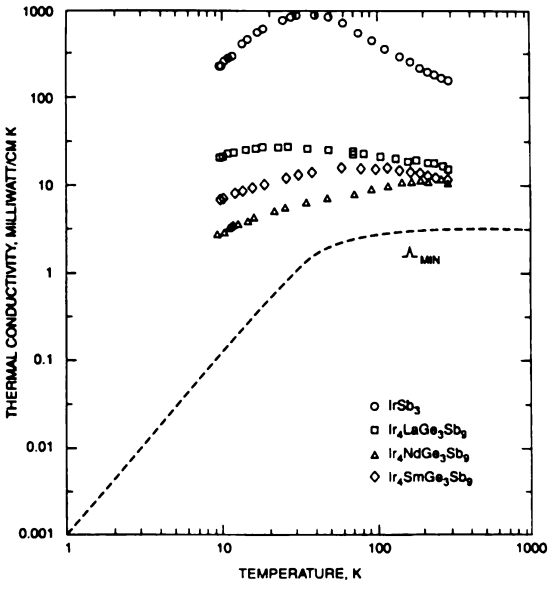

produced the phonon scattering. The lattice thermal conductivity at room temperature has dropped from 160 mW/cm K to 11 mW/cm K for the Nd-doped sample, a factor of 15 decrease. Further research is presently underway to determine whether these void occupants can be combined with mass fluctuation and strain fluctuation scattering in order to further reduce the lattice thermal conductivity. In addition other void occupants such as Bi, Ar, Kr, Xe, K, and Ti are being considered.

Charge Carriers from Dopants

The effects of the charge carriers from n-type and p-type dopants on the thermal conductivity of semiconductors has been studied in Ge, Si, SiC, GaSb, and GaAs by numerous authors[11,21-24]. In Si, both n and p dopants, when present at high concentrations so that the semiconductors are degenerate, are effective as scatterers of the very low frequency phonons. In the skutterudites $IrSb_3$ and $CoSb_3$ we have found that n-type dopants in degenerately doped samples are effective scatterers of low frequency phonons. Fig. 5 shows that at temperatures below 200K the thermal conductivity is drastically reduced. P-type dopants seem to produce a much smaller effect. The reason for the difference is not currently known.

The charge-carrier scattering of phonons has been shown to improve the efficiency of Ge-Si thermoelectric generators. Thus it could be useful in the n-type skutterudites

Figure 5.

The Lattice Thermal Conductivity of Pure, Unfilled, Polycrystalline $IrSb_3$ and single crystal $CoSb_3$ Doped with Various Levels of n-type and p-type Impurities Versus Temperature.

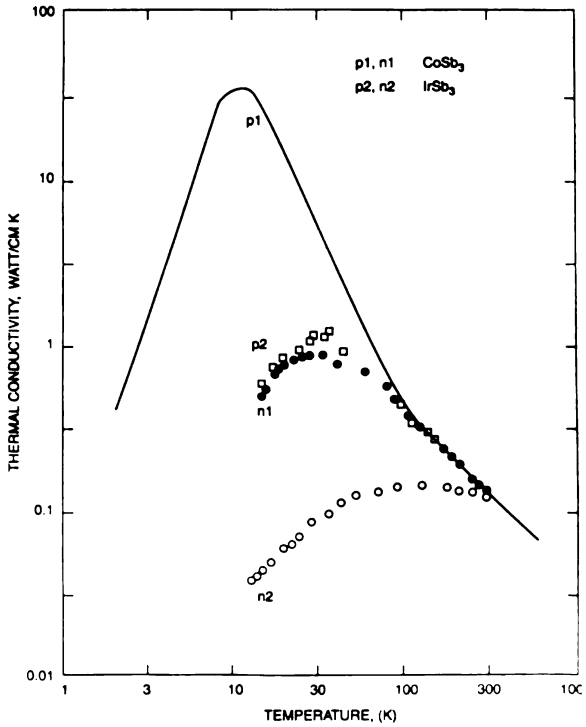

when coupled with void-filling and mass-fluctuation scattering.

Mixed-Valence Cations

In the simple binary skutterudites like $IrSb_3$ the iridium atoms each donate 3 electrons to the covalent bonding, the antimony atoms each donate 5. Thus there are 18 bonding electrons donated per formula unit. There are nine bonds. Each bond is made up of two electrons of opposite spin. This same electron counting scheme is applicable to the semiconducting ternary skutterudites. There are a number of ternary skutterudites that contain Fe, Ru, or Os atoms. These atoms tend to have mixed valences similar to iron in Fe_3O_4 or ruthenium in $RuSb_2$-$RuTe_2$ mixed crystals. In Fe_3O_4 iron occurs as both Fe^{2+} and Fe^{3+}. In $RuSb_2$ the ruthenium is Ru^{4+} while in the $RuTe_2$ it is Ru^{2+}, in the mixed crystals both valences occur. Other examples are the nominal skutterudites $FeSb_2Te$, $RuSb_2Te$, $OsSb_2Te$, and $Ru_{0.5}Pd_{0.5}Sb_3$, which are never exactly stoichiometric and possess metal ions with two different charge states.

Let us write $RuSb_2Te$ more correctly as:

$$\square_v Ru^{2+}_x Ru^{4+}_y [Sb_a Te_b]_3$$

We find experimentally that some vacancies occur on the metal sites, hence the square-denoting a vacancy - with a fractional concentration v. The sums v+x+y = 1 and a+b = 1 are equal to unity. In one case we have replaced some Sb atoms by Ge atoms on the antimony sites so that the composition is:

$$\square_v Ru^{2+}_x Ru^{4+}_y [Sb_a Te_b Ge_c]_3$$

where: a+b+c = 1. For the skutterudite $Ru_{0.5}Pd_{0.5}Sb_3$ we have:

$$\square_v Ru^{2+}_x Ru^{4+}_y Pd^{4+}_2 Sb_3$$

The compositions are collected in Table 2 along with the measured value of the lattice thermal conductivity at room temperature.

Model of Phonon Scattering by Mixed-Valence Cations

In this model the phonons are assumed to be scattered when an electron pair in the d-shell of Ru^{2+} is transferred to a neighboring Ru^{4+}. So one ruthenium atom goes from $4d^6$ -> $4d^4$ while a neighboring one goes from $4d^4$ -> $4d^6$. In the process a phonon is scattered. The scattering depends on the presence of both charge states. Thus the phonon scattering probability and hence the lattice thermal resistivity, W_g, should vary as the product of $c(Ru^{2+}).c(Ru^{4+})$ where c is the concentration in the atoms per unit volume and $W_g = 1/\Lambda_g$. Since each unit cell of volume a_0^3 contains 8 possible metal atom sites, then

$$c(Ru^{2+}) = \frac{8x}{a_0^3} \quad \text{and} \quad c(Ru^{4+}) = \frac{8y}{a_0^3}$$

and $c(Ru^{2+}).c(Ru^{4+}) = 64xy/ a_0^6$. Let us define a concentration parameter, P, as

$$P = \frac{64xy}{a_0^6}$$

Table 2.

Composition Parameters and Thermal Conductivity at 300K for Several Ruthenium Skutterudites.

Sample Number	Nominal Composition	a_o Å	Λ_g milliW/ cm K	P	v	x	y	z	a	b	c
$RhSb_3$	$RhSb_3$	9.2322	105	0	---	---	---	---	1.000	---	---
OX27	$RuSb_2Te$	9.268	33	0.79	0.104	0.799	0.097	0	0.662	0.338	---
RPS6	$Ru_{0.5}Pd_{0.5}Sb_3$	9.296	28.5	0.60	0.050	0.400	0.150	0.400	1.000	0	0
OX51	$RuSb_2Te$	9.283	20	0.95	0.094	0.785	0.121	0	0.685	0.315	0
OX52	$Ru(Ge\text{-}Sb\text{-}Te)_3$	9.286	11	1.66	0.052	0.711	0.237	0	0.666	0.272	0.062

*P in units of $10^{43}/cm^6$

We have given this in Table 2 in units of (10^{43}/cm^6). In Fig. 6 we plot W_g versus P. At P=0 we have employed the measured value of W_g for $RhSb_3$ since Rh is adjacent to Ru in the periodic table but has only one charge state, Rh^{3+}.

From Fig. 6 we conclude that the phonon scattering does depend monotonically on P. The maximum value of P will be for x=y=0.5 when $P_{MAX} = 2.5 \times 10^{43}$/cm^6. At this value W_{MAX} = 140 cm K/Watt. This converts to Λ_g = 7.1 mW/cm K at room temperature. Thus charge transfer scattering can produce a very low lattice thermal conductivity in the ruthenium skutterudites. Whether the carrier mobility and Seebeck coefficient can both be kept large at the same time is unknown.

The same sort of thermal conductivity reduction has been seen in $OsSb_2Te$ and $FeSb_2Te$ compounds where one finds Os^{2+} and Os^{4+} of Fe^{2+} and Fe^{3+}. The scattering strength of Fe is comparable to Ru while that of Os is about twice as large. These values are, so far based on the analysis of only a few samples, and therefore may be modified at a future date.

Figure 6.

The Lattice Thermal Resistivity of $RhSb_3$ and Various Ruthenium-Based Skutterudites at 300K as a Function of the Variable-Valence Scattering Parameter, P.

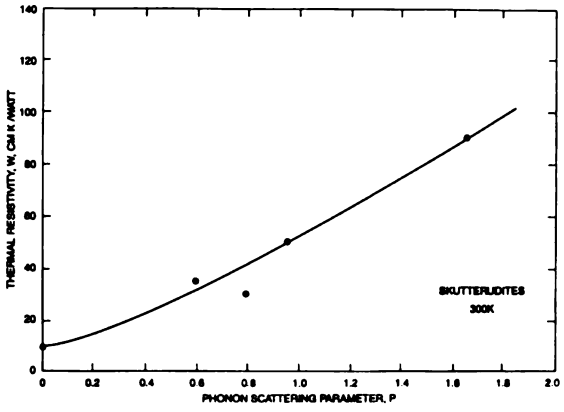

Inner Shell Excitations

The phonon scattering caused by excitation of the electrons with the f-shell or d-shell of single, isolated transition metal atoms has been studied by Slack et al. [25-27]. The rare-earth ions Sm^{3+} and Nd^{3+} incorporated into the voids in $IrSb_3$ exhibit such f-shell phonon scattering[20]. So far no d-shell excitations within single atoms have been seen in skutterudites. The f-shell transitions are rather weak phonon scatterers compared to the other scattering mechanisms that have been discussed previously.

More Phonon Scattering Mechanisms

Other defects in the skutterudite crystals such as grain boundaries, precipitates, and dislocations can produce thermal conductivity reductions. However we do not believe any of these will be useful for controlling the Λ_g in the temperature range of interest for thermoelectric devices.

Conclusions

Some results on a new family of promising thermoelectric materials with the skutterudite crystal structure have been presented. These results demonstrate that ZT values of the order of unity may be obtainable. Both n-type and p-type skutterudites possess good electrical properties although the optimum doping levels are much higher for n-type materials. This is because the electron effective mass is about 12 times larger than the hole effective mass. The room temperature lattice thermal conductivity of the antimony skutterudites is between 105 and 160 mW/cm K and needs to be reduced by a factor of about 20 in order to achieve high figures of merit. Several methods of achieving this have been described. The most effective are (a) mass and strain fluctuation; (b) void filling; (c) mixed valence electron transfer; and (d) charge carrier interactions. The good mechanical properties, the low thermal expansion coefficients, and the cubic crystal structure are also important if skutterudites are eventually employed in good thermoelectric devices.

Acknowledgment

The editor wishes to acknowledge Dr. Celia Merzbacher of the Naval Research Laboratory, Optical Sciences Division for assistance in the review of the scientific and technical details reported in the preceding article.

Biographies

Dr. Glen A. Slack received his B.S. degree in physics from Rensselaer Polytechnic Institute in 1950 and his Ph.D. in physics from Cornell University in 1956. He was employed at the General Electric Research and Development Center from 1956 to 1993. In 1993 he joined the Physics Department at R.P.I. where he is currently building up the laboratory of Novel Semiconductor Materials. He is a Fellow of the American Physical Society, the recipient of a Guggenheim

Fellowship and a Coolidge Fellowship, and has been a visiting scholar at Oxford University, Chalmers Technical University, the University of Umeä, the University of Bordeaux, and Yale University. He is the author of more than 110 scientific papers.

Dr. Slack has been working on problems in the thermal conductivity of solids for more than 40 years.

Dr. Jean-Pierre Fleurial. See page 42, Profiles in Science.

Dr. Thierry Caillat. See page 42, Profiles in Science.

REFERENCES

1. G.A. Slack, "New Materials and Performance Limits for Thermoelectric Cooling" in Handbook of Thermoelectrics", ed. by D.M.Rowe, CRC Press, Boca Raton, 1995
2. G.A.Slack and V.G.Tsoukala, J. Appl. Phys. 76 1665 (1994).
3. T.Caillat, A.Borshchevsky, and J.P. Fleurial, Proc. XIII Intern. Conf. Thermoelectrics, Kansas City, Missouri, (1994) p31-34, 58-61, Am. Inst. Phys. Conf. Proc. No. 316.
4. T.Caillat, J P Fleurial and A Borshchevsky, J. Crystal Growth 4204 (1996).
5. T.Caillat, J.P.Fleurial, and A.Borshchevsky, "Study of the Physical and Transport Properties of $CoSb_3$ Single Crystals", J. Appl. Phys. 80 (8) (1996).
6. D.T.Morelli, T.Caillat, J.P.Fleurial, A.Borshchevsky, J.Vandersande, B.Chen, and C.Uher, Phys. Rev. B52 4926 (1995).
7. J.W.Sharp, E.C.Jones, R.K.Williams, P.M.Martin, and B.C.Sales, J. Appl. Phys. 78 1013 (1 995)
8. G.A.Slack and M.A. Hussain, J. Appl. Phys. 70 2694 (1991).
9. A.Eucken and G.Kuhn, Zeit. Phys. Chem. 134 193 (1928).
10. H.D.Lutz and G.Kliche, Zeit. anorg. allgem. Chem. 480 105 (1981).
11. J.P.Dismukes, L.Ekstrom, E.F.Steigmeier, I.Kudman, and D.S.Beers, J Appl. Phys 35 2899 (1964).
12. E.F.Steigmeier, "Thermal Conductivity" ed. by R.P. Tye, Academic Press, New York, 1969, see Volume 2, Chapter 4.
13. C.J.Glassbrenner and G.A. Slack, Phys. Rev. 134 A1058 (1964).
14. N.Mandel and J.Donohue, Acta Cryst. B27 2288 (1971).
15. H.D.Lutz and G.Kliche, J. Solid State Chem. 40 64 (1981).
16. A.Borshchevsky, J. P. Fleurial, C. E.Allevato, and T.Caillat, Proc. XIII Intern. Conf. Thermoelectrics, Kansas City, Missouri, (1994) p3-6, 58-61, Am. Inst. Phys. Conf. Proc. No. 316.
17. J. P. Fleurial, T.Caillat, and A.Borshchevsky, "Thermoelectric Materials with the Skutterudite Structure: New Results", Proc. XIV Intern. Conf. on Thermoelectrics, St. Petersburg, Russia, 1995.
18. M.A.Afromowitz, J. Appl. Phys. 44 1292 (1973).
19. T.Callaway and H.C.Von Baeyer, Phys. Rev. 120 1149 (1960).
20. G. S. Nolas, G.A.Slack, D.T.Morelli, T.M.Tritt and, A.C.Ehrlich, "The Effect of Rare-Earth-Filling on the Lattice Thermal Conductivity of Skutterudites", J. Appl. Phys. 1996 - to be published.
21. G.A.Slack, J. Appl. Phys. 35 3460 (1964).
22. E.F.Steigmeier and B.Abeles, Phys. Rev. 136 A1 149 (1964).
    A.Amith, I.Kudman, and E.F.Steigmeier, Phys. Rev. 138 A1270 (1965).
23. A.G.Briggs and L.J.Challis, J. Phys. C2 1353 (1969).
24. S.R.Bakhchieva, N.P.Kokelidze, and M.G.Kekua, Phys. Stat. Sol. A83 139 (1984).
25. G.A.Slack and S.Galginaitis, Phys. Rev. 133 A253 (1964).
26. G.A.Slack, Phys. Rev. 134 A1268 (1964).
27. G.A Slack and D.W.Oliver, Phys. Rev. B4 592 (1971).

Thin-Film Superlattice and Quantum-Well Structures – A New Approach to High-Performance Thermoelectric Materials

Rama Venkatasubramanian, Center for Semiconductor Research, Research Triangle Institute, Research Triangle Park, North Carolina

Introduction

Efficient solid state thermoelectric (TE) devices are desirable for several Navy applications, such as shipboard air conditioning, cooling of special electronic components as well as on-board power generation using thermal sources. The performance of a TE device at a temperature T is essentially related to a thermoelectric *figure-of-merit* of the material, *ZT*, used to make the device. The ZT of a thermoelectric material is described by the relation

$$ZT = (\alpha^2\sigma / K)T$$

where α is the Seebeck coefficient, σ is the electrical conductivity and K is the sum-total of lattice and electronic components of thermal conductivity. The $(\alpha^2\sigma)$ term is frequently referred to as the *power factor* of the material. A conventional TE cooling device employs a p-type and an n-type segment, (also referred to as legs). Today, a vast majority of TE cooling devices employ a p-type leg consisting of a $Bi_{0.5}Sb_{1.5}Te_3$ alloy and an n-type leg consisting of a $Bi_2Te_{2.85}Se_{0.15}$ alloy.

In commercial manufacturing of thermoelectric modules, these alloyed materials are prepared as oriented polycrystalline ingots by a Bridgemann technique or a zone leveling process. The ingots are sliced into appropriate thermoelements, typically, a few mm on each side. To date, the best ZT at 300K is about 1.0 for p-type $Bi_{0.5}Sb_{1.5}Te_3$ alloys and about 0.9 for n-type $Bi_2Te_{2.85}Se_{0.15}$ alloys, not significantly higher than state-of-the-art of thirty years ago [1]. Research

on improving the ZT of these *bulk* thermoelectric materials have met with limited success since the 1960's.

However since 1960's, a variety of *thin-film deposition* techniques such as molecular beam epitaxy (MBE) [2], *organometallic vapor phase epitaxy* (OMVPE) [3] and low-pressure chemical vapor deposition (LPCVD) [4] have emerged for depositing a plethora of materials, for applications ranging from solid-state lasers to ferroelectrics. These thin-film deposition techniques have allowed the synthesis of novel materials and enabled material scientists and device engineers to apply intriguing concepts such as *superlattices* [5] and quantum-confinement in conventional and new devices. However, such techniques of epitaxial deposition and the associated analytical techniques for material characterization have rarely been investigated to improve the performance of thermoelectric materials, until recently. This is surprising since thermoelectric devices can address a substantial commercial and military market, in both solid-state cooling and power generation.

Background

In a historical note, Whall and Parker [6] suggested a possible enhancement in ZT of SiGe-thermoelectric materials by using superlattice structures, through carrier confinement in quantum wells to obtain an increased Seebeck coefficient and by modulation doping to obtain an enhancement of carrier mobility. In 1992, a National Thermogenic Workshop was organized [7] to consider various approaches to obtain a significant breakthrough in the performance of thermoelectric materials. Thin-film approaches using quantum-well structures to enhance power-factor [8, 9] and an argument for the use of superlattice structures to decrease thermal conductivity [10] were proposed in this workshop. The motivation for the use of superlattice structures to reduce thermal conductivity came from the observed reduction of lattice thermal conductivity using solid solution alloying in the Bi_2Te_3- Sb_2Te_3 and Bi_2Te_3-Bi_2Se_3 material system. In this system, the reduction in lattice thermal conductivity has been attributed to lattice distortions, from the difference between the masses of the constituent atoms, that are effective in phonon scattering, thereby impeding the flow of heat. Similarly, lattice perturbations and the atomic mass fluctuations at the superlattice interfaces, are expected to enhance phonon scattering rates. The concept of "confined" phonons [11] as well as a reduction in the thermal conductivity of GaAs/AlAs superlattice structures [12], relative to that of AlAs or GaAs and depending on the dimensions of the superlattice structure, have been experimentally demonstrated. Confined phonons imply that they do not propagate suggesting lower thermal conduction due to phonons. Also, a planar, thin-film, thermoelectric device process technology denoted as Monolithically Interconnected, Superlattice-Structured Thermoelements (MISST) [10] was proposed to concurrent-engineer the practical application of thin-film, superlattice-type structures to high-performance thermoelements.

Since then, several groups in the United States have extended the initial theoretical calculations in Ref. 8 on the potential power factor improvement in quantum-well structures [13, 14]. Some laboratories have embarked on the experimental demonstration of improved ZT at 300K in thin-film quantum-well and superlattice structures.

In this review, we will focus on the experimental results in the growth and thermoelectric properties of thin-film superlattice and quantum-well structures. A companion paper by Reinecke et. al in this issue discusses the theory behind some of the thermoelectric properties of superlattices. We will first describe some aspects of thin-film deposition of superlattice structures in thermoelectric materials. Following this, we describe some of the key results that have recently emerged with the use of quantum-confined and superlattice structures. Various approaches to the fabrication of a thin-film TE device will be described briefly. Finally, we discuss the major research issues yet to be fully addressed toward the eventual implementation of thin-film thermoelectric materials in practical, solid-state cooling and power generation systems.

Deposition of Thermoelectric Superlattice Structures

In this section we will consider two studies of epitaxial growth and characterization of thermoelectric properties of superlattice structures, where such properties have been investigated (and reported) as a function of superlattice dimension. Such a dimensional-related quantification is important to distinguish the improved properties from a superlattice approach, rather than arising purely from an epitaxial deposition process.

One study is on *n-type*, MBE-grown $PbTe/Pb_{1-x}Eu_xTe$ and related superlattice structures, grown on semi-insulating BaF_2 substrates. This system has been originally studied and reported by Harman et. al of MIT Lincoln Laboratories [15]. Second, we will describe our work on thermoelectric properties of *p-type*, OMVPE-grown Bi_2Te_3/Sb_2Te_3 superlattice structures on semi-insulating GaAs and Al_2O_3 substrates [16]. Farmer et. al of Lawrence Livermore National Laboratory have reported on sputter-deposited $Bi_{0.9}Sb_{0.1}/X$ (X=Bi_2Te_3, Bi and $PbTe_{0.8}Se_{0.2}$) superlattice structures on semi-insulating Al_2O_3 substrates [17]. However, their early results on power-factor of these sputter-deposited superlattice thin-films are inferior or about comparable to non-superlattice films of pure Bi and $Bi_{0.9}Sb_{0.1}$. Elsner et. al of Hi-Z Technology, in cooperation with Naval Research Laboratory, have reported on some significant enhancement

of thermoelectric properties of $Si/Si_{0.8}Ge_{0.2}$ superlattice structures grown on conducting Si substrates [18]. The conducting nature of the Si substrate, especially when it is lightly-doped (therefore has a high Seebeck coefficient) and is of the same polarity as the epitaxial film that is being investigated, makes the interpretation of properties of superlattices very difficult.

MBE of PbTe / $Pb_{1-x}Eu_xTe$ Superlattices

The MBE growth of PbTe and its alloys, including $Pb_{1-x}Eu_xTe$ and $Pb_{1-x}Eu_xTe_ySe_{1-y}$, have been researched in the past [19] for use in lead-salt diode lasers and detectors. Their growth have been demonstrated on single-crystal, cleaved BaF_2 substrates. The insulating nature of the BaF_2 substrates is very convenient for studying the thermoelectric properties as well. Harman et al. [15, 20] have pursued this materials system to evaluate the predicted quantum-well effects in $PbTe/Pb_{1-x}Eu_xTe$ system and its advantages for ZT improvement.

Typical $PbTe/Pb_{1-x}Eu_xTe$ (x~0.073) multi-quantum well structures are grown on BaF_2 substrates with a 2000 Å $Pb_yEu_{1-y}Te$ buffer. PbTe is the quantum-well material, typically 20 to 50 Å thick. $Pb_{1-x}Eu_xTe$, which is the barrier to provide the two-dimensional quantum-confinement of electrons in the PbTe well, is about 460 Å thick [15, 20]. The PbTe layers are left undoped and the barriers are doped with Bi [15]. This approach to doping is called modulation doping [21]. More details on the growth and charactetrization of these structures will be published soon [22].

OMVPE of Bi_2Te_3 / Sb_2Te_3 Superlattices

To our knowledge, there had been no reported OMVPE growth of Bi_2Te_3 and related materials about two years ago when we began the experimental evaluation of thermoelectric properties of Bi_2Te_3/Sb_2Te_3 superlattices. However, OMVPE, being a kinetically-limited deposition process rather than an equilibrium-driven process, has been successful in the synthesis of a variety of materials including those with miscibility gaps. Further, the availability of a wide range of organometallic precursors for Te with extremely low cracking temperatures was a good starting point.

A schematic of the thin-film Bi_2Te_3/Sb_2Te_3 superlattice structure that we have proposed as an alternative to the conventional bulk alloy is shown in Figure 1. In this review, we will consider the thermoelectric properties of two types of superlattice structures. One type is the symmetric superlattice, where the thickness of the Bi_2Te_3 and the Sb_2Te_3 layers are kept the same. The other is the non-symmetric superlattice, where the thickness of the Sb_2Te_3 layer is larger than the Bi_2Te_3 layer.

OMVPE/LPCVD growth system used to deposit the materials, has been designed to allow the fabrication of high quality superlattice structures. The OMVPE growth process is easily amenable to scaling for large-area applications, if a thin-film device fabrication demands it, as discussed in the following section on approaches to thin-film thermoelectric devices. We have grown Bi_2Te_3 and Sb_2Te_3 films on both semi-insulating GaAs substrates and Al_2O_3 substrates [23]. The growth has been achieved by a novel combination of high-temperature cracking of organometallic precursors and low substrate temperatures [24]. This new approach to OMVPE has been instrumental in obtaining single-crystalline Bi_2Te_3 films and growth of thermally stable, single-crystalline films of Sb_2Te_3.

X-ray diffraction data obtained on Bi_2Te_3 films on Al_2O_3 and GaAs indicate single-crystallinity. Low-energy electron diffraction data has confirmed the single-crystallinity of the film as well. The x-ray full-width at half-maximum, a quality parameter, of the films are comparable with a recently reported MBE-grown Bi_2Te_3 film on a Sb_2Te_3 substrate [25], in spite of a larger lattice mismatch between the Bi_2Te_3 film and an Al_2O_3 substrate visa-vis Bi_2Te_3 film and a Sb_2Te_3 substrate. The stoichiometry of Bi_2Te_3 and Sb_2Te_3 films have been confirmed by Rutherford backscattering and X-ray photoemission spectroscopy (XPS), respectively. The as-grown Sb_2Te_3 films are always p-type, determined by Hall-effect measurements. The as-grown Bi_2Te_3 films are always n-type, while the Bi_2Te_3/Sb_2Te_3 superlattice structures were always found to be p-type. More details of the growth of these materials are presented elsewhere [26].

An important concern in the growth of superlattices, in any material system, is the possibility of inter-mixing between the constituent layers of the superlattice. In this re-

Figure 1.

Schematic of a short-period p-type Bi_2Te_3/Sb_2Te_3 superlattice structure that we have investigated as an alternative to a conventional bulk alloy in p-type $(Bi_{0.25}Sb_{0.75})_2Te_3$. In this paper, when $L_S=L_B$, it is denoted as a symmetrical superlattice and when $L_S>L_B$, it is denoted as a non-symmetrical superlattice.

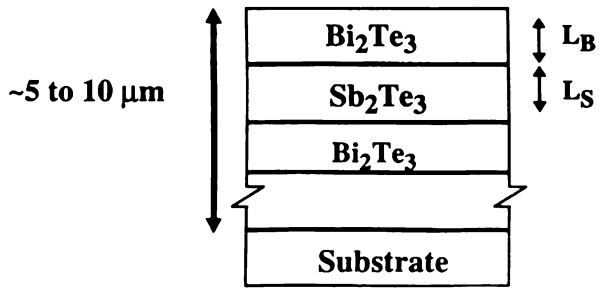

gard, it is instructive to examine the crystal structure of a layered Bi_2Te_3/Sb_2Te_3 material, along the growth direction. The schematic of this crystal structure for a ~17 Å superlattice dimension is shown in Figure 2. We note the periodic van der Walls-like bond within Bi_2Te_3 and between Bi_2Te_3 and Sb_2Te_3 layers in this structure.

Figure 2.

Crystal structure of a layered Bi_2Te_3/Sb_2Te_3 material along the growth direction. Note the presence of van der Walls-like bonding along the c-axis.

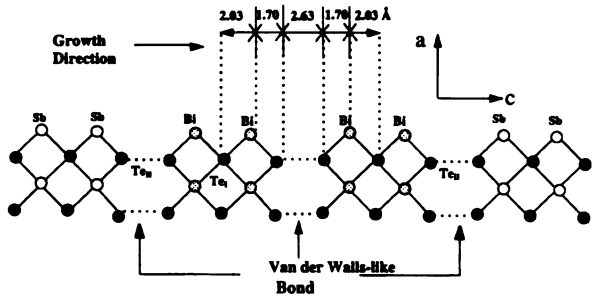

It has been predicted that this type of layered structure, with van der Walls bonding along the growth direction, lends itself amenable for obtaining abrupt surface terminations [27] thereby potentially leading to high-quality superlattice interfaces. This was evident in the XPS spectra obtained on a very thin (< 50 Å) Sb_2Te_3 layer grown on a thick Bi_2Te_3 layer. XPS data, evaluated in both normal and glancing modes, indicated a negligible presence of Bi in the surface Sb_2Te_3 layer. This provided some evidence that abrupt termination of the Bi_2Te_3 layer, prior to the growth of Sb_2Te_3 layer, was likely achieved. The quality of the Bi_2Te_3/Sb_2Te_3 superlattice structures were assessed by single-crystal x-ray diffraction. In the diffraction spectrum, clear satellite peaks (corresponding to the periodicity of the superlattices) [28] were obtained. Good agreement was obtained between the nominal value of the period estimated from growth-rates of the individual layers and the superlattice period deduced from the position of the satellite peaks. We have also recently evaluated these superlattices by double-crystal x-ray diffraction and transmission electron microscopy (TEM) [26]. The TEM data, considering that the sample preparation for microscopy with the "soft" Bi_2Te_3 and related materials are in its infancy, has indicated that good quality interfaces were achieved in the OMVPE-grown Bi_2Te_3/Sb_2Te_3 superlattices.

Thermoelectric Properties of Quantum-well and Superlattice Structures

Power Factor Enhancement in PbTe / $Pb_{0.927}Eu_{0.073}Te$ Quantum Wells

Harman et al. have recently reported on the in-plane Seebeck coefficient in PbTe quantum wells, as a function of free-carrier concentration, for a pair of quantum-well dimensions [15] and compared them to bulk and epitaxial PbTe materials. This data is reproduced in Figure 3. The excellent agreement of Seebeck coefficient as a function of doping level in epitaxial materials, visa-vis those of bulk materials, attests to the validity of the measurement of Seebeck coefficients in thin epitaxial films. The Seebeck coefficient of quantum-well structures show a significant enhancement over bulk materials only when quantum-well dimensions are about 20Å as opposed to 40 Å. This experimental investigation was done to test the theoretical model [8, 20], which predicts a large increase in power factor (and hence ZT) in multiple quantum-well structures. Good agreement was found between the experimental results and the calculations

Figure 3.

Seebeck coefficient of bulk PbTe and PbTe quantum-wells as a function of carrier concentration [15].

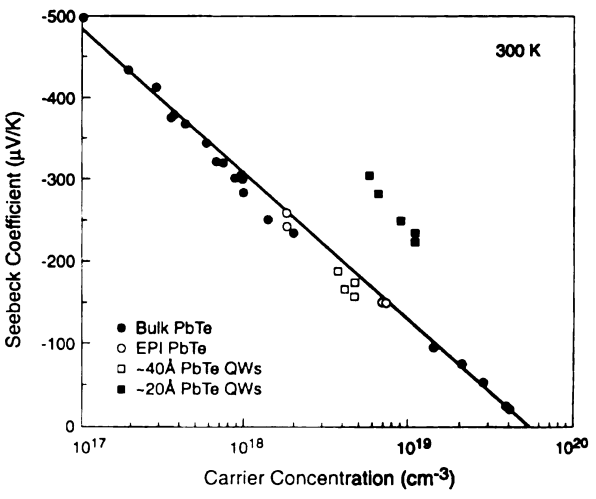

[20], giving an apparent experimental confirmation of the model. The ability to obtain higher Seebeck coefficient, for the same carrier density with apparently no loss of electronic mobility, translates to improved power factor for the 20-Å quantum-well structure. The power factor of the 20-Å PbTe quantum-well is almost a factor three better than that of bulk PbTe. Some recent work indicates that improved growth parameters can lead to higher Seebeck coefficient (also) for the 40-Å quantum-well compared to bulk PbTe.

Potential ZT in PbTe/ $Pb_{0.927}Eu_{0.073}Te$ Quantum-Well Structures

The improved power factor in the 20-Å PbTe quantum-well, in combination with an *estimated* thermal conductivity, results in a $Z_{2D}T$ *of 1.3 at 300K*. This is a factor of three higher than that of the best bulk PbTe materials [15]. The $Z_{2D}T$ is a two-dimensional figure-of-merit for the two-dimensional PbTe quantum-well and neglects the parasitic thermal conductivity of the barrier layer; when this is accounted for, a three-dimensional $Z_{3D}T$ *of 0.11* is estimated [15, 29].

Power Factor Enhancement in Bi_2Te_3 / Sb_2Te_3 Superlattices

Hall-data indicates the residual hole concentration increases in the symmetrical Bi_2Te_3/Sb_2Te_3 superlattice structures, with smaller superlattice dimension. Note here that the superlattice dimension refers to the thickness of each of the Bi_2Te_3 and Sb_2Te_3 components, which is kept about equal for the symmetrical superlattice structures. The noticeable sharp increase in residual p-type behavior with smaller superlattice dimension (achieved by more Bi_2Te_3 and Sb_2Te_3 growth switchings) suggests that Te-vacancy defects are possibly formed at the superlattice interfaces. Such defects are expected to behave as acceptors [30]. Recently, we have minimized this rapid increase in carrier concentration in short-period superlattices with higher Te-vapor pressure during OMVPE growth, consistent with this Te-vacancy argument.

The behavior of the Hall hole-mobility as a function of the superlattice dimension, for the case of symmetrical superlattice structures, is indicated in Figure 4a. Here, we notice that for all the superlattice dimensions, the hole mobility is higher than that of a corresponding $(Bi_{0.5}Sb_{0.5})_2Te_3$ alloy with a similar resistivity. Even for a superlattice dimension of ~10Å, the mobility of the superlattice structure is better than the comparable solid solution alloy. This is *evidence of avoiding or minimizing alloy scattering of carriers in* Bi_2Te_3/Sb_2Te_3 superlattices, relative to the $(Bi_{0.5}Sb_{0.5})_2Te_3$ alloy. However, we do notice a big drop in mobility when the superlattice dimension falls below the unit cell dimension of ~30 Å. The dependence of carrier mobility on the superlattice dimension for the non-symmetrical superlattice structures, with a constant Bi_2Te_3 layer thickness of ~15 Å, is shown in Figure 4b. We once again note that for a Sb_2Te_3 layer dimension >30 Å, the mobility of the superlattice structure exceeds that of a typical solid solution $(Bi_{0.5}Sb_{1.5})$ Te_3 alloy.

The dependence of the 300K Seebeck coefficient of the symmetrical and non-symmetrical Bi_2Te_3/Sb_2Te_3 superlattice structures on the superlattice-dimension is shown in Figure 5a and 5b, respectively. For the symmetrical case, we see a near 50% increase in the Seebeck coefficient with nearly a ten-fold reduction in the superlattice dimension. This increase is relatively small compared to a near 100% increase in Seebeck coefficient, in going from a 40-Å well to a 20-Å well, in the case of $PbTe/Pb_{0.927}Eu_{0.073}Te$ quantum-well system (Figure 3).

Figure 4.

Carrier mobility variation with superlattice dimension in (a) symmetrical and (b) non-symmetrical Bi_2Te_3/Sb_2Te_3 superlattice structures.

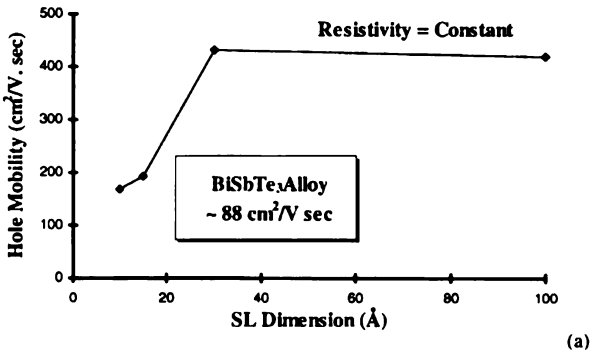

(a)

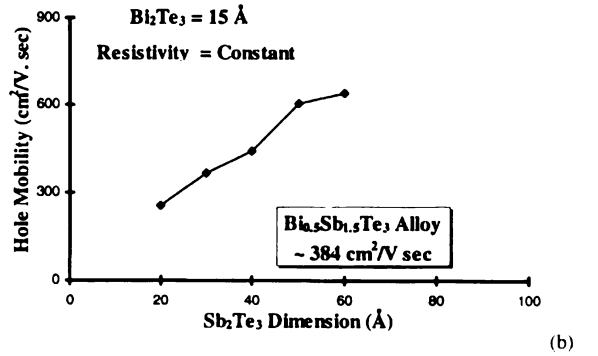

(b)

Figure 5.

Variation of the Seebeck coefficient with superlattice dimension in (a) symmetrical and (b) non-symmetrical superlattice structures.

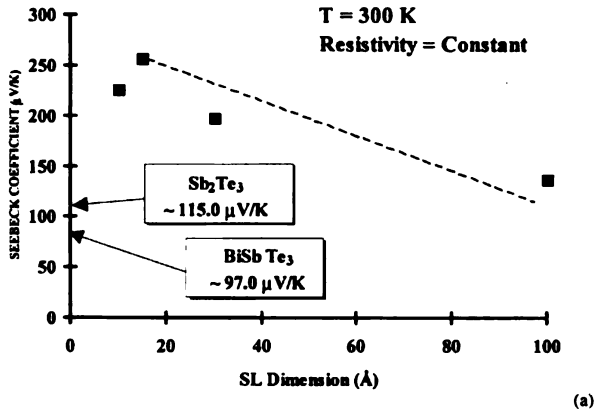

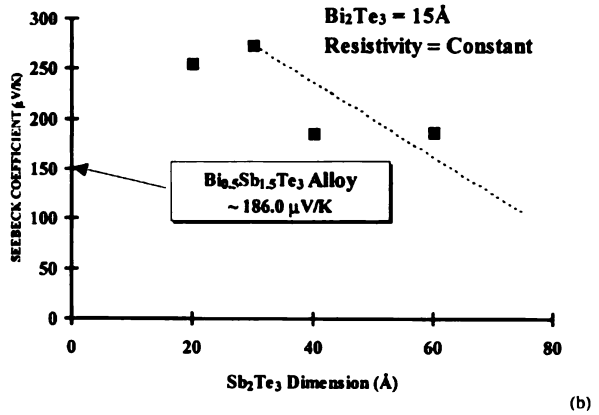

The above difference in the behavior of Seebeck coefficients with the superlattice dimension can be interpreted in terms of the likely difference in the properties of Bi_2Te_3/Sb_2Te_3 and $PbTe/Pb_{0.927}Eu_{0.073}Te$ hetero-interfaces. The bandgap difference between PbTe and $Pb_{0.927}Eu_{0.073}Te$ is about 0.31 eV at 300K, leading to a conduction-band offset of ~0.17 eV in the n-type $PbTe/Pb_{0.927}Eu_{0.073}Te$ hetero-junction [20]. This conduction-band offset provides the necessary barrier for the quantum-confinement of electrons in the PbTe-well. In contrast, the bandgap difference between Bi_2Te_3 and Sb_2Te_3 materials is expected to be less than 0.05 eV at 300K [10]. The distribution of this small bandgap difference in the Bi_2Te_3/Sb_2Te_3 superlattice system, between a valence-band offset and a conduction-band offset, has not been measured. However, if we assume that these band-offsets are about equal (~0.03 eV), we expect only a weak hole-quantum-confinement in the p-type Bi_2Te_3/Sb_2Te_3 superlattices at 300K. This could explain the slow rise in Seebeck coefficient with smaller superlattice dimensions in the Bi_2Te_3/Sb_2Te_3 system. We also note a small drop in Seebeck coefficient with decrease in superlattice dimension, in the range of 20 Å to ~10 Å, probably from a result of the sharp increase in carrier levels. The 300K Seebeck coefficients of the non-symmetrical Bi_2Te_3/Sb_2Te_3 superlattice structures also increase slowly with a reduction in the superlattice dimension as seen in Fig. 5b.

It is important to note in both Fig. 5a and 5b, the Seebeck coefficients of the short-period symmetrical and non-symmetrical superlattice structures are higher than that of a $BiSbTe_3$-alloy film and a typical $(Bi_{0.5}Sb_{0.5})_2Te_3$-alloy film, respectively. This can be attributed in part to the Fermi-level differences between the respective superlattice structure and the corresponding alloy film. The relation to obtain the Seebeck coefficient of a p-type material is given by the relation below:

$$\alpha = \frac{k}{e}\left[\frac{\int_{E=E_v}^{\infty} E^{*}\sigma(E)\,dE}{\int_{E=E_v}^{\infty}\sigma(E)\,dE} - E_f^{*}\right]$$

Here, σ is the conductivity, E^* is the reduced energy of holes in the valence band and E_f^* is the reduced Fermi-energy. For the same conductivity, the higher mobility in the superlattice (compared to the alloy) leads to a lower carrier concentration and therefore a lower hole-E_f^*. This can potentially lead to a higher Seebeck coefficient for the superlattice structure when compared to the alloy.

The effect of an improved hole mobility for a larger Seebeck coefficient is to increase the power factor in short-period p-type Bi_2Te_3/Sb_2Te_3 superlattice structures. We have observed that that the power factor of the non-symmetric superlattice structures are consistently higher than the symmetrical superlattices, due to the effect of higher mobilities for the same resistivities. We have observed a best power factor in the range of 55 $\mu W/cm\text{-}K^2$ in a non-symmetrical Bi_2Te_3/Sb_2Te_3 (15 Å/45 Å) superlattice structure at 300K.

An important concern in the measurement of thermoelectric properties of thin-film is the possible effect of the substrate. We have compared the Hall-effect carrier concentration and mobility on Bi_2Te_3/Sb_2Te_3 symmetrical superlattices (for a constant superlattice dimension) on a semi-insulating GaAs and an insulating Al_2O_3 substrate. The comparable data on the two substrates, given our observation that the morphological-quality of Bi_2Te_3 and Sb_2Te_3 films are generally better on GaAs substrates than on Al_2O_3 substrates, suggests to the absence of any effects of the substrate. Also in this regard, we have grown several thin-film p-type $(Bi_{0.25}Sb_{0.75})_2Te_3$ alloy layers on semi-insulating GaAs substrates and compared their Seebeck coefficients to bulk p-type $(Bi_{0.25}Sb_{0.75})_2Te_3$ alloy materials, as a function of free-

carrier levels. We have found good correlation [16] of the Seebeck coefficient, as a function of the free-carrier level, between these epitaxial thin-films and those of bulk materials [30]. This further attests to the validity of our measurement of the Seebeck coefficient in thin-films, similar to the above-discussed correlation in Seebeck coefficients of epitaxial-PbTe and bulk-PbTe materials.

Thermal Conductivity Reduction in Bi_2Te_3/Sb_2Te_3 Superlattices

An important objective of our experimental research effort on short-period Bi_2Te_3/Sb_2Te_3 superlattices has been to demonstrate that phonon-scattering at the superlattice interfaces can reduce the lattice thermal conductivity and then verify if it is indeed possible to obtain values lower than in solid-solution $(Bi_{0.25}Sb_{0.75})_2Te_3$ alloys [10] from additional phonon-scattering processes unique to periodic structures. For example, in a superlattice, the minimum phonon energy required to produce an Umklapp process is reduced relative to a bulk alloy. Thus a measurement of thermal conductivity is important to take further advantage of the improved electrical transport and power factor of Bi_2Te_3/Sb_2Te_3 superlattices, in the overall optimization of ZT values.

The modified 3-ω technique [31] has been used to measure thermal conductivity (λ) of thin-films from an indirect measurement of thermal diffusivity. Essentially, a thin metal strip with four pads to measure current and voltage is deposited on the film surface. The metal strip serves as the heater (by I^2 R heating) and a thermometer because of the temperature-dependent electrical resistance of the strip is related to the thermal conductivity of the thermoelectric material. Thus the thermal conductivity can be related to measured voltages. The application of an ac current (I) with an angular frequency ω causes a I^2 R heating temperature wave of frequency 2ω to diffuse into the substrate. Since the film resistance itself varies with temperature, the resistance oscillation at 2ω multiplied by the excitation current at ω produces a voltage oscillation at 3ω. The 3ω voltage can be conveniently measured by a lock-in amplifier technique.

Figure 6 shows the thermal conductivity data on both symmetrical and non-symmetrical Bi_2Te_3/Sb_2Te_3 superlattice structures as a function of the superlattice dimension. The thermal conductivity values apparently come down with a shorter superlattice dimension, although the superlattice structures in general (for periods in the range of ~100 Å or less) do indicate reduced thermal conductivities compared to bulk materials. We observe an apparent minimum thermal conductivity when the Bi_2Te_3 or Sb_2Te_3 dimension approaches ~30 Å, the unit cell dimension. For these superlattice dimensions, we obtain thermal conductivity values as low as ~2.0 mW/cm-K. *It is worth observing that both the symmetrical and non-symmetrical superlattices apparently offer about the same value for minimum thermal conductivity at a dimension of ~30Å, indicating that the thermal conductivities in these superlattices are likely dominated by phonon scattering and reduced phonon group velocities as a result of the superlattice structure, rather than the bulk-like phonon scattering processes.* It is also interesting to note that when the superlattice dimension is less than ~30 Å, the unit cell dimension, the measured thermal conductivities actually increase and tend to approach the values measured for the respective alloy films.

Figure 6.

Variation of thermal conductivity with superlattice dimension in symmetrical and non-symmetrical Bi_2Te_3/Sb_2Te_3 superlattice structures.

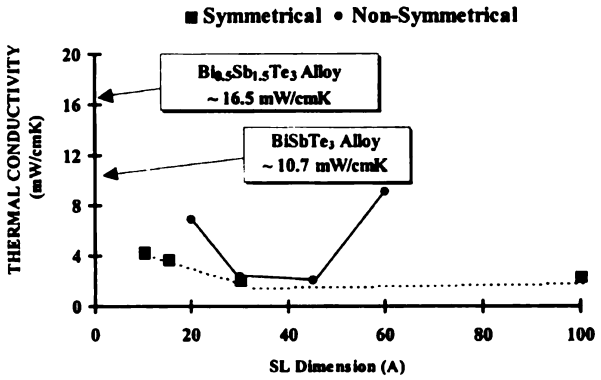

Comments on 3ω-Measured Thermal Conductivities in Superlattices

It is worth noting that the measured 3ω thermal conductivity value for the p-$(Bi_{0.25}Sb_{0.75})_2Te_3$ alloy film is ~16.5 mW/cm-K and for the p-(BiSb) Te_3 alloy film is ~10.7 mW/cm-K. These are approximately equal to the geometric mean of known thermal conductivities, along the "a" and "c" directions, in bulk crystals of these materials [1, 30]. Thus the 3ω-thermal conductivity method, at least for the frequencies (~1000 Hz) used in this study, could also be affected by the spread of the thermal wave in the direction parallel to the superlattice interfaces. It appears that the 3ω thermal conductivity value is not likely to be dominated solely by the component perpendicular to the superlattice interfaces. This was further evident in the observation that the 3ω-measured thermal conductivities in $GaAs/Al_{0.8}Ga_{0.2}As$ superlattices were comparable to the in-plane thermal conductivity values of GaAs/AlAs superlattices measured by AC calorimetry [12] and larger than the perpendicular thermal

conductivity values in GaAs/AlAs superlattices, determined by a pico-second reflectivity-optics method [32]. For example, the pico-second optics method on a ~50Å/50Å GaAs/AlAs superlattice indicated a factor-of-2 to 3 lower thermal conductivity compared to values obtained by the 3ω method or the in-plane method for similar superlattice dimensions.

In essence, we note that the thermal conductivity values of the Bi_2Te_3/Sb_2Te_3 superlattice structures need to be evaluated by a "true" through-thickness method (such as in Ref. 32) to measure the component perpendicular to the interfaces and a "true" in-plane method, with the substrate removed as in Ref. 12, to obtain the thermal conductivity parallel to the superlattice interfaces.

Potential ZT in Bi_2Te_3/Sb_2Te_3 Superlattice Structures

The power factors in Bi_2Te_3/Sb_2Te_3 superlattice structures, in this work, have been measured in a direction parallel to the superlattice interfaces. As mentioned in the previous section, the directional nature of the 3-ω thermal conductivity value is not completely clear at this point in time. In addition, unlike GaAs and AlAs materials, Bi_2Te_3 and Sb_2Te_3 materials do exhibit anisotropic thermal conductivities. This makes the determination of ZT values of the Bi_2Te_3/Sb_2Te_3 superlattice structures not straightforward.

However, as noted earlier, in the short-period Bi_2Te_3/Sb_2Te_3 superlattice structures where the thermal conductivity values are as low as ~2.0 mW/cmK, the superlattice interfaces rather than the bulk properties probably control the thermal conductivity values. So, we need to potentially correct for typical anisotropy of thermal conductivities in superlattice structures, rather than for bulk-like anisotropies. We can estimate the possible anisotropy of thermal conductivity values in Bi_2Te_3/Sb_2Te_3 superlattice structures based on some recent comparative measurement [33] of thermal conductivities in GaAs/AlAs superlattices, along both perpendicular and parallel to the superlattice interfaces. This work in Ref. 33 suggests that, in a worst-case scenario, the thermal conductivity value parallel to superlattice interfaces could be higher than that along perpendicular to the interfaces by a factor of about 2.6; similarly, we estimate that the thermal conductivities of the Bi_2Te_3/Sb_2Te_3 superlattices could be probably higher in the plane of the superlattice-interfaces by this ratio. This leads us to estimate a three-dimensional ZT_{3D} of around 2.0 at 300K for some of the best Bi_2Te_3/Sb_2Te_3 superlattice samples in the direction parallel to the superlattice interfaces. This data is indicated in Table 1. In this estimation, we have used the power factors measured at MIT-Lincoln Laboratories for the Bi_2Te_3/Sb_2Te_3 superlattices. Also shown in Table 1 are the ZT values in comparable alloy films, based on RTI-measured power factors. We note that the power factors measured at RTI on the Bi_2Te_3/Sb_2Te_3 superlattices, done similar to these alloy samples, have agreed well with the measurement at MIT-Lincoln Laboratories. Hence, the ZT enhancement in Bi_2Te_3/Sb_2Te_3 superlattice structures over comparable alloy films, grown by OMVPE, and the state-of-the-art bulk materials (typically around 0.9 to 1.0) are noteworthy.

The estimation of ZT_{3D} for the Bi_2Te_3/Sb_2Te_3 superlattices, in the direction perpendicular to the superlattice interfaces, is much more complicated and will require the measurement of Seebeck coefficient and electrical conductivity in this direction. Such an effort is in progress.

Approaches to Thin-Film Thermoelectric Devices

Recently, Farmer et. al [17] have demonstrated a miniature thermoelectric cooling device with an 8-micron-thick, sputtered, p-$(Bi_{0.25}Sb_{0.75})_2Te_3$ and n- $Bi_{0.9}Sb_{0.1}$ thin-films, respectively, on 25-μm-thick mica substrate. These devices were operated with a duty-cycle of 0.3, instead of a conventional, continuous, direct-current operation and a cooling of 5 to 10°C below the ambient was obtained. This is an encouraging result and portends well for thermoelectric devices based on high-ZT superlattice thin-films.

The results on superlattice and quantum-well structures grown by epitaxial techniques for high-ZT thermoelectric applications, although appear very promising, need to be balanced with the fact that these epitaxial techniques are ideally suited for producing thin layers and structures, typically ~ 5 to 10 μm thick, as a result of smaller growth rates. Typically, growth rates are 0.1 μm/min in OMVPE systems and 0.02 μm/min in MBE systems. These growth rates are adequate for the deposition of thin-films required for many electronic applications. However, practical thermoelectric elements require 200- to 1000-μm-thick layers [1] in the direction of heat flow, i.e., along the thermal gradient. The Peltier contact area is used to pump heat from the cold junction to the hot junction. Parasitic thermal conduction from the hot junction toward the cold junction and Joule heating oppose the Peltier-induced heat flow. A smaller thermal gradient is required to reduce this reverse flow of heat i.e., maintain certain optimum spatial separation between the hot and cold junctions. Typically, this separation is ~ 200 to 1000 μm and it would seem that it will be difficult to grow *high-quality* epitaxial *superlattice structures* to such thickness, even by present-day thin-film deposition techniques like MBE and OMVPE.

One approach [34] to utilizing the superlattice structures as high-performance thermoelectric elements, therefore, may be to process the thin-films (~5 to 10 μm) into a thermoelectric element of effective lengths of ~100 to ~500 μm using a planar monolithically-interconnected, superlattice-structured thermoelement (MISST) approach [10]. With the MISST approach, the ohmic contacts can po-

tentially generate significant I^2R heating, leading to a degradation of performance from that obtainable with an enhanced ZT. Initial modeling of the cooling-performance of the MISST device indicates that using only four segments on each of the n- and p-type element, with an epitaxial layer thickness of ~10 μm, a resistivity of ~3E-3 ohm-cm for the superlattice material, a Peltier contact resistivity of 1E-6 ohm-cm^2, an ohmic-contact resistivity of 5E-7 ohm-cm^2, an effective device ZT of ~1.5 may be obtained with an intrinsic ZT of ~2.3. Therefore, good quality ohmic contacts at each of the vertical segment are necessary to reduce I^2R losses, which can affect the overall cooling efficiency. We note that the use of a limited number of segments in the MISST device in conjunction with a reduction in radiative heat loss from the ohmic-contact surfaces, and minimization of thermal conduction losses through the supporting-superstrate like Kapton, would help ameliorate the parasitic thermal exchange with the ambient.

The MISST concept, if successful, can alleviate the necessity of epitaxially growing thick epitaxial superlattice-type layers, as required in other possible approaches to fabrication of a thin-film thermoelectric device [9]. The MISST device processing technique can enable the cost-effective fabrication of high-performance thermoelements from superlattice-type materials as well as non-superlattice thin-film materials. Fairly simple, conventional microelectronic processing is required to fabricate these thermoelements. Two sets of wafers need to be processed, one for the n-type leg and the other for a p-type leg, which are then interconnected to form a cooling element. The attachment of the thermally insulating superstrate like Kapton will enable the removal of the growth-substrate. This superstrate provides mechanical support for the interdigitated n-type and p-type legs. While a smaller thickness of the Kapton superstrate is preferable for reducing the parasitic thermal conduction loss, a larger thickness will facilitate device handling.

Near-Term Research Issues

In earlier sections, we pointed out several aspects of thermoelectric properties of both PbTe quantum-well structures and Bi_2Te_3/Sb_2Te_3 superlattices that merit a closer look. Specifically, in MBE-grown $PbTe/Pb_{0.927}Eu_{0.073}Te$ structures, the requirement of a fairly thick (460 Å) $Pb_{0.927}Eu_{0.073}Te$ barrier compared to the quantum-well (20 Å) results in a substantial degradation of an estimated, effective 3-dimensional ZT compared to an excellent ZT_{2D} of ~1.2 for the PbTe quantum-well. There is a clear need to measure thermal conductivity of these $PbTe/Pb_{0.927}Eu_{0.073}Te$ structures, by methods such as 3-ω, to obtain an estimate of $Z_{3D}T$. The thermal conductivity results on Bi_2Te_3/Sb_2Te_3 superlattice structures [16] should be an incentive to explore these $PbTe/Pb_{0.927}Eu_{0.073}Te$ structures as well. As suggested by Harman et. al [15], other

Table 1.

Potential ZT in Bi_2Te_3/Sb_2Te_3 superlattice samples.

Sample #	MIT-LL Power Factor	RTI Power Factor	Through-Thickness Thermal Conductivity ($K_\perp$)	Estimated In-Plane Thermal Conductivity (K_a)	Estimated In-Plane ZT at 300 K	Material type	Comment
	(μW/cm-K^2)	(μW/cm-K^2)	(mW/cm-K)	(mW/cm-K)			
7-253	37.8		4.35	11.3	**1.0**	SL Period ~ 20 Å	$t_{Bi2Te3} = t_{Sb2Te3}$
7-258	40.7		2.05	5.3	**2.3**	SL Period ~ 60 Å	$t_{Bi2Te3} = t_{Sb2Te3}$
7-223	28.3		4.3	11.2	**0.8**	SL Period ~ 20 Å	$t_{Bi2Te3} = t_{Sb2Te3}$
7-270	19.3		2.4	6.2	**0.9**	SL Period ~ 200 Å	$t_{Bi2Te3} = t_{Sb2Te3}$
7-327	31.8		2.1	5.5	**1.7**	SL Period ~ 60 Å	$t_{Bi2Te3} = 1/3\ t_{Sb2Te3}$
7-323	32.4		3.7	9.6	**1.0**	SL Period ~ 30 Å	$t_{Bi2Te3} = t_{Sb2Te3}$
7-260		24.1	16.5	16.5	**0.44**	$Bi_{0.5}Sb_{1.5}Te_3$ Alloy	
7-214		1.8	10.7	10.7	**0.05**	$BiSbTe_3$ Alloy	

quantum-well/barrier combinations such as $Bi_zSb_{1-z}/Pb_xEu_{1-x}Te_ySe_{1-y}$ or a suitable alternative need to be explored to obtain higher $Z_{2D}T$ of up to ~8.0 and correspondingly $Z_{3D}T$ of near 3.0. This should help overcome some of the restrictions posed by the requirement of thick barrier layers in the quantum-well approach.

The early results on thermoelectric properties of Bi_2Te_3/Sb_2Te_3 superlattice structures appear to suggest that it may be possible to break the traditional, conflicting requirements for high electrical conductivity and low thermal conductivity encountered in bulk thermoelectric materials. Superlattices may offer a route to minimize carrier scattering and obtain improved transport properties including thermoelectric power-factor, by avoiding solid-solution alloying; yet the superlattice interfaces can enhance phonon scattering rates and reduce lattice thermal conductivity. One of the key issues in this material system remains - what are the conduction and valence band offsets so that a better theoretical understanding of the observed enhancement in thermoelectric properties can emerge. Another key issue is the accurate measurement of the thermal conductivity in superlattice structures, along specific directions.

From an experimental standpoint, it is worth noting the importance of high-quality Bi_2Te_3/Sb_2Te_3 superlattice structures on improvement in thermoelectric properties. We have observed that the effect of an intentional disorder in the superlattices is to reduce the Seebeck coefficient and increase the thermal conductivity. The disorder was simulated by intentionally making the Bi_2Te_3 component of the superlattice as an alloy layer. Such controlled studies of the Bi_2Te_3/Sb_2Te_3 superlattice in conjunction with measurements of hetero-interface properties are urgently needed. A major issue remains the reliable measurement of all three thermoelectric properties of thin-film structures, namely the Seebeck coefficient, the electrical conductivity, and the thermal conductivity, both parallel and perpendicular to the superlattice interfaces. Uher and Moreli discuss some of these aspects in a companion paper in this issue.

Development and testing of thin-film thermoelectric devices employing some of the superlattice structures (with the higher estimated ZT values) are needed. Thin-film device design optimization will include identification of the necessary dimensions based on thermoelectric material parameters. Significant process development issues will have to be addressed depending on the thin-film device approach employed in the fabrication. The device process development such as joining the n-type and p-type superlattice elements together, aligning and joining them to an electrical path, and providing for the structural rigidity of the resulting structure, are expected to be significant engineering problems that can be overcome once we are convinced that we do have ZT>1 in thermoelectric materials based on superlattice structures.

Acknowledgments

The author acknowledges the technical contributions of Mr. Thomas Colpitts, Mr. Eric Watko, Mr. Mike Mantini and Mr. Dave Malta during the course of this work. The author also acknowledges Dr. Ted Harman of MIT Lincoln Laboratories for the verification of power factors in the Bi_2Te_3/Sb_2Te_3 superlattice structures as well as many valuable comments during the review of this manuscript.

The editor wishes to acknowledge Dr. Ted Harman of MIT Lincoln Laboratory for assistance in the review of the scientific and technical details of the article and for volunteering to assist in measuring properties of thin film structures reported in this article.

Biography

Dr. Rama Venkatasubramanian received his Ph.D. in Electrical Engineering in 1988 from Rensselaer Polytechnic Institute, Troy, New York. He was a recipient of the Allen B. Dumont Prize at Rensselaer for outstanding academic achievement. Prior to his graduate work at Rensselaer, he obtained his B.S in Electrical Engineering in 1983 from the Indian Institute of Technology, Madras, India. He is a recipient of the National Talent Search Scholarship during his undergraduate work. Since 1989, he has been with the Center for Semiconductor Research, Research Triangle Institute, in North Carolina. Presently, he is a Senior Research Engineer working in the area of thermoelectrics, photovoltaics and other electronic materials for device applications. He has over 75 publications in the area of heteroepitaxy, characterization of electronic materials, novel optoelectronic materials based on quantum-confined structures, thermoelectrics, photovoltaics and other devices.

REFERENCES

1. F.D. Rosi and E.G. Ramberg, "Evaluation and Properties of Materials for Thermoelectric Applications," in Thermoelectricity, Ed. by P. H. Egli, John Wiley and Sons, NY (1960).
2. A.Y. Cho and J.R. Arthur, Progress in Solid State Chemistry, G. Somorjai and J. McCaldin Eds. **10**, (1973), p.157.
3. G.B. Stringfellow, *Organometallic Vapor Phase Epitaxy: Theory and Practice*, Academic Press, London, (1989).
4. M.E. Jones and D.W. Shaw, *Growth from the Vapor, from Treatise on Solid State Chemistry*, **5**, N.B. Hannay, Ed., Plenum, New York **(1976).**
5. L. Esaki and R. Tsu, IBM J. Res. **Dev., 14, 61**

(1970).
6. T.E. Whall and E.H. C. Parker, Proc. of First European Conf. on Thermoelectrics, D.M. Rowe, Ed., 51 (1987) and references there in.
7. 1st National Thermogenic Cooler Conference, Sept. 17, 1992, Fort Belvoir, VA.
8. L.D. Hicks and M.S. Dresselhaus, "The Effect of Quantum Well Structures on the Thermoelectric Figure of Merit," Presented at the 1st National Thermogenic Cooler Workshop, Sept. 17, 1992, Fort Belvoir, VA.
9. T.C. Harman, "PbTeSe/BiSb Short-Period Superlattice as a New Thermoelectric Cooler Material," Presented at the 1st National Thermogenic Cooler Workshop, Sept. 17, 1992, Fort Belvoir, VA.
10. R. Venkatasubramanian, "Organometallic Epitaxy of Bi_2Te_3 and Related Materials and the Development of Planar, Monolithically-Interconnected, Superlattice-Structured, High-Efficiency Thermoelectric Elements," Presented at the 1st National Thermogenic Coler Workshop, Sept. 17, 1992, Fort Belvoir, VA.
11. B. Jusserand and D. Paquet, "Confined and Propogative Vibrations in Superlattices," in Heterojunctions and Semiconductor Superlattices, Ed. by G. Allan, G. Bastard, M. Launoo, and M. Voos, Springer Verlag, 1986.
12. T. Yao, Appl. Phys. Lett., **51**, 1798 (1987).
13. D.A. Broido and T.L. Reinecke, Appl. Phys. Lett., **67**, 1170 (1995).
14. J.O. Sofo and G.D. Mahan, Proc. of the 13th International Conf. on Thermoelectrics, AIP Conf. Proc., **316**, 239 (1995).
15. T. Harman, Proc. of ARPA Thermoelectric Materials Workshop, Arlington, VA, November 1995.
16. R. Venkatasubramanian, Proc. of ARPA Thermoelectric Materials Workshop, Arlington, VA, November 1995.
17. J. C. Farmer, Proc. of ARPA Thermoelectric Materials Workshop, Arlington, VA, November 1995.
18. N.B. Elsner, S. Ghamaty, J.H. Norman, J.C. Farmer, R.J. Foreman, L.J. Summers, M.L. Olsen, P.E. Thompson, and K. Wang, Proc. of the 13th International Conf. on Thermoelectrics, AIP Conf. Proc., **316**, 328 (1995).
19. D.L. Partin, J. Electronic Materials, **13**, 493 (1984).
20. G. Dresselhaus, Proc. of ARPA Thermoelectric Materials Workshop, Arlington, VA, November 1995.
21. R. People, J.C. Bean, and D.V. Lang, J. Vac. Sci. Technol., **A3**, 846 (1985).
22. T. Harman, M.M. Manfra, and D.L. Spears, Submitted to J. Electron. Materials.
23. R. Venkatasubramanian, T.S. Colpitts, M. Mantini and D. Malta, Proc. of 14th International Conf. on Thermoelectrics, St. Petersburg, in press (1996).
24. U.S. Patent Provisional Application Serial No. 60/016, 710.
25. A. Mzerd, D. Sayah, J.C. Tedenac, and A. Boyer, J. Cryst. Growth, **140**, 365 (1994).
26. R. Venkatasubramanian and T.S. Colpitts, Presented in the VIII International Conf. on OMVPE, Cardiff, England, June 1996.
27. O. Lang, R. Schlaf, Y. Tomm, C. Pettenkofer, and W. Jaegermann, J. Appl. Phys., **75**, 7805 (1994).
28. B.E. Warren, X-Ray Diffraction , Reading, Mass., Addison-Wesley, (1969).
29. J. Prater, Proc. of ARPA Thermoelectric Materials Workshop, Arlington, VA, November 1995.
30. H. Scherrer and S. Scherrer, Proc. of the 12th International Conf. on Thermoelectrics, Yokohama, H. Mastubara Ed., 90 (1994).
31. D.G. Cahill, M. Katiyar, and J.R. Abelson, Phys. Rev. B, **50**, 6077 (1994).
32. W.S. Capinski and H.J. Marris, "Thermal Conductivity in GaAs/AlAs Superlattices," Paper presented at the March 1996 American Physical Society Symp. on Semiconductors: Transport in Superlattices I; R. Venkatasubramanian, "Thermal Conductivity Reduction in Superlattice Structures," Paper presented at the March 1996 American Physical Society Symp. on Semiconductors: Transport in Superlattices I
33. G. Chen, C.L. Tien, X. Wu, and J.S. Smith, J. Heat Transfer, **116**, 325 (1994).
34. Another approach is to process the 10-mm-thick films into thermoelements of proportionately smaller areas compared to bulk materials.

Profiles in Science

Jean-Pierre Fleurial

Dr. Fleurial earned his Ph.D. in solid state physics and materials science from the National Polytechnique Institute of Lorraine, France, in 1988, during which he developed new growth techniques and theoretical models for high quality single crystals of Bi_2Te_3. In 1988, Dr. Fleurial came to JPL as a National Research Council Resident Research Associate and joined the permanent staff in 1990. He was first involved with the optimization of Si-Ge alloys for thermoelectric power generation. He has calculated ternary and quaternary phase diagrams of Si-Ge alloys, and also performed diffusion and solid solubility studies, liquid phase epitaxial growth of Si-Ge. More recently, Dr. Fleurial has been actively engaged in the study of novel promising thermoelectric materials, in particular compounds with the skutterudite structure. He is also involved in thermoelectric microcoolers and high thermal conductivity materials for resolving thermal management issues. Dr. Fleurial currently leads the JPL Thermoelectric Team and is the active Secretary of the International Thermoelectric Society.

Thierry Caillat

Dr. Caillat earned his Ph.D. in materials science from the National Polytechnique Institute of Lorraine, France, in 1991. During his Ph.D., he conducted experimental and theoretical research on high quality single crystals of p-type Bi_2Te_3-Sb_2Te_3 alloys grown by a novel technique, the traveling heater method. After this research, Dr. Caillat received a National Research Council Fellowship to pursue studies of new semiconducting materials for thermoelectric applications at JPL. He joined the permanent staff at JPL in 1994. In the last five years, he has played a key role in identifying several families of promising compounds for thermoelectric applications, including skutterudites and b-Zn_4Sb_3-based materials. He has been elected to serve as a Board Member of the International Thermoelectric Society from 1996 to 1999.

Profiles in Science (continued)

JPL's Thermoelectric Team, Materials and Device Technologies Group

The staff of Jet Propulsion Lab's (JPL's) Thermoelectrics Team in the Electric Power Systems Section is considered by the international community as a leader in developing thermoelectric materials and understanding thermoelectric power generation and cooling technology. Jean-Pierre Fleurial and Thierry Caillat are noted members of the team receiving support from the Office of Naval Research (ONR). The Team has a proven record of establishing unique facilities as dictated by the needs of a particular study and is widely known for its outstanding materials preparation and characterization capabilities. A wide variety of preparation techniques are exploited: crystal growth and powder metallurgy for bulk materials and various deposition processes for thin films. The electrical resistivity, Hall effect, Seebeck coefficient, thermal diffusivity and the heat capacity can be measured from 4K to 1300K. In addition, equipment built for testing devices at high temperatures and for extended periods of time is considered a key capability.

The Team has also pioneered the development of a comprehensive solid state physics model for the thermal and electrical transport properties of a given material over its full temperature range of usefulness to use as a tool for guiding experimental and for predicting the maximum performance likely to be achieved. In the past 5 years, several programs were initiated on the development of new thermoelectric materials with high thermoelectric efficiencies for space and terrestrial applications. Recent results obtained at JPL and confirmed by other laboratories have shown that ZT (figure of merit) values significantly larger than 1 could be obtained. A new growing area for the Team is the development of thermoelectric microcoolers and high thermal conductivity materials such as diamond for the thermal management of high density power electronics. These JPL programs receive support from ONR, National Aeronautics and Space Administration (NASA), other federal agencies, and private industries.

Thermoelectric Property Measurements

Ctirad Uher, Department of Physics, University of Michigan, Ann Arbor, MI

As discussed elsewhere in this journal, the most important parameter determining whether a given solid is a potentially useful thermoelectric material is the figure of merit $Z = S^2\sigma/\kappa$ or its dimensional equivalent ZT. Here S is the thermoelectric power or the Seebeck coefficient, σ is the electrical conductivity, κ is the thermal conductivity and T is the absolute temperature. Thus, to assess a given material for its thermoelectric potential necessitates measuring the three essential parameters S, σ, and κ. The measurements should be carried out over a wide enough temperature range to gain insight about the trend in the transport behavior and to establish the domain over which the figure of merit is maximized. Often one desires to have more detailed information about the transport properties and an inquiry into the carrier density, the dominant carrier type, mobilities, effective masses and scattering times is relevant and helpful in revealing the overall transport behavior. Such expanded property measurements then include the whole gamut of transport investigations with the Hall effect as clearly the most important one. The singular importance of the Hall effect is the reason why I include it in the review of the transport properties which determine the figure of merit of the thermoelectric materials.

1. Electrical Resistivity

Electrical resistivity is perhaps the most frequently performed measurement on a conducting solid. Because of its conceptual simplicity such a measurement might appear as a straightforward exercise requiring no special considerations. This is not so in practice and, especially in investigations of thermoelectric materials, great care must be used to assure accurate and reliable experimental results.

The measurements of the resistivity can be done by a variety of techniques and the preferred one depends on factors such as the size of a specimen, its shape, magnitude of the resistivity, desired accuracy of the data, available instrumentation and, to a degree, taste and preference of the person conducting the measurements. Before I describe the experimental techniques most frequently applied to measurements of the resistivity it is worthwhile to note the range of

resistivities one encounters in thermoelectric materials. As is stated elsewhere in this journal, the carrier concentration in practical thermoelectrics falls within the range 10^{25}-10^{26} m^{-3} which implies that these materials have rather low values of resistivity somewhere in the 10^{-5} Ω-m range. Thus, accurate measurements necessitate the use of high sensitivity instrumentation. Furthermore, because the resistivity is low, the contact resistance is comparable to the sample resistance and one should avoid using a two probe configuration where the same two contacts serve the dual role of carrying the sample current and sensing the potential difference. For any kind of reliable measurements the use of four probe techniques with well separated current and voltage contacts is essential.

1a. Four-probe bar measurements

Perhaps the most frequently used technique employs a sample in the form of a parallelepiped (bar) with two pairs of contacts (four probes), Fig.1a. One pair serves to inject current through large-area ohmic contacts at the ends of the bar and the other pair, separated from the current contacts, measures the voltage drop along the length of the bar via small-area contacts. It can be shown by a relatively straightforward analysis[1] that by insetting the voltage contacts by a distance not shorter than the width of the sample, the sample current over the distance delineated by the voltage probes will be axial and the equipotentials will remain essentially planar and normal to the bar axis even for highly nonuniform current contacts. The voltage probes are typically held in place by either pressure or by means of a solder or a variety of conducting pastes and epoxies.

Frequently, point contacts may be too resistive and it is preferable to prepare the specimen in the form of a bridge with long and narrow side-arms to which large-area contacts can conveniently be attached. An example of a bridge-shaped sample is given in Fig.1b. Although no current flows through the side-arms they do cause distortions of the equipotentials in their vicinity. Fortunately the effect is rather small for side-arms with the width substantially smaller than the width of the sample and one should aim to make them as narrow as mechanical strength allows. Bridge-shaped samples are a popular geometry and they have an added advantage of being convenient for measuring of the Hall effect in which case either one of the opposing pairs of side-arms could be used to pick up the transverse (Hall) voltage.

The electrical resistivity ρ for the above two sample geometries is given as

$$\rho = \frac{V}{L}\frac{wt}{I} = R\frac{A}{L} \qquad (1)$$

where R is the resistance, L the distance between the voltage probes and A the cross-sectional area of the sample. Thus, this method requires an accurate electrical measurement to determine R as well as a precision mechanical measurement to specify the dimensions of the sample (geometrical factor A/L). A typical experimental set-up to measure the resistivity of a bar or bridge-shaped sample includes a standard resistor of resistance R_s in series with the sample in order to determine the actual current in the circuit $I = V_s/R_s$. The simplicity of this experimental technique is its main draw and appeal. However, when used to measure the electrical resistivity of thermoelectric materials, one needs to be aware of its shortcomings. The chief problem is that the voltage probes pick up the total potential which may or may not consist of contributions from sources other than Ohm's law and it is difficult to account for some of these effects. If one could assume strictly isothermal conditions there would be no problem. Unfortunately one frequently encounters standing thermal gradients ΔT across the sample (either imposed by improper experimental set-up or due to excessive Joule heating) and, because of the large thermopower of thermoelectric materials, these standing thermal gradients contribute thermoelectric voltage $\Delta V = S\,\Delta T$ which is superposed on the truly resistive voltage drop. One can deal with the thermoelectric contributions which originate in the standing thermal gradients simply by reversing the current flow and taking the average of the two readings. A far more serious problem concerns the Peltier effect contribution. As is well known, a passage of current through a junction between two dissimilar metals is accompanied by the heat flux density and this leads, depending on the direction of the current, to liberation or absorption of heat at the junction. Since one usually does not have available fine wire-probes made of the same material as the sample under study, one obviously faces the problem associated with the Peltier heat at the two current contacts. Because the Peltier effect is linear in current, current reversal changes the sign of both the resistive voltage and the Peltier effect and, one cannot separate the re-

Figure 1a.
Bar-shaped sample with a typical arrangement of probes for measurements of the electrical resistivity.

Figure 1b.
Bridge-shaped specimen suitable for measurement of the resistivity and Hall effect. Pads for attachment of contacts are shaded.

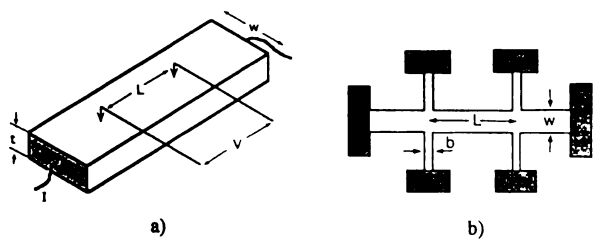

spective contributions by averaging the two readings. The net effect is thus an apparent increase in resistivity which, for a good thermoelectric material such as Bi_2Te_3 amounts up to 1/3 of the total resistivity.

The most effective way to deal with the Peltier contribution is to use alternating current in combination with a lock-in amplifier or to introduce an electromechanical chopper which converts the dc current into a square-wave alternating current of suitable frequency. Since it takes a finite time to establish the thermal gradient due to the Peltier heat while the resistive voltage sets in instantaneously, the idea is to switch the current polarity before the thermoelectric contribution can build up. Because one can use accurate potentiometers or high sensitivity digital voltmeters to pick up the demodulated signal and one avoids the problems of stray signals associated with wide frequency band ac meters, the chopped dc is preferable to alternating current. Chopping frequencies of several tens of Hz are typically perfectly adequate to suppress the Peltier effect contribution. Potentiometric circuits utilizing the electromechanical choppers have been described in the literature[2,3].

1b. The van der Pauw technique

The requirement of a bar-shaped or bridge-shaped sample to ensure uniform current flow and well defined equipotentials represents a serious constraint on the sample geometry. It is often very inconvenient to process a sample into a bar-shaped form and one would rather use a measuring technique which is less restrictive in terms of the required sample geometry and suitable for samples of irregular contour or plane lamella. The technique which satisfies these criteria is based on the conformal mapping of two-dimensional fields and was developed by van der Pauw[4]. This technique has found widespread use in recent years and its only essential requirement is that the sample be of uniform thickness, structurally homogeneous, and singly connected, i.e., not having isolated holes.

Consider a plane lamella of uniform resistivity ρ and thickness δ with four line contacts on the edge separated by distances a, b, and c as shown in the inset of Fig. 2. We are interested in the potential at terminals 3 and 4 as a result of the current I introduced at the terminal 1 and removed at the terminal 2. It is easy to show that the resistance $R_{12,34}$ defined as the ratio $\frac{V_{34}}{I_{12}}$ equals

$$R_{12,34} = \frac{V_{34}}{I_{12}} = \frac{\rho}{\pi\delta} \ln \frac{(a+b)(b+c)}{b(a+b+c)} \qquad (2)$$

By commuting the electrodes, i.e., using terminals 1 and 4 as voltage electrodes while injecting the current into the half-plane via the terminal 2 and removing it at the terminal 3, the resistance $R_{23,41}$ becomes

$$R_{23,41} = \frac{V_{41}}{I_{23}} = \frac{\rho}{\pi\delta} \ln \frac{(a+b)(b+c)}{ac} \qquad (3)$$

A simple manipulation and the fact that b (a+b+c) + ac = (a+b) (b+c) allows one to combine Eqs.2 and 3 into a single equation containing the desired resistivity ρ of the lamella,

$$\rho = \frac{\pi\delta}{\ln 2}\left[\frac{R_{12,34} + R_{23,41}}{2}\right] f\left(\frac{R_{12,34}}{R_{23,41}}\right) \qquad (4)$$

Here f is the asymmetry function which depends only on the ratio $R_{12,34}/R_{23,41}$. A plot of the asymmetry function f versus the resistance ratio $R_{12,34}/R_{23,41}$ is given in Fig.2. The experimental procedure to determine the resistivity using the van der Pauw technique thus consists of measuring the two resistivites $R_{12,34}$ and $R_{23,41}$, using Fig.2 to determine the value of the asymmetry function f corresponding to the resistance ratio $R_{12,34}/R_{23,41}$ and inserting the values into Eq.4 to determine the resistivity of the material.

Figure 2.

The asymmetry function f as a function of the resistance ratio $R_{12,34}/R_{23,41}$. The inset shows a sample in the form of a semi-infinite slab of thickness δ with four line-contacts separated by distances a,b and c along the edge of the slab. Current enters the sample at the contact 1 and leaves it at the contact 2. Potential difference is measured between contacts 3 and 4.

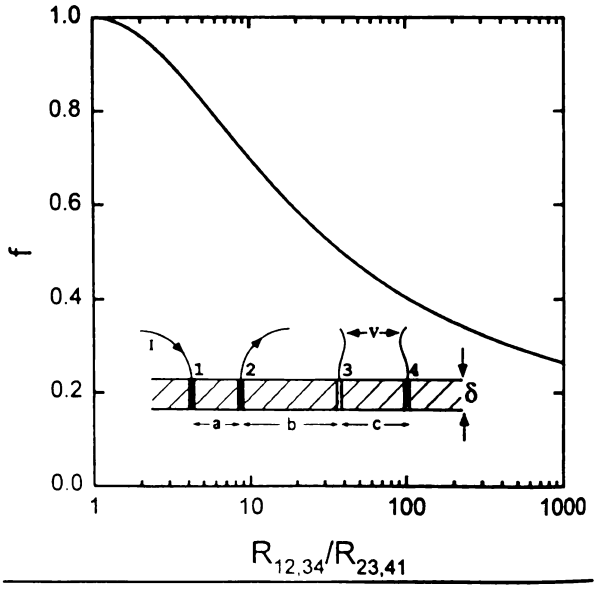

While Eq.4 applies to an arbitrarily shaped lamella, there is an advantage in using symmetrical shapes such as discs or squares contacted in a symmetrical fashion. For instance, if the specimen is a perfect circle with the contacts along the orthogonal diameters, then obviously $R_{12,34} = R_{23,41}$, the asymmetry function f has value of unity, and Eq.4 becomes

$$R \equiv \frac{\rho}{\delta} = \frac{\pi}{\ln 2} R_{12,34} \qquad (5)$$

where R stands for the sheet resistance measured in "ohms per square."

The location and size of the contacts is crucial for the accuracy of resistivity measured by the van der Pauw technique. A theoretical assumption of line-contacts attached at the edges of the lamella is not always viable in practice and it is preferable to place the contacts on top of the structure close to the outer edge. The price one pays for violation of the assumed edge-placement of the contacts and for their finite size is an error introduced in the measurement of resistivity. Van der Pauw and subsequently a number of authors[5,6] considered various electrode layouts and sample shapes and calculated the error introduced by each specific configuration, including the so-called clover-leaf sample geometry. In general, the finite size of contacts and their displacement from the edge tend to result in the measured resistivity which is smaller than the actual resistivity of a material under study. Planar shape of the samples including thin-films deposited on a variety of substrates tend to smooth out any standing thermal gradients better than do the bar-shaped specimens. The van der Pauw technique is thus a useful method of assessing the electrical resistivity of thermoelectric materials.

One should note that the electrical resistivity is also often measured by the collinear four-point probe technique[7,8]. Although used rather sporadically on thermoelectric materials (due to small voltages developed between the closely spaced voltage probes as a result of relatively low resistivity of thermoelectric materials), numerous versions of this technique, including a number of commercially available set-ups, have found widespread use in evaluating materials which typically have resistivities in the range 10^{-3} - 10^{1} Ω-m. Although not as accurate as the techniques where the geometrical factor of the sample is well defined, the four-point probe might be useful for rapid scanning of production ingots of thermoelectric materials. For a detailed description of this deceptively simple technique and how to account for various correction factors the reader is referred to the original literature[9-11].

2. Seebeck Coefficient

As the definition $S = \Delta V/\Delta T$ implies, measurement of the Seebeck coefficient, or the thermoelectric power, as the Seebeck coefficient is frequently called, involves a simultaneous determination of a thermoelectric voltage ΔV arising as a consequence of an imposed temperature difference ΔT between two points along the sample length. To get an accurate value of S, both ΔV and ΔT must be measured with precision and that requires certain special considerations.

Experimental arrangements to determine the Seebeck coefficient usually involve one of two configurations illustrated in Fig. 3. In the first one, a sample is provided with a heater (a small resistor, wire-wound heater, or thin-film strain gauge resistor) at one end and the other end is attached (soldered, epoxied or by other means that provide good thermal link) to a heat sink. Thermal and potential differences are then measured between two points along the length of the sample. Depending on the temperature range of interest, sample size and desired accuracy, one can use small calibrated resistance thermometers or, more typically, thermocouples to determine ΔT, and either fine gauge copper wires or the legs of the thermocouples to measure the Seebeck voltage. In the other popular configuration, shown in Fig. 3b, the sample is clamped between two reasonably large copper blocks and both ΔV and ΔT are measured between the blocks. Because of the inherently low thermal conductivity and high Seebeck coefficient of the thermoelectric materials and consequently an insignificant contribution of interfaces to the overall thermal and potential gradients, it makes little difference which of the two experimental set-ups is employed. For other materials where the contact resistance might introduce large interfacial gradients the layout of Fig. 3a is always the preferred one. It should be noted that measurements of the Seebeck coefficient do not require good vacuum. In fact, the presence of some inert gas might be beneficial to

Figure 3.

Experimental set-up for the measurement of the Seebeck coefficient using copper-constantan thermocouples.
3a. Temperature sensors attached to the sample.
3b. Temperature sensors attached to the heat source and sink.
Numbers 1 and 2 designate copper and constantan wires, respectively.

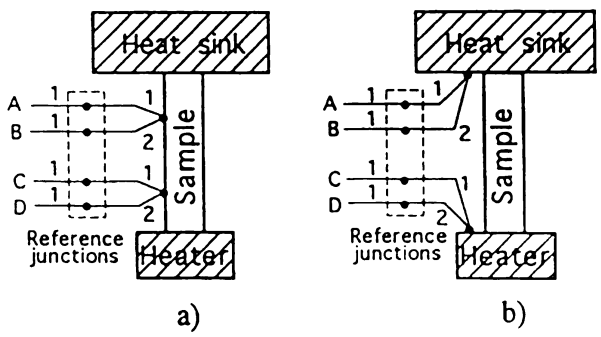

improving the thermal contact. However, because it is convenient to carry out measurements of the Seebeck coefficient together with the measurements of the thermal conductivity, and the latter requires good vacuum, the studies are most often done under adiabatic conditions.

Assuming one uses temperature sensors of reputable origin, the success of the experiment hinges primarily on the quality of the thermal contact at the thermocouple junctions. An ideal thermal contact is achieved by soldering the thermocouple junction to the sample. If one desires to use a differential thermocouple, it is essential to remember that at least one of the two junctions must be insulated from the sample otherwise the emf generated by the thermocouple is shorted via the sample and an error reading results. Alternative ways of attaching the thermocouple junctions rely on various glues and epoxies and one may also opt for inserting the thermocouple junctions into tiny holes drilled in a specimen.

Attention paid to the reference junction is just as important. For room temperature measurements and for investigations at elevated temperatures one usually keeps the reference junctions at an ambient temperature. All that is needed is a small Dewar flask filled with water and covered with a polystyrene cap through which is inserted a thermometer and glass tubes filled with oil. Thermocouple junctions are immersed in the oil which facilitates good and stable thermal contact. Alternatively, one can use commercially available ice reference points which are capable of maintaining the temperature at 0 ± 0.1°C. Measurements below the room temperature are normally done in a cryostat an integral part of which is a copper sample block or copper "pot" which can serve as a robust thermal grounding post. The temperature of this copper post is carefully monitored using a platinum thermometer or some other high sensitivity resistance thermometer. Because of their low sensitivity at liquid helium temperatures, thermocouples must eventually be replaced by resistance thermometers if one wishes to study the Seebeck effect below about 10K. This of course avoids the problem with thermocouple junctions but adds a new one - how to cope with much more bulky resistance thermometers especially if the sample is small.

The choice of a thermocouple depends very much on the temperature range of interest and on how much stray heat can one tolerate to reach the sample. Basically, the desire is to maximize the thermocouple reading and to minimize the heat path into/from the sample along the leads. Because of its very high thermal conductivity, if copper forms one leg of a thermocouple, it should be a very thin wire. In general, one should only use thermocouple wires that come from a reputable source and for which exist calibration tables traceable to the national standard.[12] One should avoid using old, strained and "kinking" thermocouples as these may generate spurious signals. If one makes his/her own thermocouple junctions, one should always test the efficacy of the couple by comparing the emf generated at two fixed temperatures (e.g., the ice point and liquid nitrogen) and compare the readings with the calibration tables. Special attention needs to be paid to measurements at high temperatures. One should not only periodically recheck the thermocouple calibration but it is also essential that the wires brought out from a high temperature environment to the measuring instrumentation are not interrupted at points where large temperature differences are likely to exist. It is always preferable to use capillary tubes and pass the wires uninterrupted.

Although the propensity for errors arising from measurements of ΔT is far greater than for measurements of ΔV, and the errors are usually more serious , it is, nevertheless, a prudent practice to ascertain that ΔV is the true Seebeck voltage. The key point to keep in mind is the fact that the Seebeck voltage measured is the property of a couple formed by the sample and the leads, $S_{measured} = S_{sample} - S_{leads}$. As we already noted, the connecting leads could be the legs of the thermocouples or a pair of separate wires. In either case, one must correct for the absolute thermopower of the leads in order to obtain the absolute thermopower of the sample. Thermopower of the copper wires, the material most frequently used as the Seebeck voltage probes, does not exceed a couple of $\mu V/K$ at 300K while typical values of the Seebeck coefficient of thermoelectric materials are in excess of 200 $\mu V/K$. Thus, for thermoelectrics, the omission to correct for the thermopower of copper leads does not lead to a serious error. This is not so for other materials and in any case it is a good practice to present the data in their correct form. Tables providing thermopower values as a function of temperature for pure Pb wire which serves as the standard reference material for calibration purposes are available in the literature.[13] Furthermore, the discovery of high temperature superconducting perovskites (superconductors have zero absolute Seebeck coefficient at temperatures $T < T_c$) has greatly extended the temperature range over which the absolute Seebeck coefficient of any material can quickly and conveniently be determined.[14]

I wish to note that the Seebeck coefficient can also be determined using the Harman method discussed in section 4. In this case a passage of dc current through a sample suspended in a vacuum (adiabatic conditions) results in the voltage across the sample V_a and the temperature difference ΔT. By subtracting the ohmic voltage V_i (measured under the isothermal conditions) from the voltage V_a and dividing by ΔT one obtains the Seebeck coefficient of the sample with respect to the measuring leads. Correcting for the thermopower of the leads yields the absolute Seebeck coefficient of the sample. Though simple in principle, it is not advisable to rely on this method for an accurate determination of the Seebeck coefficient. The reason is a small temperature difference ΔT and the fact that the adiabatic and isothermal voltages V_a and V_i do not always (especially at lower temperatures) differ by a margin large enough to achieve, after subtraction, good enough accuracy.

3. Thermal Conductivity

Of the three transport properties that determine the figure of merit of a thermoelectric material, the thermal conductivity is technically the most demanding one but also the most sensitive to the nuances of microstructure and composition. This latter attribute has in fact been used to great effect in increasing the figure of merit of a given material system. Traditionally, thermoelectric materials have been developed by selecting systems with reasonably large power factors (the power factor is the numerator $S^2\sigma$ in the figure of merit) and then systematically decreasing the thermal conductivity by altering the microstructure, defect and impurity content, or chemical composition. This means that when searching for potentially useful thermoelectric materials or when optimizing their thermal conductivity, the experimental technique must be flexible enough to accommodate samples with a wide range of thermal conductivities. While the heat flux, thermal gradient, and thermal conductivity are analogous to electrical current flow, potential difference, and electrical conductivity in an Ohm's Law experiment, accurate thermal measurements are far more difficult to realize in practice than their electrical analogue. This is chiefly due to the fact that while in an electrical resistivity experiment current leakage paths can be virtually eliminated, *it is impossible to completely suppress all heat leakage paths in a thermal conductivity experiment.* The diligent experimentalist must always be aware of the existence of heat leaks in his experimental apparatus and take special care to minimize them with respect to the heat flow through the sample.

I now discuss several methods for measuring the thermal conductivity of thermoelectric materials and highlight their relative advantages and disadvantages. The choice of the appropriate method is a strong function of the sample size and geometry, material type, and temperature range of interest, and in many cases it may be desirable to use more than one method to insure an accurate determination of the absolute magnitude of the thermal conductivity.

3a) The Longitudinal Steady-State (LSS) Technique

This technique is the thermal analogue of the four-probe bar measurement of electrical resistivity discussed in section 1a. For this type of measurement, a long bar-shaped or cylindrical sample is preferred. It has the advantages of providing an absolute measurement of the thermal conductivity over a wide temperature range using fairly simple and inexpensive instrumentation. Its chief disadvantages are limitations on sample size (generally only samples longer than a few millimeters can be measured) and sample geometry (the method is unsuitable for thin film materials and for samples with highly irregular shape), and the susceptibility to errors due to heat losses especially in measurements on low thermal conductivity materials. The generic experimental set-up is shown in Fig.4. One end of the sample, of cross-sectional area A, is secured by means of epoxy, solder, or by clamping to a temperature controlled heat sink. This heat sink can be the cold tip of a liquid nitrogen or liquid helium cryostat, the cold head of a closed cycle refrigerator, or even a heated plate. An electrical heater is attached in a similar manner to the free end of the sample. This heater may be a small wire wound resistor, a strain gauge, or an evaporated metal film. For a given current I and voltage V across this electrical heater, an amount of power P = IV will be produced. At two points, spatially separated by a distance L along the sample, are affixed temperature sensors which measure the temperatures T_h and T_c of the hot and cold side of the sample. When the heater is energized, a heat flux Q=P/A will flow down the sample and a temperature difference ΔT will be developed. Under steady-state condition, and assuming all of the Joule heat generated by the heater flows down the sample, the thermal conductivity can be written as

$$\kappa = \frac{P}{\Delta T}\frac{L}{A} \qquad (6)$$

Thus by measuring the heater power, the temperature difference along the sample, and geometrical factor L/A the thermal conductivity is determined. Clearly the accuracy of this method depends on the accuracy to which the quantities P, ΔT, and L/A can be measured. The power P is specified by

Figure 4.

Longitudinal steady-state technique to measure thermal conductivity of a bar shaped sample of cross-sectional area A. After the heater is energized with power P, a temperature difference $\Delta T = T_h - T_c$ is measured between two points separated by a distance L along the sample.

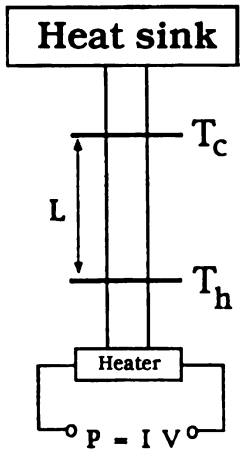

the product of I and V and both quantities can be measured to within one part in 10^4. The uncertainty in the geometrical factor L/A can be as small as 1 % for large, long samples and as large as 20 % for short samples or specimens with irregular shape.

The most critical parameter in the steady state measurement of κ is the temperature difference ΔT. The accuracy to which this quantity can be measured is a function of the type of temperature sensors used and the temperature range of the measurement. The two most popular types of sensors for measuring sample temperatures in a steady-state experiment are resistance thermometers and thermocouples. Each of these sensors has its advantages and drawbacks and the choice largely depends on sample size and geometry and temperature range of interest.

Resistance thermometers offer a highly accurate measurement of the absolute temperature because they possess a strongly temperature dependent and well characterized and reproducible resistance. They are commercially available from many sources[15] and can be purchased already calibrated, so that a measurement of the resistance of the sensor provides a very accurate determination of the absolute temperature. A notable drawback of resistance thermometers is their relatively bulky size which makes it difficult to accommodate these thermometers on samples of short length.

For smaller samples the use of fine wire thermocouples is the preferred technique and the issues pertaining to their proper use as discussed in section 2 are equally relevant here. Caution should also be exercised when using thermocouples in a magnetic field. The Seebeck coefficients of the thermocouple materials can be a quite strong function of field and their field dependence can also differ from strand to strand. The experimentalist who wishes to measure the thermal conductivity of a specimen in a magnetic field using thermocouples should take every precaution to ensure the field dependence of the sensor signal is well characterized.

Up to now I have tacitly assumed that all of the heat generated by the heater flows down the length of the sample and into the heat sink; in an actual experiment this condition is never achieved. The challenge to the experimenter is to minimize the alternate means of heat transfer to ensure that virtually all the heat flows down the length of the specimen. Let us consider the main sources of heat loss.

When the heater in Fig.4 is energized, heat has the following alternate paths: i) conduction down the length of the sample; ii) conduction and convection in the surrounding medium; iii) conduction along the heater and temperature sensor leads; and iv) radiation to the surroundings. The goal is to minimize mechanisms ii)-iv) with respect to the desired mechanism i). Heat transfer via mechanism ii) can be virtually eliminated by placing the measuring apparatus in a vacuum chamber evacuated to less than 10^{-5} Torr. Conduction along the sensor and heater leads can be made insignificantly small by using long, thin wires which can be coiled to fit into the experimental space. The chief limitation on the steady-state measurement is heat loss from the heater and the sample by radiation. These radiative losses depend on the 4th power of the absolute temperature, and thus at low temperatures (say below 100 K or so) they can generally be neglected. At higher temperatures and for samples with small thermal conductance, radiation losses can become substantial. These losses can to some extent be minimized by surrounding the sample with a radiation shield thermally anchored to the heat sink, or better yet, provided with a temperature profile along its length matching that across the sample. This will minimize the temperature difference between the radiating surfaces and thereby minimize heat transfer by radiation. In any case it is desirable to have some estimate of the magnitude of the radiation losses in a given experimental setup. This can be done either by modeling the system using Stefan's Law and the appropriate value of emissivity, or by measuring the total heat losses directly, e.g., by replacing the sample with a very long, thin sample of low thermal conductivity such as glass, energizing the heater, and observing the temperature profile along the sample. Even with all these precautions, one really cannot hope to make accurate measurements of thermal conductivity using the steady-state technique much above room temperature on any material of thermal conductivity less than a few hundred mW cm^{-1} K^{-1}. Thus in order to characterize materials for high temperature applications, other techniques are called for.

3b) The Radial Steady-State (RSS) Method

Among the best known experiments utilizing the radial steady-state method are those measuring the thermal conductivity of silicon and germanium up to the melting point.[16] In this technique, the sample is a cylinder of length L and heat is made to flow radially out from the center of the sample; see Fig.5. Thus a heater wire must be placed along the axis of the sample and two thermocouples placed at two radial positions r_1 and r_2. In this geometry the thermal conductivity is given by

$$\kappa = \frac{P \ln(r_2 / r_1)}{2\pi L \Delta T} \qquad (7)$$

The sample must be slit in half in order to insert the heater and thermocouple wires and then clamped tightly back together. The sawn faces must be smoothly polished so that they fit neatly together in order to eliminate any conduction, convection, or radiation along the interface. Although this technique is conceptually very simple and elegant, it is difficult to realize in practice because large samples (for instance 1 cm in diameter by several centimeters long) are required.

3c) The 3-ω Method

While the LSS technique described in section 3a offers the distinct advantages of relative simplicity and a direct measurement of the thermal conductivity, it has two main drawbacks: radiation losses limit its use at high temperatures, and in general it cannot be used to measure thin film materials. A technique developed over the last ten years which can overcome both of these difficulties is the 3-ω technique.[17] Intended originally for measurements of the thermal conductivity of bulk glasses in the 30-750 K temperature range, it has since been refined and adapted to measure thermal conductivity of thin films. Typical samples are 1 cm square plates a few millimeters thick, or a thin film deposited on a substrate. Onto the surface of the sample is evaporated a thin metal line (such as silver or platinum) which serves the dual purpose of heater and thermometer. A current through the heater at frequency ω produces a temperature oscillation at a frequency of 2ω. Since the resistance of the heater-thermometer increases with temperature it also oscillates at 2ω. This resistance oscillation multiplied by the original current oscillation at frequency ω produces a voltage oscillation across the strip at frequency 3ω, whence the method's name. By solving the heat transfer equation for a narrow line source on the surface of an infinite half volume, this voltage can be directly related to the thermal conductivity of the material. A nice feature of the method is that by increasing ω, regions closer and closer to the surface of the sample can be probed, i.e., at high enough frequency the method will measure the thermal conductivity of a film on a substrate. Before applying this technique to a broad range of materials, an important point must be remembered: the technique as originally developed was to measure thermal conductivity of electrically insulating materials. If one wishes to apply this technique to a thermoelectric material (a rather good electrical conductor), an electrically insulating layer must be placed between the heater/thermometer and the sample. The experiment then measures the sum of the thermal resistance of the insulating layer and the sample, as well as the boundary resistances at each interface. In principle it should be possible to separate out these contributions by varying the frequency or simply minimizing the contribution of the insulating layer by making it very thin, but such modifications have not yet been investigated in detail. The 3-ω technique does, however, provide the potential of directly measuring the thermal conductivity of thin film thermoelectric materials. Films as thin as 10 microns can be measured using the original 3-ω technique without modification, and recently it has been demonstrated[18] that the method can be extended to probe films as thin as 3000 Å. In addition, the method is essentially free from errors due to radiation losses, and thus may be useful in measuring bulk materials at high temperatures. The reason the radiation losses do not enter into consideration is because they are proportional to the characteristic length scale of the measurement, which can be made very small in the 3-ω technique by using photolithography to define the heater/thermometer.

Figure 5.

A radial steady-state thermal conductivity measurement. A heater H is placed along the axis of a cylindrical sample of length L. A temperature difference $\Delta T = T_h - T_c$ is measured between two points r_1 and r_2 along the radius of the cylinder.

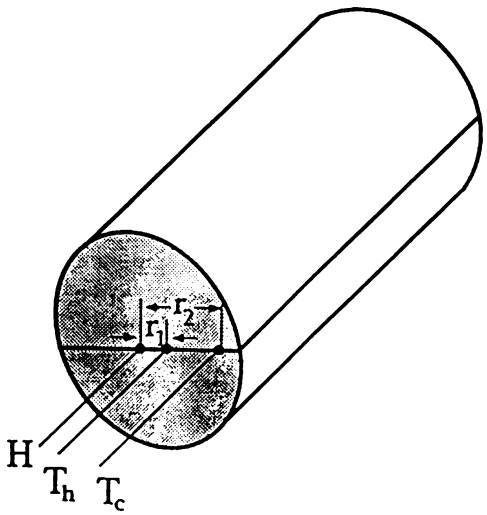

3d) Transient Method of Measurement

Several transient techniques have been described in the literature[19,20] and all are variations to some degree of the original transient thermal wave experiments of Ångstrom.[21] These methods monitor the temperature rise on the back surface of a sample when the front surface is exposed to a heat wave that has a time dependence. A modern, laser-based version of the method[22] consists of a pulsed laser heat source, a vacuum furnace, and detection, amplification and analysis systems. The front and back surfaces of the sample must be covered with a coating to absorb the radiant incident energy. The laser is pulsed with a duration on the order of 1 ms and total energy output on the order of 10 J. The temporal dependence of the temperature rise on the back surface of the sample as recorded by a suitable infrared detector is related to the thermal diffusivity of the sample. As in the case of the 3-ω technique, radiation losses can be kept small by reducing the size and thickness of the sample; this however, requires a pulse of shorter duration since the pulse duration must remain small with respect to the transit time of the heat wave through the sample. A potential pitfall of this technique is the reliable and reproducible production of an absorbing

layer on the sample, which can cause difficulty when adhesion and thermal expansion problems arise at high temperatures. In addition, the determination of the thermal conductivity from the measured diffusivity requires knowledge of the heat capacity C of the material since $\kappa = DC\rho$, where ρ is the mass density. Thus C must be measured independently or calculated from the crystal structure and elastic constants. In spite of these drawbacks and the rather more expensive instrumentation required compared to traditional steady-state methods, transient thermal diffusivity measurements have become a popular approach of determining the thermal conductivity of thermoelectric materials above room temperature.

We conclude this section by describing two experimental approaches used to identify the mechanisms by which heat flows in a thermoelectric material, information which is crucial when developing new thermoelectrics and optimizing their properties.

3e) Separating the Electronic and Lattice Thermal Conductivities

The thermal conductivity of a solid is composed of two contributions: that due to the charge carriers, κ_c, and that due to lattice vibrations, or, phonons, κ_p. The measured thermal conductivity is the sum $\kappa = \kappa_c + \kappa_p$. For carrier concentrations below about 10^{26} m^{-3} the electronic component of thermal conductivity is usually negligible in comparison to κ_p. However, in some materials κ_p itself is very small (this of course is just what one desires for a thermoelectric), and in these cases κ_c can be an appreciable fraction of the total thermal conductivity even at carrier concentrations below 10^{25} m^{-3}. In the course of understanding and optimizing the properties of a given material, it is essential to know the individual contributions of phonons and carriers to the total heat conductivity. Generally this is done by either estimation of the carrier component using the Wiedemann-Franz (W-F) law or by suppression of κ_c using a magnetic field.

An estimation of the carrier thermal conductivity using the W-F law is by far the easier of the two methods as the only required information is the magnitude of the electrical resistivity, and this is normally obtained as part of the routine of evaluating the thermoelectric properties such as described in section 1. The W-F law states that, if the carriers in the system are undergoing scattering processes in which the change of energy of the carrier is small compared to the thermal energy $\kappa_B T$ (elastic scattering), then $\kappa_c = L_o T/\rho$ where $L_o = 2.45 \times 10^{-8}$ V^2 K^{-2} is the Sommerfeld value of the Lorenz number and ρ the electrical resistivity. When the carrier scattering is not elastic, the Lorenz number is smaller than L_o and the Wiedemann-Franz law provides an upper limit to the carrier thermal conductivity.

In circumstances when the W-F law is known to break down and an exact determination of κ_c is desired, one can attempt a separation of the thermal conductivity into its two components by using a magnetic field. A magnetic field applied transverse to the thermal current can suppress the carrier thermal conductivity when the field is large enough to achieve the classical high field regime specified by $\omega_c \tau >> 1$ or equivalently, $\mu B >> 1$. Here ω_c is the cyclotron frequency, τ the scattering time and μ the carrier mobility. Physically this condition implies that the carriers are "trapped" in several cyclotron orbits before being scattered and cannot transport their heat content down the thermal gradient. Consequently the heat conduction proceeds only via lattice vibrations. The high-field condition can actually be achieved only in fairly high mobility materials. For instance for B = 5 T, the product μB equals unity for $\mu = 2000$ cm^2 V^{-1} s^{-1}. As a function of magnetic field one monitors a decrease and eventual saturation of the thermal conductivity at a value equal to κ_p. Even if the mobility is not large enough to achieve the high field condition, extrapolation techniques have been developed which allow κ_p to be determined.[23,24]

4. Direct Measurements of ZT

Instead of measuring the transport parameters that specify the figure of merit in separate experiments, Harman[25] showed that the figure of merit can be conveniently determined in a single experimental run, the technique nowadays known as the Harman method. In section 1a we drew attention to the existence of the Peltier heat that necessarily arises when a dc electric current passes through the sample and what complications this leads to in measurements of the resistivity. In the Harman method this same phenomenon is turned into a virtue. Consider a sample of a good thermoelectric with cross-sectional area A and length L suspended by thin wires in a vacuum of order 10^{-5} torr and through which passes a direct current I for long enough time so that a steady-state is reached. Assume no heat loss along the connecting leads nor any loss by radiation to the surroundings. The potential difference across the sample V_a is made up of a purely ohmic voltage V_i augmented by a thermoelectric voltage $S\Delta T$ which has its origin in the temperature gradient resulting from the Peltier effect (remember, the Peltier heat is generated at one end and absorbed at the other end and this sets up a thermal gradient across the sample). Using the definition of the figure of merit, $z = S^2/\rho\kappa$, and some straightforward manipulation, it is easy to show that the dimensionless figure of merit can be written as

$$ZT = \frac{V_a}{V_i} - 1 \qquad (8)$$

Hence, in principle, by measuring the adiabatic and isothermal resistivities (voltage V_a with a direct current and voltage V_i with a chopped dc of equal magnitude) one can readily determine the dimensionless figure of merit ZT.

In practice it is not possible to provide total thermal isolation of a sample from its surroundings and small heat losses along the wires supporting the sample and losses due to radiation from the end contacts and from the sample surface are inevitable. Correction terms which need to be applied are given in a book by Goldsmid[26]. With a judicious choice of the connecting leads and appropriate sample dimensions the figure of merit at room temperature can be measured with an accuracy better than 2%.

5. The Hall effect

The Hall effect represents a powerful experimental tool which provides insight into the nature of transport, the density of carriers, the type of conduction, and the carrier dynamics. Measurements of the Hall effect have become not only a standard weapon in the armory of a solid state physicist seeking to understand transport behavior of solids but also an integral part of the quality control process in essentially every branch of solid state electronics. Although the thermoelectric figure of merit does not explicitly depend on the value of the Hall constant, the information gained from the Hall measurements is truly indispensable for a thorough understanding of the carrier transport in thermoelectric materials. It is for this reason that I include here a brief description of the Hall measurements.

The Hall effect is a manifestation of the Lorentz force acting on a free charge carrier moving in a solid. As the carriers are deflected to one edge of the sample (the top edge in the case of electrons and the configuration of Fig. 6a) they set-up a transverse electric field which opposes further deflection and pile up of the charge. At a steady-state the transverse electric field, called the Hall field, exactly balances the Lorentz force. In experiments one normally does not measure electric fields but rather voltages. Writing the current density as $j_x = I/wt$ where I is the current and wt the cross-section of the sample, and applying magnetic field along the z-axis, the Hall voltage V_H becomes

$$V_H = \frac{IB_z}{t}\frac{1}{nq} = R\frac{IB_z}{t} \qquad (9)$$

Please note that it is the thickness t (the dimension in the direction of the magnetic field) and not the width w (the spacing between the Hall voltage probes) that enters in the Eq. 9.

The quantity R defined as

$$R = \frac{1}{nq} \qquad (10)$$

is the Hall constant. Eqs. 9 and 10 are the essence of the Hall effect measurement. The direction of the transverse electric field and therefore the sign of the Hall effect depend on the sign of the charge carrier. The established convention is that when q is negative (electrons), the Hall coefficient R is taken as negative. Fig. 6a, in fact, depicts the situation where the charge carriers are electrons. Furthermore, Eq. 10 facilitates a straightforward determination of the carrier density. It holds very well for metals and strongly degenerate semiconductors because here the carriers participating in the conduction process occupy a narrow energy range on the order of $\kappa_B T$ around the Fermi level. Having nearly the same energy and therefore equal velocities, all carriers will be deflected in a given magnetic field by approximately the same amount. In nondegenerate semiconductors, on the other hand, the carriers do not have the same velocities and they will be deflected in a magnetic field by different amounts. However, even in this case, the correction to Eq. 10 is small and can be accounted for by introducing a constant A on the right-hand side of Eq. 10 which never departs very far from unity. For instance, in a covalent solid where the carriers scatter on acoustic vibrations, the mean-free path is independent of energy and the constant A equals to $3\pi/8 \sim 1.17$. In ionic semiconductors, at temperatures above the Debye temperature, the carriers scatter predominantly on optical phonons, and the constant has a value A = 1.11.

By combining the Hall measurements with that of the electrical resistivity, one arrives at an important transport parameter known as the Hall mobility, $\mu_H = \sigma|R|$. As discussed elsewhere in this journal issue, the mobility is one of

Figure 6a.
Hall effect for a single band of free electrons.

Figure 6b.
Hall effect for a solid with a band of electrons and a band of holes.

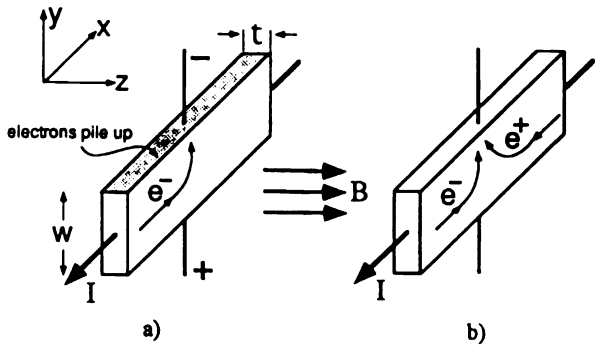

the critical parameters which serves as a criterion whether a given material is a good thermoelectric or not. Large values of μ_H are desired, and materials possessing a large value of the mobility are also expected to show significant changes in their transport behavior when subjected to an external magnetic field.

If more than one group of carriers participate in the conduction process we have more than one Lorentz force and we must treat the steady-state as arising from the equality of currents (magnetic field-generated deflection current balanced by the current due to the Hall field) rather than the equality of the Lorentz force and the Hall field. For a frequently arising situation of the mixed conduction (one band of electrons with $\sigma_1=nq\mu_n$ and $R_1=-1/nq$, and a band of holes with $\sigma_2=pq\mu_p$ and $R_2=1/pq$) a general expression valid for all field strengths is[27]

$$R=\frac{1}{q}\frac{\left(n\mu_n^2-p\mu_p^2\right)+\mu_n^2\mu_p^2(n-p)B^2}{\left(n\mu_n+p\mu_p\right)^2+\mu_n^2\mu_p^2(n-p)^2B^2} \qquad (11)$$

Obviously, when the material is perfectly compensated, i.e., when n=p the field dependence disappears. If, in addition to being compensated, the mobilities of the electrons and holes are the same, then the Hall coefficient becomes zero. In the limit of large fields and large mobilities, or more precisely, when $\mu_nB>>1$ and $\mu_pB>>1$, Eq. 11 reduces to

$$\lim_{B\to\infty} R=\frac{1}{q(n-p)} \qquad (12)$$

and the high-field Hall coefficient is a measure of the carrier imbalance. It is noteworthy that Eq.12 applies regardless of the shape of the Fermi surface or the nature of scattering.

In principle, the configuration of Fig.6 coupled with Eq.9 or, in the case of two-band conduction Eq.11, provides for a straightforward determination of the Hall constant. However, it should be remembered that the Hall voltage signal is rather small, typically several orders below the ordinary resistive voltage generated in the same sample with the same current, and one must minimize systematic errors.

The most critical issue in the Hall measurements is a probe alignment. Although one can align Hall probes on thin film structures very accurately using lithographic techniques, in bulk samples one usually is not so fortunate and probe misalignment is always present. In addition to the Hall voltage, the misaligned probes inevitably pick up resistive voltage which is proportional to the degree of misalignment. To eliminate the effect of probe misalignment one reverses the magnetic field and measures the Hall voltage again. The true Hall voltage is then obtained by subtracting the two readings,

$$V_H=\frac{V_H(B)-V_H(-B)}{2} \qquad (13)$$

In fact, it is a good practice to reverse not just the magnetic field but also a direction of the current and calculate the Hall voltage from the mean of all four readings.

Another important consideration in Hall effect measurements is the length-to-width ratio L/w of the sample. In short samples with large width w (and current contacts over the entire width w) the measured Hall voltage would clearly be smaller than the value based on Eq. 9 because the Hall field is effectively shorted. It has been show[28] that in order to eliminate the shorting effect of the current contacts, the length-to-width ratio should not be smaller than 3. It should be realized that one does not solve the problem by merely making the current contacts smaller. It is true that the shorting of the Hall voltage is then not as serious as before but this comes at a cost of making the current distribution highly inhomogeneous, perhaps even a greater problem.

Equations describing the Hall effect, just as Eq. 1 for the electrical resistivity, assume that the measurements are made under isothermal conditions., i.e., in the absence of any thermal gradients. We have already pointed out that this is an unrealistic scenario when investigating electrical resistivity of thermoelectric materials with dc currents. The use of a chopped dc current, the best remedy identified then, is also the best approach in measurements of the Hall effect.

For completeness, we note that the Hall effect can also be measured using the van der Pauw arrangement discussed in section 1b. Referring to Fig. 2, van der Pauw derived[4] the formula for the Hall mobility

$$\mu_H=\frac{\delta}{B}\frac{\Delta R_{24,13}}{\rho} \qquad (14)$$

where δ is the thickness of the plane lamella, B is the magnetic field, ρ is the resistivity, and $\Delta R_{24,13}$ is the change of the resistance $R_{24,13}$ due to the magnetic field. Again, the clover-shaped sample geometry has a distinct advantage in providing a relatively large Hall signal at low level of dissipation.

Conclusion

An increased sensitivity to environmental concerns with regard to waste heat and the deleterious nature of chemical refrigerants and compressed gases has once again brought the development of new thermoelectric materials and devices to the forefront. Whether the search for new and more efficient materials will be successful hinges directly on our ability to measure accurately the fundamental transport properties of these systems. This is all the more true when it is realized that many of the materials being investigated today are from

classes of solids whose transport properties are virtually unknown and potentially unusual and exotic in nature. Whether the observed effects are representative of the actual properties of the material or are an artifact of an ill-fated experimental technique is a critical issue which every researcher must consider on a case-by-case basis.

In this review I have attempted to outline the most popular and useful techniques for measuring the transport properties of thermoelectric materials, and have highlighted the advantages and drawbacks of each. As I have pointed out, the choice of a particular technique and its successful application depends on the type, size, and shape of the material, the temperature range of interest, the desired accuracy of the data, and, to a large extent, the particular researcher's taste and experience. As new and more interesting materials are discovered and developed, their accurate characterization remains a challenge requiring serious attention, and it is hoped that this review will assist researchers in choosing and implementing the techniques best suited for their particular needs and tasks.

Acknowledgments

The author wishes to acknowledge Dr. Donald Morelli (General Motors Research and Development Center) for his assistance in preparing this manuscript.

The editor wishes to acknowledge Dr. Alexander Ehrlich of the Naval Research Laboratory, Materials Science Division for assistance in the review of the scientific and technical details reported in this article.

Biography

Dr. Ctirad Uher received his B.S. and Ph.D from New South Wales University in Australia in 1972 and 1975, respectively. He was a postdoctoral associate at the Michigan State University during 1976-78, the Queen Elizabeth II Fellow at CSIRO in Sydney from 1978 until 1980 when he moved to the University of Michigan. In 1986 he spent a year as a von Humboldt Fellow at the Max Plank Institute in Stuttgart and in 1989 he was awarded D.Sc from the New South Wales University. At the University of Michigan he served as an Associate Chair and Associate Dean for Research and in 1994 became Chair of the Department. His research focuses on the conducting processes in solids, search for novel thermoelectric materials, and thermal transport in high-temperature superconductors. Dr. Uher has been supported by ONR since 1992. He is the author of over 130 publications including several review articles on heat transport in solids.

REFERENCES

1. D. J. Ryden, AERE Report 6996, UKAEA, Harwell (1973).
2. T. M. Dauphinee and E. Mooser, Rev. Sci. Instrum. **26**, 660 (1955).
3. W. D. Edwards, J. Sci. Instrum. **42**, 432 (1965).
4. L. J. van der Pauw, Philips Res. Rep. **13**, 1 (1958).
5. R. Chwang, B. J. Smith, and C. R. Crowell, Solid-State Electron. **17**, 1217 (1974).
6. J. M. David and M. G. Buehler, Solid-State Electron. **20**, 539 (1977).
7. L. Valdes, Proc. I.R.E., **42**, 420 (1954).
8. F. M. Smits, Bell Syst. Tech. J. **37**, 711 (1958).
9. A. Uhlir, Jr., Bell Syst. Tech. J. **34**, 105 (1955).
10. D. E. Vaughan, Brit. J. Appl. Phys. **12**, 414 (1961).
11. D. S. Perloff, Solid-State Electron. **20**, 681 (1977).
12. R.L. Powell, W.J. Hall, C.H. Hyink, L.L. Sparks, G.W. Burns, M.G. Scroger, and H.H. Plumb, *Thermocouple Reference Tables Based on the IPT-68*, National Bureau of Standards, Monograph 125 (1974).
13. R.B. Roberts, Philos. Mag. **36**, 91 (1977).
14. C. Uher, J. Appl. Phys., **62**, 4636 (1987).
15. A wide selection of sensors is available from Lakeshore Cryotronics Inc, 64 East Walnut Street, Westerville, OH 43081.
16. C.J. Glassbrenner and G.A. Slack, Phys. Rev. **134**, A1058 (1964).
17. D.G. Cahill, Rev. Sci. Instrum. **61**, 802 (1990).
18. D.G. Cahill, in Thermal Conductivity 22, ed. T.W.Tong, Technomic Publishing, Lancaster, PA, 1994, p.33.
19. R.L. Rudkin, R.J. Jenkins, and W.J. Parker, Rev. Sci. Instrum **33**, 21 (1962).
20. C. Wood and A. Zoltan, Rev. Sci. Instrum. 55, 235 (1984).
21. A.J. Ångström, Annal. Phys. 114, 513 (1861).
22. G.B. Kokos, K.A. Gschneidner, Jr., B.A. Cook, and B.J. Beaudry, J. Appl. Phys. **66**, 2356 (1989).
23. S.A. Aliev, I. Ya Korenblit, and S.S. Shalyt, Sov. Phys. Solid State **8**, 565 (1966).
24. C. Uher and H.J. Goldsmid, Physica Status Solidi (b) **65**, 765, (1974).
25. T. C. Harman, J. Appl. Phys. **29**, 1373 (1958).
26. H. J. Goldsmid, *Electronic Refrigeration*, Pion Publishers, London (1986).
27. E.H. Putley, *The Hall Effect and Related Phenomena*, Butterworth & Co., London (1960).
28. I. Isenberg, B.R. Russell, and R.F. Greene, Rev. Sci. Instrum. **19**, 685 (1948).

Research Notes

Thermoelectric Power Studies at the Naval Research Laboratory

by Alexander Ehrlich

In response to the needs and opportunities represented by thermoelectrics, the Naval Research Laboratory has developed a research thrust which is integrated in the Navy's overall thermoelectric research program. This thrust includes the theoretical work of Singh et. al. and Reinecke et. al. which has been reviewed elsewhere in this volume. The first involves the calculation of electronic and phononic structure which are a central issue in the thermoelectrically important parameters making up Z. The latter work explores the potential for figure of merit enhancement by quantum confinement of the electrons in the thermoelectric material, i.e. using very thin films or fine wires as the active thermoelectric material.

The Naval Research Laboratory has developed a flexible state of the art experimental capability for measuring the various electrical transport phenomena needed to evaluate new materials for their potential use in thermoelectric applications. This has put NRL in a position to evaluate new classes of materials which appear promising, as well as become a center for evaluating materials developed specifically for these applications by a variety of institutions. This work is now being carried out by Drs. Wendy W. Fuller-Mora and Alexander C. Ehrlich in the Transport and Electronic Structure Section, headed by Dr. Ehrlich and Dr. Valerie Browning. A dedicated thermoelectric apparatus capable of measuring the Seebeck coefficient (thermoelectric power) and electrical conductivity from room temperature to four degrees Kelvin, with data acquisition taking place in a semiautomated way as the temperature is swept between the limits of interest, has been developed. A second apparatus designed to obtain accurate measurements of thermal conductivity on much larger samples of a specific geometry and also capable of measuring S and σ on these samples has been constructed and employed to measure metallic systems. It is currently being modified to achieve accuracy on the semiconductors which constitute most of the practical thermoelectric materials. This apparatus is capable of measurements at room temperature and above and also a computer collects data in a semiautomated manner. Dr. Kevin Stokes, an NRL post-doc, is also developing an experimental capability to measure thermal conductivity by a method known as the 3 omega technique. This recently developed approach to the problem largely avoids the errors caused by unknown heat loss present, to a degree, in other approaches to the measurement of thermal conductivity.

The existence of these apparatus' has resulted in collaborations with a number of laboratories including academic, industrial and governmental institutions. For example, a number of examples of both filled and unfilled skutterudites compounds prepared by Slack et. al. at RPI have been characterized. With Marlow Industries of Dallas, Texas the possibility of accurate, direct measurements of all the parameters in Z, including thermal conductivity, has been explored. Dr. David Demske of the Naval Surface Weapons Center, White Oak is developing techniques for making quantum wires to achieve enhanced Z's. The development is being coordinated with NRL to facilitate the process as well as to assure that the materials are geometrically and otherwise suitable for measurement as the development continues.

An interdivisional effort to develop aerogels as thermoelectric materials will be undertaken at NRL. Dr. Karen Swider, Dr. Debra Rolison (Chemistry Division), and Dr. Celia Merzbacher (Optical Sciences Division) will develop electrically conducting aerogels and characterize them by a variety of techniques. The goal is to employ the unique structure of aerogels to enhance thermoelectric performance (e.g. by exploiting the lower dimensional structure of these materials which may give rise to quantum confinement). Additionally, a collaborative effort between Jerry Meyer (Optical Sciences Division) and Northwestern University researchers Ketterson and Wong is also underway. This effort seeks to exploit quantum-confined carriers in bismuth for next-generation thermoelectric cooling devices.

Thermoelectric Cooling Systems

by Gordon Duval

Thermoelectric (TE) cooling systems are currently less efficient than conventional vapor compression systems, and therefore, are not widely used. As part of the Chloro-fluorocarbons Replacement program, Naval Sea Systems Command (NAVSEA) has funded research into improving thermoelectric material efficiency. Recent breakthroughs in this research could make TE attractive for future ships. System level studies have shown that the total ship electric power requirement for a decentralized TE cooling system with improved TE units, approaches the power required by a conventional centralized vapor compression system. Decentralization also results in cost savings due to reduced ventilation ductwork, the elimination of an isolated fan room, and modular construction.

Thermoelectric air conditioning units (TEAC) were developed and installed on the USS DOLPHIN, AGSS 555 in the early 1970s. Westinghouse Model 21E and 22K/L, one-half ton units (10 modules per cabinet) were used in the forward electronic space, the pump room and the engine room. Eventually module replacement became necessary. Having learned where the problem areas were, redesign was in order. Advanced design TEAC modules (Figure 1) have been developed and manufactured at Naval Surface Warfare Center Carderock Division (NSWCCD), Annapolis; and two prototype modules are currently aboard the DOLPHIN in the forward compartment (with four original modules). These modules utilize standard TE materials. They are 50% lighter and projected to be cheaper to manufacture than the original modules. An additional four modules will be manufactured and installed later in FY97, continuing the TE operational presence begun in 1971.

The TE material research program was in the past divided into three separate tasks, improving the standard TE material, bismuth telleride; improving TE material configurations (both short range); and developing a new family of TE materials based on multilayer superlattices (long range). Current work at Massachusetts Institute of Technology (MIT) and Lincoln Labs has the potential to substantially increase the figure of merit (ZT). This effort has focused on the use of two-dimensional quantum well multilayer superlattices (QWSL) material systems. Theoretical models of these systems have demonstrated a potential for large increases by using quantum well structures (atomic level layering of TE material) which constrain electron and phonon interaction to two dimensions. Lincoln Labs is working with MIT to fabricate these multilayer systems through molecular beam epitaxial (MBE) techniques. Experimental measurements in FY96 have confirmed ZT values greater than 2.3 for these PbTe quantum wells. It should be noted that for bulk PbTe material, ZT=.6 (approx.) is the best measured. Work will continue in FY97 to reduce barrier thickness, improve thermal conductivity measurements, and obtain higher three dimensional ZT values.

Figure 1

Water-to-air thermoelectric cooling module. NSWCCD prototype.